

GEOLOGY AND GOLD-SILVER DEPOSITS IN THE
SAN JOSE MINING DISTRICT, SOUTHERN SAN MATEO
MOUNTAINS, SOCORRO COUNTY, NEW MEXICO

by,

Eugene W. Cox

Submitted in Partial fulfillment of
the Requirements for the Degree of
Master of Science in Geology

New Mexico Institute of Mining and Technology
Socorro, New Mexico

1985

CONTENTS

	PAGE
ABSTRACT.....	1
INTRODUCTION.....	3
Study Area.....	3
Objectives of Study.....	8
Methods of Investigation.....	8
STRATIGRAPHY AND PETROGRAPHY.....	10
Tertiary Extrusive Rocks.....	12
Rock Spring Formation (upper tuff and upper agglomerate members).....	12

Vicks Peak Tuff.....	13
Lower interval (basal vitrophyric zone and lower welded zone).....	15
Upper interval (upper welded and partially welded zones).....	16
Springtime Canyon Quartz Latite Lava.....	19
Ash-Flow Tuff Unit of Milliken Park.....	21
Tertiary Intrusive Rocks.....	22
Quaternary Alluvium, Colluvium, and Talus.....	23
STRUCTURE.....	24
Faults and Fracture Systems.....	24
ALTERATION.....	29
Alteration products observed in sample thin- section and detected by X-ray diffraction analyses.....	29

LANDSAT IMAGERY.....	36
ECONOMIC GEOLOGY.....	41
History of the San Jose Mining District.....	41
Description of ore deposits and distribution of mineralization.....	42
DISCUSSION AND CONCLUSIONS.....	51
Practical Features for Exploration.....	56
SELECTED BIBLIOGRAPHY.....	58
ACKNOWLEDGEMENTS.....	80
PLATES.....	82

LIST OF FIGURES

- 1) Map overlay on a Landsat image showing general locations of the study area, mountain ranges and the Rio Grande in south-central New Mexico..... 4
- 2) Map showing the general location, geographical features, routes of access, and land status of the study area. Also shown are previous and ongoing geologic studies in the southern San Mateo Mountains..... 5 and 6
- 3) Generalized structural map of the study area showing target areas for exploration..... 25
- 4) Vertical variation of minerals detected by X-ray diffraction analyses of samples taken in the 90 foot exploration shaft in Milliken Park..... 32
- 5) Zonation of minerals detected by X-ray diffraction analyses in samples taken across the quartz breccia vein at the Taylor shaft..... 34

- 6) Reproductions of the enhanced and ratioed composite Landsat images of the study area (a, b, and c)..... 37, 38, and 39
- 7) Graphs showing Au, Ag, and Au/Ag values of samples taken in five mineralized zones plotted in order of increasing Au content..... 48
- 8) Geologic map of an area in the San Jose Mining District..... POCKET
- 9) Cross-section A to A' from Casa Grande north-east to Indian Peak..... POCKET
- 10) Cross-section B to B' east to west across the central part of the study area..... POCKET
- 11) Map showing locations of samples listed in Appendix IV. Au/Ag ratios indicated for separate mineralized zones. Directional drilling site locations also shown..... POCKET

LIST OF TABLES

1) Stratigraphy of the San Jose Mining District.....	11
2) Mean, range, and standard deviations of of Au, Ag, and As values (ppm), and Au/Ag from analyses of sample groups taken in five mineralized zones in the study area.....	47

APPENDICES

I. Sample preparation and semiquantitative X-ray analyses of alteration products.....	65
II. Intensity values for argillic and other minerals detected by X-ray diffraction analyses.....	69
III. Rhyolite Mine sample map (Neubert, 1983).....	72
IV. Geochemical analyses data.....	73

ABSTRACT

Precious-metal deposits in the San Jose Mining District of Socorro County, New Mexico occur within a complexly fractured area on the southeastern flank of the San Mateo Mountains. Cross-cutting faults and fracture systems in the area are a product of regional extension and volcanotectonic activity within the proposed boundaries of the Nogal Canyon Caldera. Epithermal mineralization in felsic volcanic host rocks is surrounded by broad argillic-ferric alteration zones apparent in enhanced satellite imagery.

Upper members of the Rock Spring formation, the upper and lower intervals of Vicks Peak Tuff, Springtime Canyon Quartz Latite lava, and the tuff unit of Milliken Park are distinct Tertiary volcanic units exposed in the study area. This series of discontinuous tuffs and lavas was deposited during eruptions associated with formation of the Nogal Canyon Caldera. Thickening of flow units across faults and discordant contacts between flow units indicate repeated faulting and eruptive events. Late-stage silicic intrusive rocks are locally exposed in the area.

Gold and silver deposits in the San Jose Mining District contain anomalous concentrations of arsenic, mercury, and antimony. Geochemical analyses of rock samples and stream sediments show subeconomic concentrations of copper, lead, zinc, and molybdenum. Platinum, palladium, beryllium,

niobium, and lanthium have also been detected in samples taken in the area. Mineralized felsic volcanic rocks contain quartz, adularia, alunite, albite, pyrite (commonly oxidized), limonite, goethite, hematite, and wad. Argillic alteration products surrounding deposits include kaolinite, illite (sericite and hydromica inclusive), smectite, and mixed-layer clays.

Banded quartz veins, low-pH alteration, and hydrobrecciation in mineralized zones are attributed to episodic fracturing, boiling, and hydrothermal eruption. In this model gold, silver, and associated minerals and trace elements are concentrated during hydrothermal activity initiated by magmatism and pressure release. Intensified argillic alteration, silicification, and oxidation apparent in mineralized zones are attributed to repeated pulses of hypogene fluids followed by thermal collapse and supergene recharge.

INTRODUCTIONStudy Area

The study area includes approximately 6 square miles of the Cibola National Forest in the southeastern San Mateo Mountains of south-central Socorro County, New Mexico. The area is located within the San Jose Mining District 48 miles southwest of Socorro, New Mexico. The San Mateo Mountains reach a maximum elevation of 10,252 feet (3125 m) at Vicks Peak, about one and a half miles west of the study area. The elevation in the study area ranges from 6750 feet to 8490 feet. The general location of the study area and mountain ranges in south-central New Mexico is shown in Figure 1. Geographic features, routes of access, land status, and areas covered by previous and on-going geologic studies are shown in Figure 2.

The southern San Mateo Mountains are a generally northeast-dipping uplift located in the eastern part of the Cenozoic Mogollon-Datil volcanic field. The Mogollon-Datil field is an erosional remnant of a broad Tertiary-aged bimodal volcanic complex bordering the Rio Grande rift, the Colorado Plateau, and the southern Basin and Range province. Incomplete geologic mapping and reconnaissance in the eastern part of the Mogollon-Datil volcanic field indicate at least five ignimbrite-erupting calderas (Osburn and Chapin,

1983). Mineral deposits in the area are spatially associated with Tertiary resurgent calderas and volcanic centers (Elston, 1978).

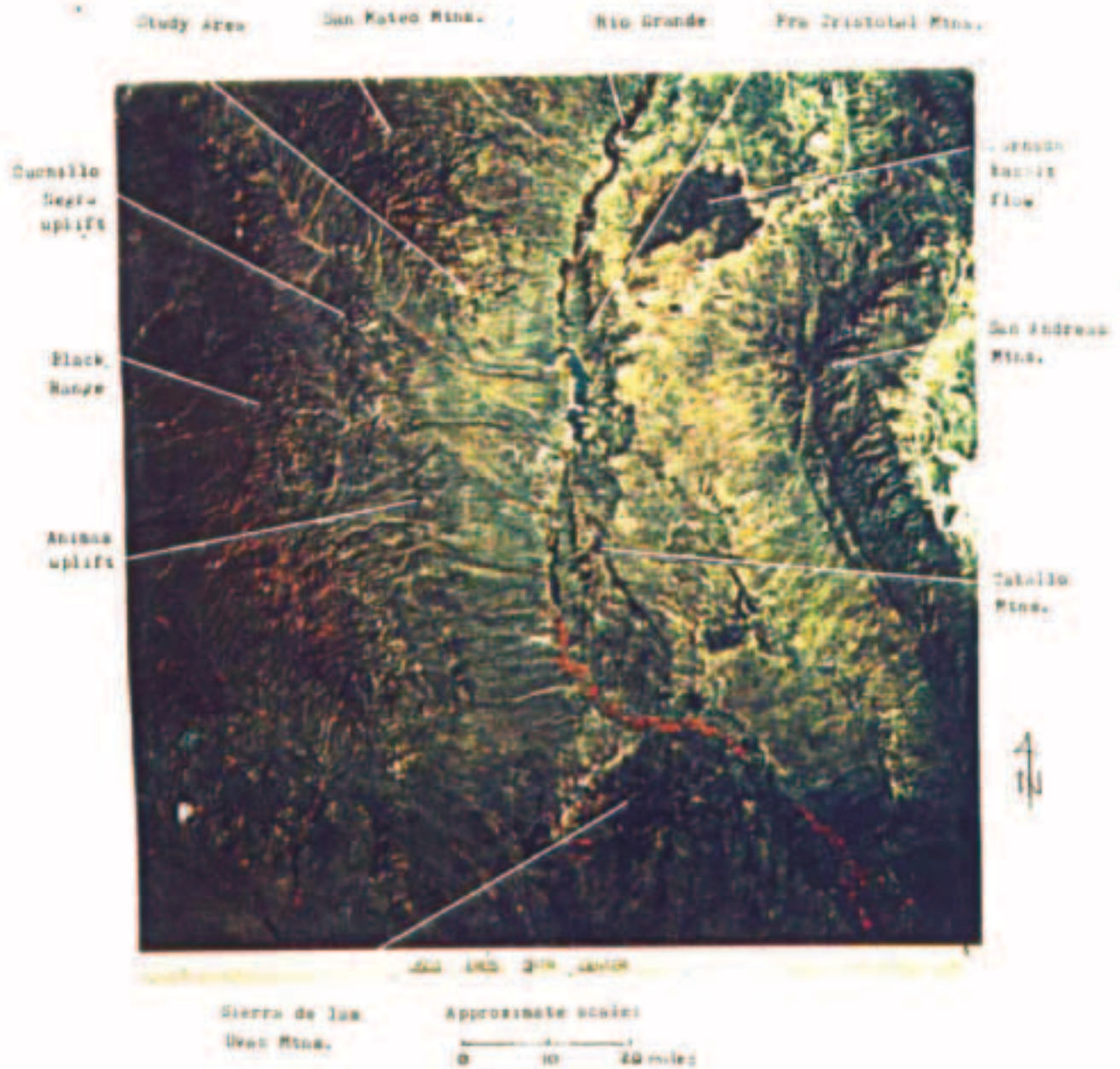
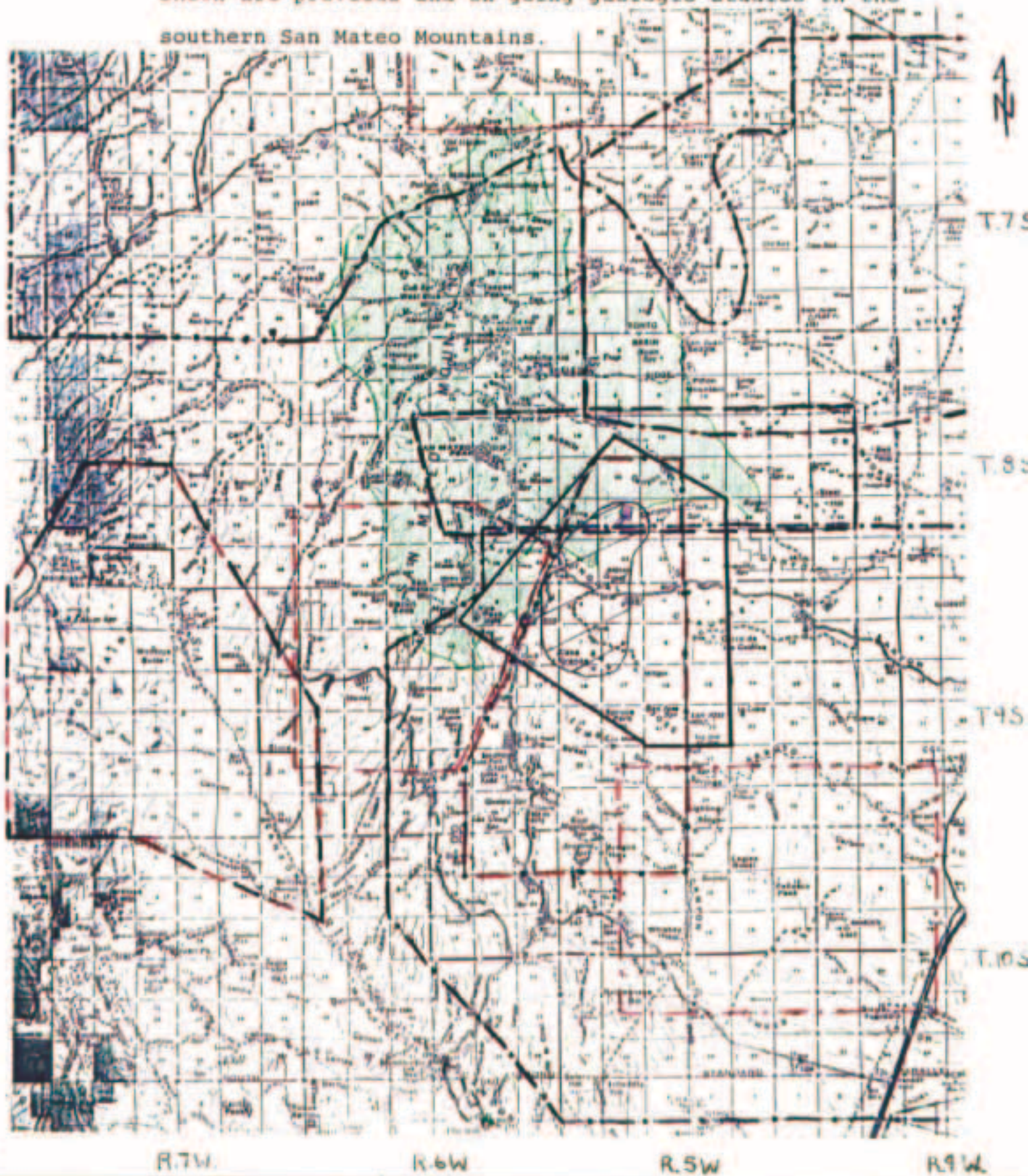


Figure 1. Map overlay on a Landsat image showing the general locations of the study area, mountain ranges, and the Rio Grande in south-central New Mexico.

Figure 2. The general location, geographical features routes of access, and land status of the study area. Also shown are previous and on-going geologic studies in the southern San Mateo Mountains.



Areas outlined in Figure 2.

- | | | | |
|---|-----------------------------|---|------------------------|
|  | Apache Kid Wilderness |  | Patented Mining Claims |
|  | Study Area | | |
|  | S.G. Lasky, 1932 | | |
|  | J.W. Furlow, 1965 | | |
|  | S.A. Farkas, 1969 | | |
|  | E.G. Deal, 1973 | | |
|  | F. Maldonado, 1974 | | |
|  | G. Atwood, 1982 | | |
|  | J. Foruria, 1984 | | |
|  | C.A. Ferguson, 1985 | | |
|  | M.L. Hermann, (in progress) | | |
|  | C.E. Hesse, (in progress) | | |

Detailed mapping in the study area has revealed complex stratigraphic and structural relationships. The study area is located in a volcanotectonic depression within the boundaries of the Nogal Canyon Caldera proposed by Deal and Rhodes (1976). Recent sampling and analyses in the area indicate widespread mineralization of gold and silver within broad, complex fracture zones in a thick sequence of ignimbrites, lavas and intrusive rocks. Breccia-hosted epithermal gold-silver deposits are silicified, pyritized, argillically altered, and stained by yellow, orange, red, brown, and black iron and manganese oxides and hydroxides (limonite, goethite, hematite and wad).

Reported information from past exploration and mining in the San Jose Mining District, in addition to recent detailed geologic mapping, interpretation of enhanced satellite imagery, aerial photographs, and geochemical, petrographic, and X-ray diffraction analyses, have been used in this report to describe epithermal mineralization in the area. Information from preliminary directional drilling by Exxon Minerals Company during the summer of 1985 will provide further valuable information. Continued work in the area may lead to discovery of large-scale, bulk-minable, precious-metal deposits.

Objectives of Study

The primary objectives of this study are: 1) to map and describe the Tertiary volcanic rocks and the complex structural framework in the study area, 2) determine the sequence of possible cauldron-related volcanotectonic events, and 3) to study the epithermal mineralization and alteration associated with hydrothermal systems.

Methods of Investigation

Detailed geologic mapping was done at a scale of 1/12,000 on a base map consisting of an enlargement of part of the Vicks Peak, and Steel Hill topographic quadrangles of the U.S. Geological Survey 7 1/2-minute series. Natural color aerial photographs, obtained from the U.S. Forest Service, Cibola National Forest series CIB, 1974 (scale 1:15,840) aided mapping of the area. Mapping in the field was done during 1984 and 1985.

False color composite Landsat images, taken May 17, 1973 (scale: 1:1,109,000), were useful in delineating large-scale structural features and hydrothermal argillic-ferric alteration in the study area. The images were produced, expanded, and enhanced using hardware and software provided by the Technology Application Center of the University of New Mexico during the fall of 1984.

Thirty-six thin-sections, prepared from samples collected throughout the study area, were examined using a Nikon binocular polarizing and reflecting microscope. The modal contents of minerals in lithologic units were estimated, and other petrographic features including the effects of welding, devitrification, mineralization, and alteration were observed. Petrographic rock names are from Travis (1955). Photomicrographs of selected thin-sections are included in the Plates section of this report.

Semiquantitative X-ray diffraction analyses of twenty-four samples were made August through December, 1983 at New Mexico Institute of Mining and Technology in Socorro, New Mexico. X-ray diffraction traces of clay-sized sample separates were obtained in untreated, glycolated, and heated runs. These data were used to estimate the variable comparative content of detectable minerals in hydrothermally altered rock samples.

Geochemical data shown in this report include analyses reported by the U.S. Geological Survey (Griffitts and others, 1971), the U.S. Bureau of Mines (Neubert, 1983), Foruria (1984), and analyses provided by the current owners of the Apache lode mining claims located in the study area. Concentrations of gold, silver, arsenic, mercury, and antimony in rock samples were determined using atomic absorption analyses and fire assays. Anomalous concentrations of gold, silver, platinum, copper, lead, zinc, molyb-

denum, arsenic, antimony, beryllium, bismuth, niobium, and lanthanum in the area have been detected using spectographic analyses of rock samples and stream sediment concentrates. One bulk sample was tested with cyanide for the leachability of gold.

STRATIGRAPHY AND PETROGRAPHY

Rock units exposed in the study area include Tertiary volcanic rocks, and Quaternary alluvium and colluvium. A thick sequence of Tertiary ignimbrites, lavas, intrusives, and sedimentary rocks in the southern San Mateo Mountains overlie Mesozoic, Paleozoic, and Precambrian basement rocks composed of folded and sheared argillaceous and clastic sedimentary rocks, limestones, igneous and metamorphic rocks. Basement rocks are known from drill holes and surface exposures outside the study area (Table 1).

Table 1: STRATIGRAPHY OF THE SAN JOSE MINING DISTRICT

PERIOD	UNITS	THICKNESS
QUATERNARY	Alluvium, colluvium, terrace deposits, and talus	0-50 m (0-164 ft)
TERTIARY	Tuff unit of Milliken Park	35 m (115 ft)
	Springtime Canyon Quartz Latite	15-700 m (50-2300 ft) (Deal & Rhodes, 1976)
	Vicks Peak Tuff	488-1220 m (1600-4000 ft) (Hermann, unpubl.)
	Spears Formation	Rock Spring Formation
Red Rock Ranch Formation		1000 m (3281 ft) (Farkas, 1969; Deal & Rhodes, 1976)
PERMIAN	Abo Formation	0-210 m (0-680 ft) (Kottlowski, 1963)
PENNSYLVANIAN	Madera Limestone	640-914 m (2100-3000 ft) (Kottlowski, 1963)
	Sandia Formation	0-100 m (328 ft) (Kottlowski, 1963)
ORDOVICIAN	Upham Dolomite	0-60 m (0-197 ft) Kelley & Furlow, 1965; Kottlowski, 1963)
PRECAMBRIAN	Metasedimentary, intrusive, and extrusive rocks of basaltic, intermediate, and granitic composition	

Tertiary Extrusive RocksRock Spring Formation

The upper tuff and upper agglomerate members of the Rock Spring Formation are the oldest rocks exposed in the study area. These units are part of the upper Rock Spring Formation which is composed of interbedded andesitic to latitic lavas, tuffs, and breccias. Deal and Rhodes (1976) suggest a lithic-rich agglomerate in the upper Rock Spring Formation formed as an ignimbrite lahar during the early stages of development of the Nogal Canyon Caldera. The Rock Spring Formation is approximately 2000 feet (609.6 m) thick three miles south of the study area (Farkas, 1969).

The upper members of the Rock Spring formation were mapped as a single unit in the west-central part of the study area. Locally exposed outcrops are hydrothermally altered along faults. Thin-sections of the upper tuff member contain 30% feldspar phenocrysts composed of orthoclase and plagioclase, and about 10% biotite phenocrysts within a dark microcrystalline matrix. Commonly these minerals are replaced by sericite, and opaque iron oxide (Plates 1a, b). The upper agglomerate member is similarly altered and contains poorly-sorted lithic fragments supported in a cryptocrystalline matrix.

Vicks Peak Tuff

The Vicks Peak Tuff is the dominant rock unit in the study area. Lasky (1932) mapped and described the Vicks Peak Tuff in the southern San Mateo Mountains as "brown rhyolite". Furlow (1965) called it the Rhyolite of Vicks Peak, and Farkas (1969) later named it the Vicks Peak Rhyolite. The unit was recognized to be an ignimbrite and was redefined as the Vicks Peak Tuff by Deal and Rhodes (1976). These authors suggested its eruptive source is the Nogal Canyon Caldera of the southern San Mateo Mountains. The Vicks Peak Tuff, sampled north of the study area, has been dated to be 31.3 ± 2.6 Ma by Bornhorst and others (1982), and 28.46 Ma by Kedzie and others (1984).

Deal and Rhodes (1976) suggested the Vicks Peak Tuff is more than 2165 feet (650 m) thick in the southern San Mateo Mountains. Flows of Vicks Peak Tuff up to 800 feet thick extend across the San Mateo, Datil, eastern Gallinas, Bear, Lemitar, Magdalena, and northern Jornada del Muerto mountains, and the Sierra Cuchillo, northern Black Range, Joyita Hills in south-central New Mexico (Osburn and Chapin, 1983; Maldonado, 1974). Ferguson (1985) measured a section of Vicks Peak Tuff more than 800 feet (244 m) thick in the northern San Mateo Mountains approximately 12 miles north of the study area. Maldonado (1974) found a 1200 foot (360 m) thick section of Vicks Peak Tuff in a structural depression

in the Sierra Cuchillo about 7.5 miles southwest of the study area.

A section of Vicks Peak Tuff more than 4000 feet (1200 m) thick in areas west of the study area is indicated by ongoing investigation west of the Rock Spring fault (Hermann, unpublished). The Vicks Peak Tuff is approximately 1600 feet (480 m) thick in adjacent areas east of the Rock Spring fault. This great difference in thickness must have resulted from down-to-the-west movement along the Rock Spring fault before and/or during early eruptions of the Vicks Peak Tuff.

Exposures of Vicks Peak Tuff 35 miles north of the study area in the Bear and Gallinas Mountains are crystal-poor (Osburn, 1984). In the northern San Mateo Mountains the lower interval of the Vicks Peak Tuff is crystal-poor compared to the upper interval which contains up to 15% phenocrysts of potassium feldspar (Ferguson, 1985). Similarly, phenocryst content of the Vicks Peak Tuff in the southern San Mateos ranges from 2% - 4% potassium feldspar in its lower interval to 5% - 15% in its upper interval. In the study area the lower interval is composed of a thin basal vitrophyre and a thick densely welded zone which were mapped as a single unit. The upper moderately and partially welded zones were mapped as a single unit designated as the upper interval of the Vicks Peak Tuff.

The lower interval of the Vicks Peak Tuff is composed of the following distinct zones:

1. The basal vitrophyric zone of the Vicks Peak Tuff exposed in the west-central part of the study area is composed of a gray densely welded, spherulitic, devitrified layer approximately 20 feet thick. This layer contains approximately 2% phenocrysts of commonly perthitic sanidine and abundant opaque crystallites. The microcrystalline matrix has a recognizable vitroclastic texture and perlitic cracking is common. The vitrophyric zone locally contains spherulites up to 4 inches in diameter. Cracks and microbrecciation in samples contain quartz, pyrite, and limonite (Plates 2a, b).

2. The lower densely welded zone of the Vicks Peak Tuff is brownish gray, fine-grained, and porphyritic. In the study area this part of the section is approximately 700 feet thick. Multiple flow units in the lower welded Vicks Peak form columnar jointed exposures which contain 2 - 4% sanidine phenocrysts in a microcrystalline matrix. Quartz and potassium feldspar occur as thin polycrystalline intergrowths within abundant small flattened gas cavities. In some zones devitrified pumice forms small, rounded, flattened white patches. Dark xenoliths or magma clots are locally abundant in welded flows near the top of the lower interval of Vicks Peak Tuff.

The upper interval of the Vicks Peak Tuff is composed of the following distinct members:

1. A gray, flow-banded, moderately welded zone approximately 600 feet thick overlies the welded zone of the lower interval. Separate flow units in this zone contain 5% - 8% sanidine phenocrysts up to 2.5 mm in length which are commonly perthitic. Biotite content generally increases upward in the section forming up to 2% of the rock. The microcrystalline matrix, composed of polycrystalline potassium feldspar and quartz contains microcrystalline ferromagnesian minerals, zircon, and finely divided opaque minerals. The vitroclastic texture is commonly recognizable in devitrified samples.

2. The top 100 to 300 feet of Vicks Peak Tuff is moderately to partially welded. The degree of welding decreases upward and locally abundant pumice and gas cavities commonly contain polycrystalline vapor-phase minerals including potassium feldspar and quartz. Phenocryst content in this part of the upper interval consists of 8% - 15% commonly broken sanidine and approximately 2% biotite. Axiolitic structures are can be recognized in the microcrystalline matrix which contains crystallites of zircon and finely-divided opaque minerals.

Separate flow units in the upper interval of Vicks Peak Tuff include a dark dense flow which forms a thick sheeted zone that is up to 300 feet thick in some areas. This

sheeted zone is exposed below light colored, columnar caprock above Casa Grande peak, Indian Peak, and topographically lower areas between Nogal Canyon and San Jose Arroyo (Plate 3). It has irregular, sometimes vertical foliation. This relatively permeable, structurally weak unit is brecciated, altered, and mineralized along faults and fracture systems in the study area. Irregular bands of limonite from oxidized pyrite appear to have formed as broad diffusion fronts along fractures (Plate 4). Foruria (1983) found more than 5% alunite in samples taken on Indian Peak.

In the study area the Vicks Peak Tuff is vertically zoned and contains irregular layers with variable amounts of phenocrysts, xenoliths, vapor-phase minerals, pumice, lithic fragments, gas cavities, and spherulites. Multiple flow units are devitrified, altered, and mineralized. Welding breaks between flow units are not apparent. Generally phenocryst content, vapor-phase mineralization, abundance of gas cavities, and pumice content increases upward in the section. Dark co-mingling xenoliths in some flow units of the Vicks Peak Tuff appear to have mixed to produce hybrid zones.

Polycrystalline potassium feldspar and quartz in gas cavities and pumice fragments in the Vicks Peak Tuff are attributed to vapor-phase mineralization by ascending gas expelled during welding and devitrification. Vapor-phase mineralization and devitrification in thick ash-flow tuffs are thought to be enhanced by volatile transfer during welding (Smith and Ross, 1961; Smith, 1960). Vertical foliation in the upper poorly-welded zone may have resulted from gas streaming during this process. Discontinuous sheeted fracturing in some flow units may have developed during cooling.

Disseminated hydrothermal mineralization in pumice fragments, gas cavities, and pore space is common in the upper interval of Vicks Peak Tuff (Plates 5a - h). Primary phenocrysts and vapor-phase mineralization in the Vicks Peak Tuff sampled in the study area commonly show the effects of hydrothermal alteration. Felsic minerals throughout the section have undergone variable degrees of potassic metasomatism. Gas cavities and pores are commonly lined by adularia and quartz crystallites. Patches and lamellae in perthitic sanidine phenocrysts are preferentially replaced and altered. Ferromagnesian minerals are commonly sericitized and replaced by opaque crystallites.

Stretched pumice fragments in the Vicks Peak Tuff generally have a normalized northwest-southeast lineation in the study area. These give a striated appearance to some

exposures. The abundance, size, and degree of stretching are generally greatest in flow units of the upper interval of Vicks Peak Tuff. Spherulites are locally abundant in the basal vitrophyric zone and other thick laterally discontinuous zones in the Vicks Peak Tuff. Commonly spherulites in densely welded zones contain slit-like structures enclosed by discolored outer rinds which may have formed following welding by devitrification of gas-charged glassy fragments.

Springtime Canyon Quartz Latite Lava

A gray porphyritic lava known as the Springtime Canyon Quartz Latite commonly overlies the Vicks Peak Tuff in the northern half of the study area. Lasky (1932) referred to this laterally discontinuous unit as "porphyritic rhyolitic cap rock". Furlow (1964) called the Springtime Canyon Quartz Latite a rhyolitic tuff, and mapped it along Springtime Canyon and San Mateo Peak where it measured up to 2300 feet (700 m) thick. Farkas (1969) mapped exposures of Springtime Canyon Quartz Latite lava northeast of the study area and suggested it is entirely an intrusive rock. Foruria (1984) mapped broad flows of Springtime Canyon Quartz Latite lava 2 miles northeast of the study area.

In the study area the Springtime Canyon Quartz Latite contains approximately 20% medium to coarse grained tabular feldspar phenocrysts up to 7 mm in diameter, 5% biotite, and 3% quartz. The microcrystalline matrix contains polycrystalline feldspar, quartz, and lesser amounts of biotite, zircon, and opaque crystallites. Approximately 1% zircon in the rock commonly occurs as individual crystallites and as inclusions in biotite. Lamellae and internal patches of exsolved albite in perthitic sanidine phenocrysts commonly are altered and selectively replaced by argillic minerals. Subhedral biotite is commonly sericitized and replaced by opaque iron oxide (Plates 6a - d).

Locally preserved massive flows of Springtime Canyon Quartz Latite lava up to 100 feet (30 m) thick pinch out to the south below the ash-flow tuff unit of Milliken Park in the central part of the study area. Coarsely porphyritic flows are commonly trachytic, autobrecciated, and contain clasts of Vicks Peak Tuff. Exposures of Springtime Canyon Quartz Latite lava are strongly altered and mineralized along fracture systems.

Ash-Flow Tuff Unit of Milliken Park

The tuff unit of Milliken Park is the youngest extrusive rock exposed in the study area. This ignimbrite unit dips eastward where it lies above Springtime Canyon Quartz Latite and Vicks Peak Tuff on structurally low fault blocks in the study area. Other exposures of the tuff unit of Milliken Park have not yet been located by reconnaissance mapping in surrounding areas. Because of its limited extent and compositional similarity to Springtime Canyon Quartz Latite and Vicks Peak Tuff it appears to represent a late eruptive phase of the Nogal Canyon Caldera volcanic sequence. Farkas (1969) did not distinguish this unit from the Vicks Peak Tuff. Foruria (1984) lumped it with the Springtime Canyon Quartz Latite.

The base of the tuff unit of Milliken Park is composed of thin, locally exposed vitrophyric and unwelded zones below up to 115 feet (35 m) of a brownish gray, moderately welded zone. The welded portion contains 30% broken potassium feldspar phenocrysts and 5% biotite phenocrysts which are commonly broken and altered to sericite. The dark glassy matrix has a layered, vitroclastic texture and contains up to 3% opaque crystallites. Pumice, lithic fragments, and gas cavities are locally abundant. Microscopic perlitic cracking is evident in thin-sections (Plates 7, 8a - d).

Tertiary Intrusive Rocks

Small, widely-spaced silicic dikes in the study area penetrate fractured zones within faulted blocks of Vicks Peak Tuff. These orange-red hypabyssal rocks are locally exposed along traces of northeast and east-west trending faults and fractures. Exposures within narrow fractures are porous, trachytic, vertically foliated, argillically altered, and surrounded by mineralized zones containing vein quartz, pyrite (commonly oxidized), limonite, hematite, wad, and anomalous gold and silver. Rocks surrounding dikes are brecciated, altered, and mineralized (Plate 9).

Sanidine is the dominant phenocryst in locally exposed dikes in the study area. Samples contain about 15% tabular sanidine crystals 1 to 4 mm long which commonly have perthitic exsolution along lamellae and patches. These milky translucent crystals are commonly rimmed and have poorly preserved birefringence and chatoyancy. Many sanidine phenocrysts are deeply embayed by sericite and argillic alteration products. The rock also contains about 5% quartz forming polycrystalline pore fillings and rounded crystals 0.01 to 0.10 mm in diameter. The matrix contains up to 20% hematite and limonite, and 5% pore space. Samples commonly contain oxidized pyrite and small black spherical blobs of wad less than 5 mm in diameter (Plates 10, 11a - d).

Possible eruptive centers of Springtime Canyon Quartz Latite within the proposed boundaries of the Nogal Canyon Caldera include those mapped and described by Lasky (1932), Furlow (1964), Atwood (1983), and Hermann (unpubl.). These include large intrusive stocks outside the study area located along what appear to be ring fractures in the Nogal Canyon Caldera. Dikes exposed in Springtime Canyon adjacent to the Pankey vein, and outside the western margin of the study area along the Apache Kid wilderness trail are other possible sources of latitic lavas in the area.

Quaternary Alluvium, Colluvium, and Talus

Alluvium, composed of locally derived material deposited during periods of heavy runoff, is confined to present day stream channels located between structurally high blocks in the study area. Steep canyons and drainages are commonly covered by talus, and bordered by colluvium composed of poorly-sorted unconsolidated broken rock fragments and soil cover. This material commonly covers contacts, structures, and mineralized zones in the study area.

STRUCTURE

Many structural features in the southern San Mateo Mountains have been generally treated in previous geologic studies. Lasky (1932) mapped and described northeast trending fault-filling veins in the area including the Pankey, Rhyolite, and Big It veins, and other unnamed roughly east-west trending veins of the San Jose Mining District. Furlow (1965) mapped the east-west trending faults along Nogal Canyon, and Springtime Canyon. Segments of the Rock Spring fault in the western part of the study area, have been generally mapped and described by Farkas (1969) and Foruria (1984). Griffitts and others (1971), and Foruria (1984) show the general locations of the Indian Peak fault and other prominent linear features in their reconnaissance maps of the area.

Faults and Fracture Systems

Detailed geologic mapping along the base of the southeast slope of Vicks Peak reveals a complex system of faults and fracture systems bordering generally northeast tilted fault blocks (Figure 3). Layering, flattened pumice fragments, and gas cavities can be used to estimate the strike and dip of ignimbrites and lavas in these areas. Discontinuous unit thickness across faults and discordant contacts

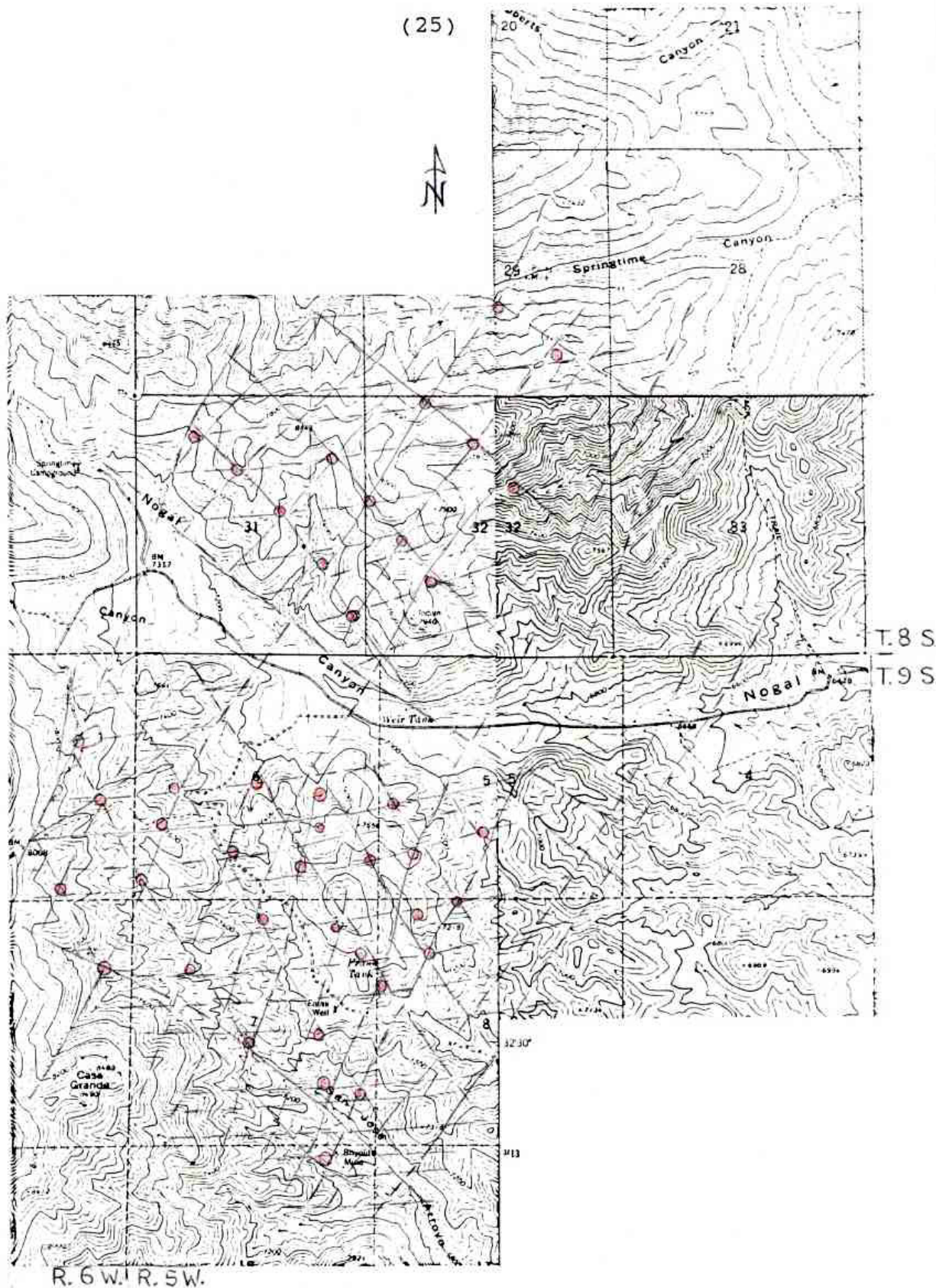


Figure 3. Generalized structural map of the study area. Red circled areas are altered breccia zones situated along intersecting faults and fractures systems. These areas should be sampled and evaluated during continued exploration.

between stratigraphic members of the Vicks Peak Tuff, the Springtime Canyon Quartz Latite lava, and the tuff unit of Milliken Park indicate repeated eruptive and tectonic activity. Block jostling has intensified fracturing in the area. Commonly older faults have been reactivated and fault intersections are brecciated, hydrothermally altered, and mineralized.

Northeast trending down-to-the-west normal faulting is developed regionally in the southern San Mateo Mountains. In the study area northeast trending faults form concentric traces along the southeast slope of Vicks Peak. This series of extensional faults include the Rock Spring, Pankey, Indian Peak, and Rhyolite faults. The lower interval of Vicks Peak Tuff appears to be drag folded along northeast trending faults indicating that movement might have occurred before the unit was thoroughly welded.

The Rock Spring fault which trends N. 25 E. near the western margin of the study area has experienced more than 2000 feet (600 m) down-to-the-west vertical displacement (Hermann, unpubl.). The Vicks Peak Tuff is more than 4000 feet (1200 m) thick west of the Rock Spring fault and contains a thick lithic-rich section not found to the east in the foot wall of the fault. This substantial thickening and brecciation west of the Rock Spring fault indicates that movement occurred during early eruptive phases of Vicks Peak Tuff (Plate 12).

The Pankey fault trends about N. 40 E. from Pankey Mine in Springtime Canyon south through the central part of the study area. In the north slope of Springtime Canyon the Pankey fault is filled by a mineralized quartz vein. South of Springtime Canyon the vein is not exposed along the fracture trace of the Pankey fault in structurally lower blocks (Plates 13, 14). The trace of the Pankey fault is partially concealed in the complexly fractured area south of Springtime Canyon. Between Nogal Canyon and the San Jose Arroyo the Pankey fault has experienced approximately 350 feet down-to-the-west displacement. About 300 feet of movement is evident on the Pankey fault north of Springtime Canyon.

The Indian Peak fault is another northeast trending normal fault crossing the central part of the study area. About 300 to 400 feet down-to-the-west vertical displacement is evident along the Indian Peak fault in the central part of the study area. Hydrothermal alteration is common along the trace of the fault. Strongly silicified wall rocks along the Indian Peak fault are exposed on the southern slope of Nogal Canyon.

The Rhyolite fault trends approximately N. 25 E. through the southeastern part of the study area about one mile east of the Pankey fault. Two roughly parallel fractures form the trace of the Rhyolite fault. The combined down-to-west displacement across these fractures is more than 600 feet. Fault-bounded blocks in the hanging wall of

the Rhyolite fault are cross-cut by closely-spaced inter-connecting fractures. Brecciated rocks in these fractured zones are extensively altered and mineralized.

A series of closely-spaced northwest and approximately east-west trending faults and fractures cross-cut northeast trending faults in the study area. Up to 300 feet down-to-the-west movement is evident along some northwest trending normal faults which generally dip more than 70 degrees to the southwest. Vertical displacement along steeply dipping east-west trending normal faults is quite variable ranging from 10 to 300 feet.

The central part of the study area is bounded by two near parallel normal faults, trending N. 60 W. along Nogal Canyon and the San Jose Arroyo. Differences in elevations of distinct members of the Vicks Peak Tuff bordering these faults indicate the Nogal Canyon fault is down to the south and the San Jose fault is down-dropped to the north. Both the San Jose fault and the Nogal Canyon fault have undergone about 300 to 500 feet of vertical displacement. East-west extensional subsidence between these faults increased the degree of block rotation and fracture concentration in the central part of the study area compared to adjacent areas.

ALTERATION

Potassium metasomatism is common in volcanic rocks of the eastern Mogollon-Datil volcanic field (Osburn, 1978; Eggleston, 1982). This type of alteration has been attributed to wide-spread geothermal activity in areas in south-central New Mexico which have undergone Tertiary rotational normal faulting and 20% - 100% crustal extension (Osburn, 1978; D'Andrea-Dinkelman and others, 1983). More intense hydrothermal alteration in the study area is evident in thin-sections and X-ray diffraction traces of samples of the upper members of the Rock Spring Formation, the Vicks Peak Tuff, the Springtime Canyon Quartz Latite, the tuff unit of Milliken Park, and rhyolitic intrusive rocks.

Hydrothermal activity associated with breccia zones, quartz veins, and rhyolite dikes in the study area has resulted in progressive mineral alteration in permeable host rocks. Primary feldspar phenocrysts and crystallites observed in thin-section are commonly replaced by sericite, alunite, and argillic alteration products. Ferromagnesian minerals are replaced by biotite, sericite, and opaque crystallites. Oxides and hydroxides of iron and manganese liberated during this process commonly fill pore space. Zircon crystallites in these rocks are not affected in altered samples.

Distinct vertical and horizontal zoning of low-pH alteration products is evident in mineralized zones in the study area. X-ray diffraction analyses of clay-sized sample separates indicate variable relative concentrations of kaolinite, illite (sericite and hydromica inclusive), smectite, mixed-layer clays, quartz, orthoclase (adularia inclusive), albite, and alunite. Similar alteration assemblages commonly occur in mineralized felsic rocks and are believed to be genetically related to fracturing, sealing, and boiling (Meyer and Hemley, 1967; Buchanan, 1981).

Procedures for determining comparative amounts of argillic minerals in samples using X-ray diffraction techniques are outlined in Appendix I of this report. The method used produced unitless numeric values (parts in 10) which represent semiquantitative content of major clay groups. Relative content of other minerals in clay-sized sample separates were estimated by comparing representative X-ray diffraction peak intensities. Peak intensities from X-ray diffraction analyses are listed in Appendix II.

Figure 4 shows the vertical variation of fine-grained mineral separates indicated by X-ray diffraction analyses of four samples taken in the 90 foot shaft in Milliken Park. Sample traces have sharp, distinct, relatively intense kaolinite peaks. Less intense, broadly dispersed illite and smectite peaks represent varieties of lower crystalline quality. Other broad peaks and ripples in diffraction traces are similar to calculated patterns by Brindley and Brown (1981) for clays with randomly interstratified illite-smectite mixed-layer clay.

Comparatively high amounts of illite (sericite and hydromica inclusive), smectite, mixed-layer clays, and quartz are indicated at the 60 foot level. This assemblage of expandable clays, and associated with quartz and adularia represents a low-permeable zone that may be related to boiling. The 30 foot level shows a marked increase of kaolinite and silver content compared to the other shaft samples. Below the 60 foot level there is an apparent increase of kaolinite and decrease of other detectable argillic constituents. Gold values in the four samples taken in the 90 foot shaft ran 0.02 to 0.03 ounces per ton (0.62 - 1.00 ppm).

Figure 4. The vertical variation of argillic and nonargillic clay-sized mineral separates from four chip samples taken at 30 foot intervals in the 90 foot exploration shaft in Milliken Park detected by X-ray diffraction analyses. Results of analyses for gold and silver are also indicated.

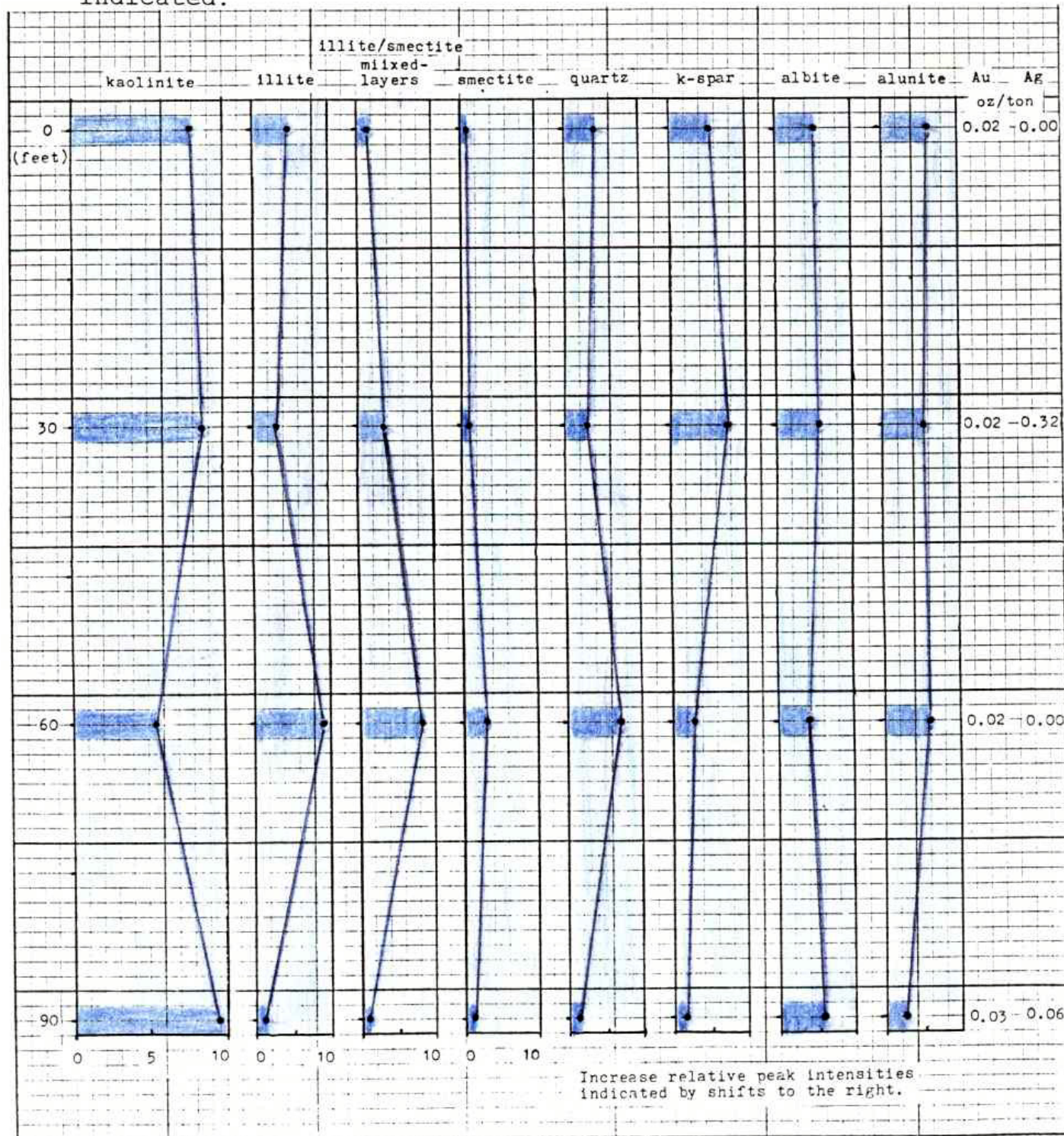
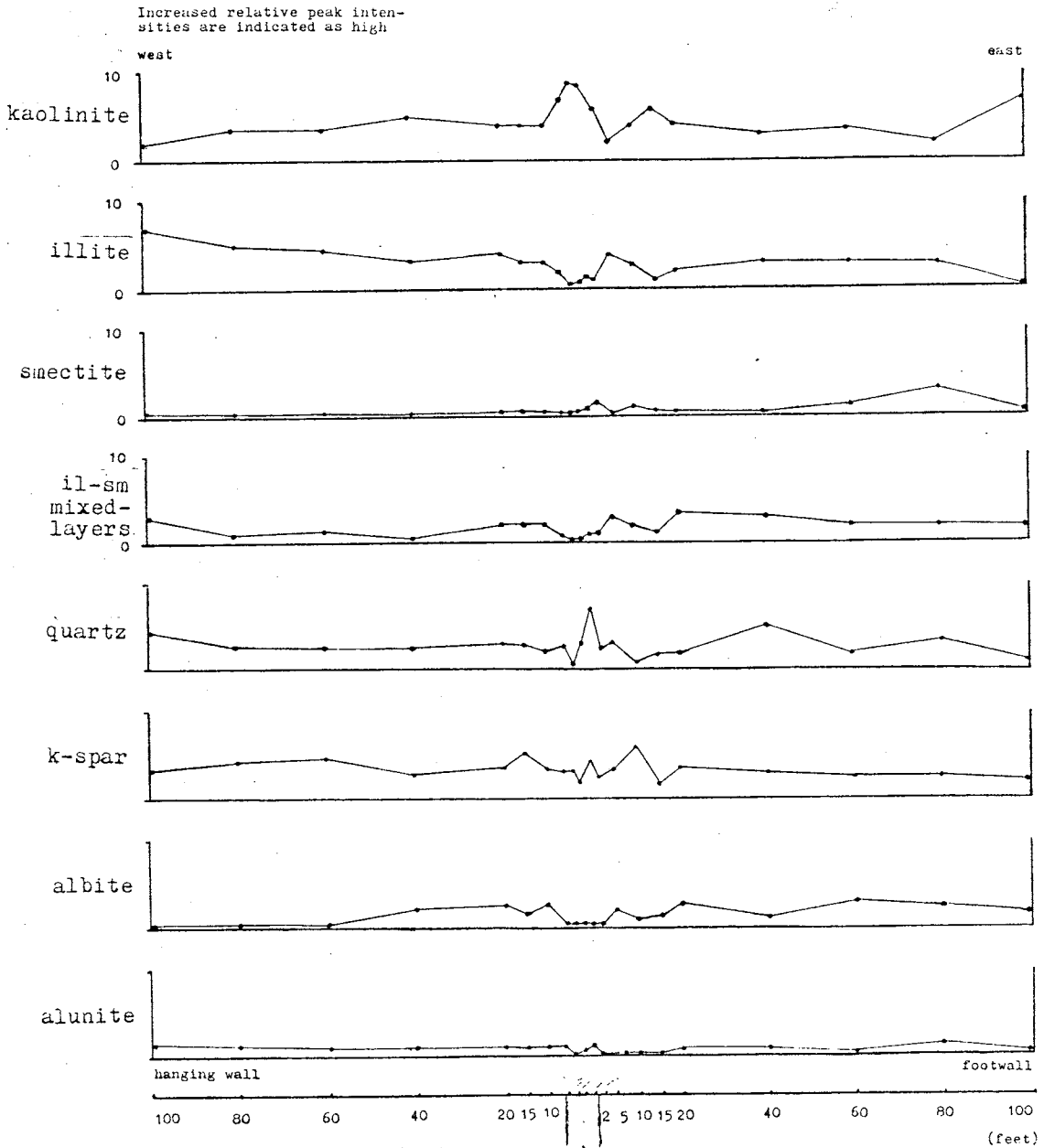


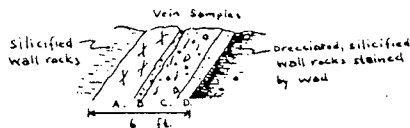
Figure 5 graphically shows the results from X-ray diffraction analyses of samples taken at closely-spaced intervals across the vein and wall rocks at the Taylor shaft. Comparative numeric values for argillic minerals are semiquantitative unitless values (parts in 10). Peak heights of other minerals in X-ray diffraction traces were compared directly to estimate intensities. A generally inverse relationship between kaolinite and other argillic minerals is evident. High kaolinite content occurs in the central part of the vein and at 15 and 100 feet to the east in the footwall. The selvage bordering the vein contains comparatively high amounts of illite (sericite and hydromica inclusive), smectite, and mixed-layer clays. Samples also show an inverse relationship between potassium alteration products and albite.

Figure 5. Variable content and zonation of alteration products detected by X-ray diffraction analyses of twenty outcrop samples taken across the brecciated amethyst bearing quartz vein exposed at the Taylor shaft.



Sample locations and distances east and west of the central quartz vein indicated.

Four samples taken across the six feet wide vein exposed at the Taylor shaft. Samples designated A, B, C, and D.



- A. Silicic zone, gray quartz
- B. Red hematitic breccia zone
- C. White argillic zone, unconsolidated breccia containing Mn & Fe oxides
- D. Greenish argillic zone, fine-grained gouge

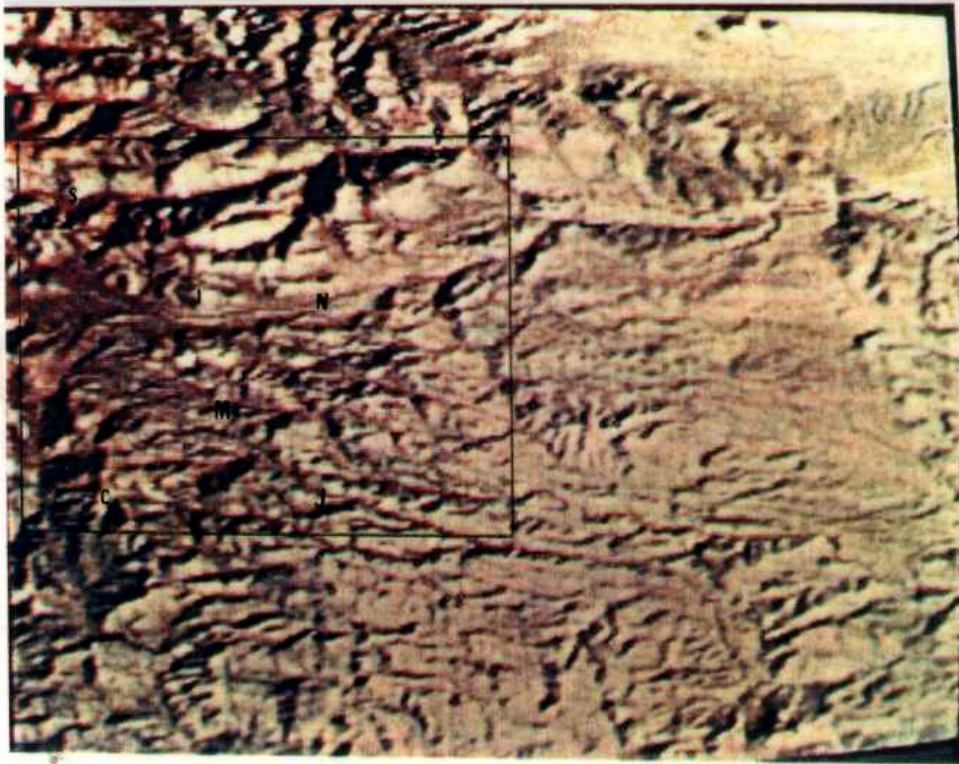
Foruria (1984) used X-ray diffraction analyses to detect zoned argillic alteration products across the Pankey fault in the Pankey Mine area. This work indicates a narrow kaolinized zone in the central part of the fault surrounded by an illite zone, and an outer smectite zone. The alteration along the Pankey vein is similar to zones detected across the vein exposed at the Taylor shaft. The width of the altered zone in densely welded Vicks Peak Tuff forming walls along the Pankey vein is much narrower than that detected in more permeable moderately to poorly welded tuff surrounding the Taylor shaft.

Argillic alteration and silicification in the Pankey vein and the vein exposed at the Taylor shaft are attributed to dynamic processes of boiling, secondary pyrite oxidation, and the action of near-surface sulfur-oxidizing bacteria (Buchanan, 1981; Crone and others, 1984; Schoen and others, 1973). Barren, vein-like silicic residues of silicified ash-flow tuff in the study area, such as those exposed in the south-facing slope of Nogal Canyon and in the west-facing slope northeast of Milliken Park, appear to have been formed by supergene alteration along fractures. Wall rocks surrounding these silicic ribs are not hydrothermally altered as they are around mineralized quartz veins attributed to hypogene mineralization.

LANDSAT IMAGERY

Vincent and Rouse (1977) used Landsat data and various techniques of spectral classification in exploration for a copper porphyry deposit in the southern San Mateo Mountains of Socorro county, New Mexico. Although their work revealed the anomalous argillic-ferric alteration in the region surrounding the study area, copper mineralization was not found so the area was deemed to be "economically unimportant".

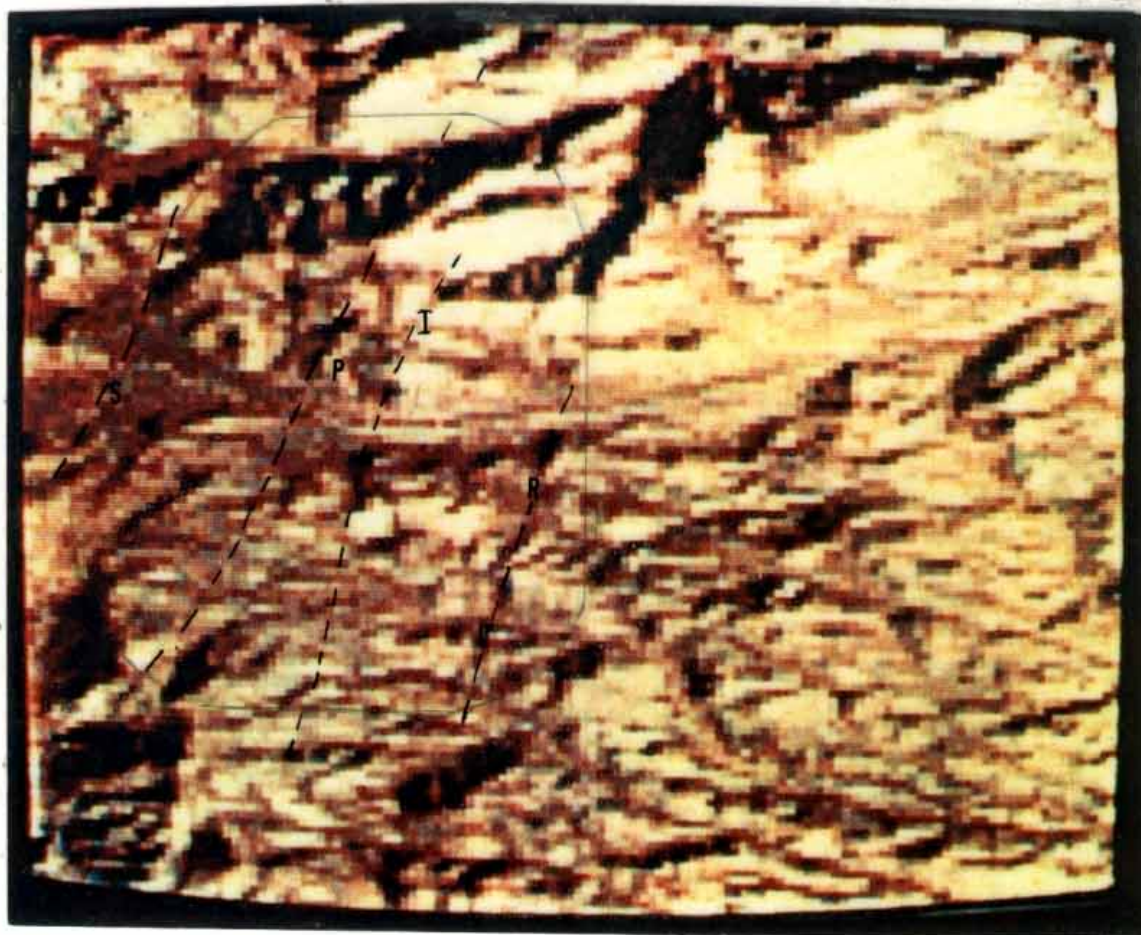
The color composite images of the southeastern San Mateo Mountains, reproduced in Figures 6a, b, and c, were taken May 17, 1973 from the Landsat-1 satellite multi-spectral scanner system (MSS). These images have a spacial resolution of approximately 259 x 187 feet (78 x 56 m), and a four channel spectral range of 0.5 to 1.1 m designated as bands 1, 2, 3, and 4. The images shown in this report were obtained with the Remote Image Processing System (RIPS), and microprocessor-based analysis software developed by the Earth Resources Observation Systems (EROS) Data Center. The images were photographed from a color monitor.



Approximate scale: 1 inch = 1.9 miles



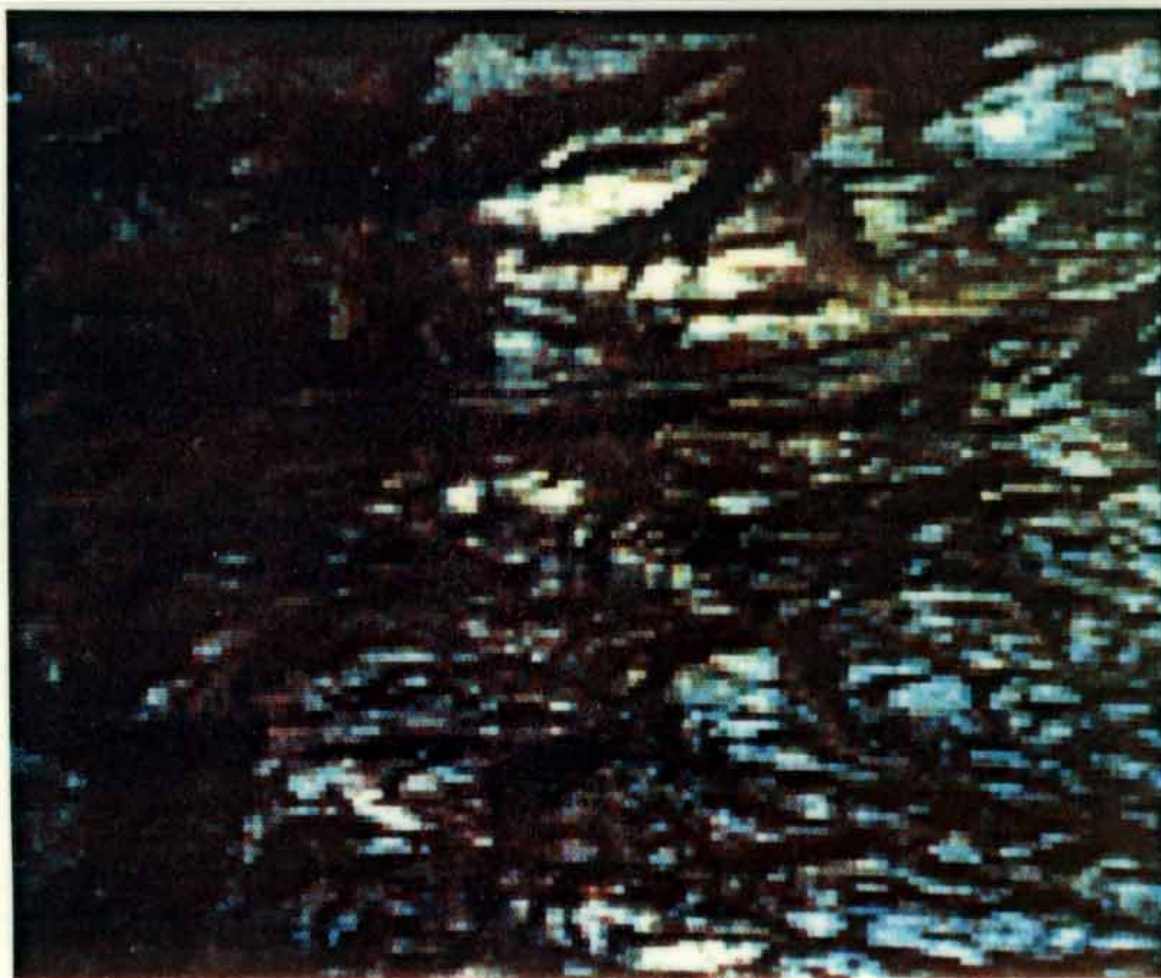
Figure 6a. A Landsat-1 frame of approximately 71 square miles (185 km^2) on the southeast flank of the San Mateo Mountains. The locations of Springtime Canyon (S), Nogal Canyon (N), San Jose Arroyo (J), Casa Grande peak (C), Indian Peak (I), and Milliken Park (M) are shown. The blocked-in area in the figure is enlarged, enhanced, and reproduced in Figures 6b and c.



Approximate scale: 1 inch = .81 miles



Figure 6b. The locations of the study area and positions of major northwest trending faults including branching traces of the Rock Spring fault (S), the Pankey fault (P), the Indian Peak fault (I), the Rhyolite fault (R), and cross-cutting east-west linear features in the area.



Approximate scale: 1 inch = .81 miles



Figure 6c. A ratioed false color composite with a scale similar to 6b, produced with ratioed bands displayed as 1/2 (red), 2/4 (green), and 3/4 (blue).

Figures 6a, and b were produced with channels designated as 1 (blue), 2 (green), and 4 (red). This combination shows the structural grain of the area while minimizing the effects of vegetation and shadows. Color differences reflect differences in lithology, vegetation, aspect, and slope which darken the image especially in the western part of the study area. The band ratios used to produce Figure 6c were used by Rowen and others (1974) to discriminate similar hydrothermally altered zones in southern Nevada. The white, yellow, and blue colored areas (pixels) in Figure 6c generally correspond to argillic-ferric zones in the study area. The low spectral and spacial resolution, and the effects of slope and aspect limit the usefulness of the Landsat data in exploration.

ECONOMIC GEOLOGYHistory of the San Jose Mining District

A prospector named Johnson reportedly discovered gold in Springtime Canyon around 1900 (North, 1983). The area remained inactive until the summer of 1931 when Tom Hellyer rediscovered high-grade ore at the Pankey vein in the northern part of the area known as the San Jose Mining District (sometimes included in the San Mateo Mountain Mining District) (Lasky, 1932). The district produced approximately \$33,000 worth of gold and silver between 1932 and 1941, a period in which gold prices remained stable at \$20.67 per fine ounce troy until 1934 when the price rose to \$35.00 per ounce, and while generally rising silver prices averaged about \$.60 per fine troy ounce (US Bureau of Mines Mineral Yearbooks, 1933-1941). Three train cars of ore shipped from the area by Nogal Mines, Inc. to the El Paso smelter in 1932 brought \$8.64 per ton, and equally weighted samples taken from all the veins in the San Jose Mining District averaged \$5.00 per ton (Lasky, 1932).

Reported production for the San Jose Mining District indicates that approximately 888 troy ounces of gold and 12,917 troy ounces of silver were produced from 1932 to 1941 (North, 1983). The Pankey Mine and to a lesser extent the Rhyolite mine were the primary producers. Three lode mining

claims, shown in Figure 1, were patented along and adjacent to the Pankey vein in Springtime Canyon. The northern and western borders of these patented claims lie on the southern boundary of the Apache Kid Wilderness. Mineralization of gold and silver occurs in the wilderness along the northern extensions of the Pankey and Rhyolite faults (Foruria, 1983).

Description of Ore Deposits and Distribution of Mineralization

The Pankey Mine (also known as the Nogal Mine) is located in section 29, T. 8 S., R. 5 W. along the Pankey vein in the northern part of the San Jose Mining District. The mine consists of a 555 foot adit which is stoped to the surface along part of its length, a 30 foot raise, and two winzes measuring 75 and 19 feet. Lasky (1932) reported the ore produced at the Pankey Mine during the 1930's was composed of cryptocrystalline, banded, cockade, and comb-structured quartz containing native gold and silver, cerargyrite, and silver sulphosalts, limonite, pyrite, and calcite. Lasky also reported minor occurrences of copper mineralization, black manganiferous calcite, and fluorite.

The USGS wilderness mineral survey by Neubert (1983) gives analyses of 12 chip samples taken in the Pankey Mine reported to contain as much as 0.146 ounces per ton (4.54 ppm) of gold, and 6.0 ounces per ton (186.62 ppm) of silver. Lasky (1932) reported that limonitic ore produced from the

Pankey Mine averaged 0.225 ounces per ton (7.00 ppm) gold, and 10.50 ounces per ton (326.58 ppm) silver. The southern extension of the Pankey fault splits and intersects other faults and fracture systems in the study area forming brittle fracture zones. Samples from these zones contain anomalous gold and silver values.

Mineralized zones in the vicinity of the Rhyolite Mine and along San Jose Arroyo are located about 3.5 miles south of the Pankey Mine in sections 7, 17, and 18, T. 9 S., R. 5 W. The adit of the Rhyolite Mine and other workings in the San Jose Arroyo to the north are presently blocked by fallen rock at the base of steep canyon walls (Plate 15). A map of the Rhyolite Mine showing sample locations, and analyses by Neubert (1983) is reproduced in Appendix III. The mine consists of about 225 feet of drifts and cross-cuts, and 50 feet of shafts and winzes. Neubert (1983) reported that one sample from the mine, composed of hydrothermally altered, gougy breccia stained by iron oxide contained 0.17 ounces per ton (5.29 ppm) gold, and 0.06 ounces per ton (1.87 ppm) silver.

Neubert (1983) reported that an undisclosed number of samples taken in the central part of the San Jose Mining District contained no detectable gold or silver. More recent sampling and analyses in the area however show substantial gold and silver values in some mineralized zones, and widespread anomalous concentrations of Au, Ag, As, Hg,

and Sb. Results of analyses for Au, Ag, As, Hg, Sb, Pt, Cu, Pd, Zn, Mo, Be, Nb, and La reported by the USGS, US Bureau of Mines, and Foruria (1984), and analyses provided by the current owners of the Apache claims are listed in Appendix IV. Sample locations are shown in Figure 11.

A 25 foot exploration adit and a caved-in shaft are located in section 5, T. 9 W., R. 5 S., within a broad mineralized zone along branching traces of the Rhyolite fault near where it intersects the San Jose fault (Plate 16). Moderately welded Vicks Peak Tuff in the area is extensively brecciated, silicified, and altered below caprocks composed of the tuff unit of Milliken Park. Silica infilling in matrix supported quartz breccias commonly contains fine-grained pyrite and hematite (Plates 17a, b). Samples from the area contain up to 0.30 ounces per ton (9.33 ppm) gold and 0.20 ounces per ton (6.22 ppm) silver.

A 90 foot exploration shaft is located in section 7, T. 9 W., R. 5 S., less than one mile north of the Rhyolite Mine, in an area known as Milliken Park. Mineralized rocks in the area are intensely fractured where the Rhyolite fault intersects east-west and north-northwest trending faults. Brecciated walls of the shaft, composed of the upper interval of Vicks Peak Tuff, are silicified, argillically altered, and stained by limonite and wad. Chip samples taken at 30 foot intervals in the shaft, ran 0.02 to 0.03 ounces per ton (0.62 - 1.00 ppm) gold and up to 0.32 ounces per ton (10.02

ppm) silver. One exceptional sample, taken along the Rhyolite fault at a silicified breccia pipe located approximately 400 feet north of the exploration shaft, ran 0.48 ounces per ton (14.93 ppm) gold, and 0.40 ounces per ton (12.44 ppm) silver. Lasky (1932) reported that samples taken in Milliken Park in 1929 averaged \$3.00 per ton.

The Taylor exploration shaft is located along a north-west trending vein in the west-central part of section 5, T. 9 W., R. 5 S., about one quarter mile south of Nogal Canyon. The vein fills a down-to-the-west normal fault striking N. 25 W., dipping 65 degrees west. The shaft, which is about 20 feet deep, exposes a 6 foot wide brecciated quartz vein containing successive generations of intergrown, microcrystalline, banded, crustified, white, gray, black manganiferous, and amethystine quartz. Lamellar and hackly textures indicate calcite dissolution (Plate 18). The broad silicified zone bordering the vein is argillically altered and stained by limonite and wad.

Samples from the Taylor vein have run up to 0.75 ounces per ton (23.33 ppm) gold, and 5.60 ounces per ton (174.18 ppm) silver (Foruria, 1984). A standard 48 hour bottle-roll cyanide leach test of a 15 pound dump sample indicated better than 75% extraction of gold from oxidized ore assayed at 0.05 ounces per ton (1.56 ppm) gold. Panning loosely consolidated material from the central part of the vein has produced several gold micronuggets.

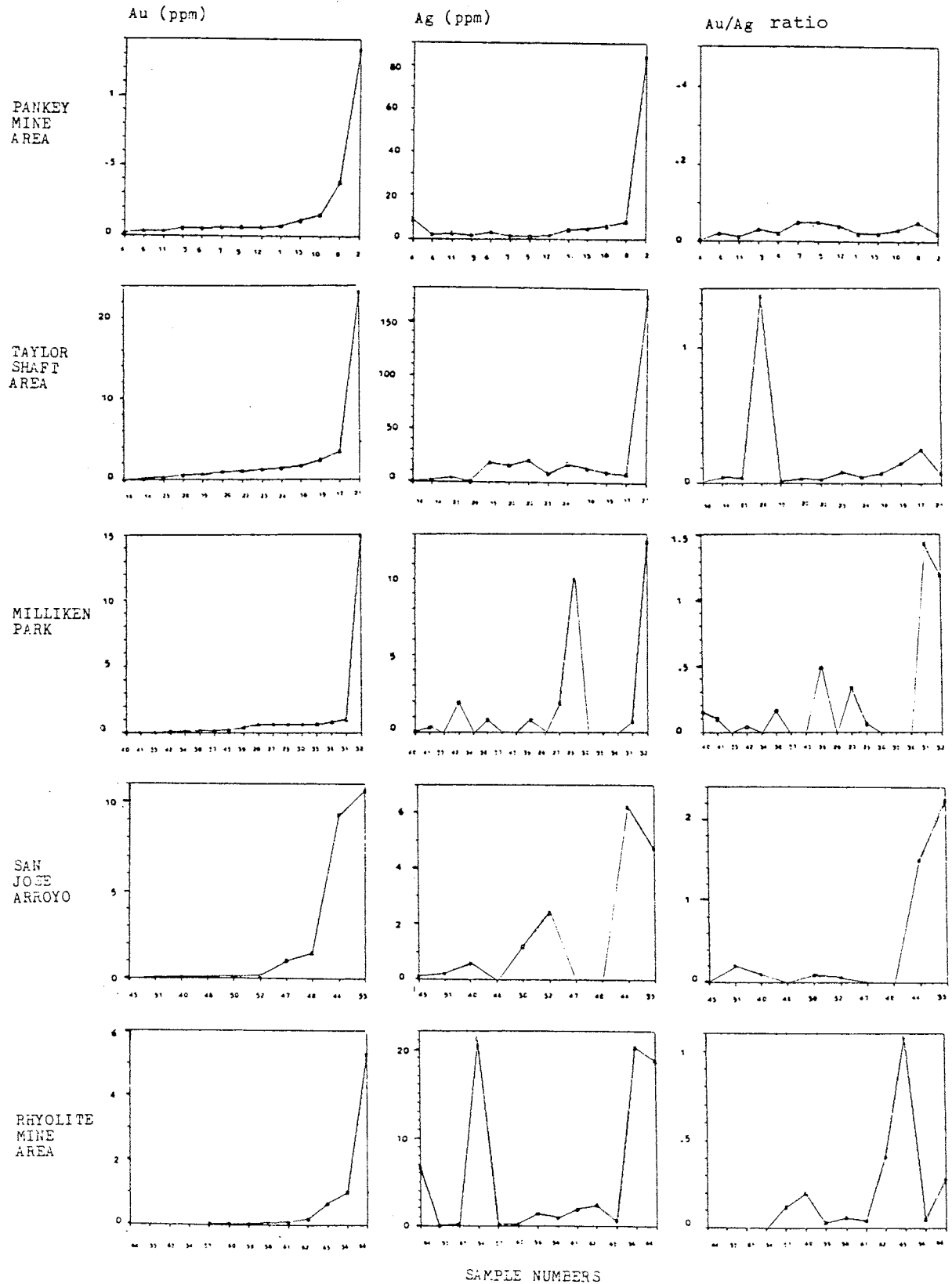
Table 2 shows the mean (average), range (difference between the highest and lowest values), and standard deviation for Au, Ag, As values (ppm), and Au/Ag ratios calculated from geochemical analyses of samples taken in five mineralized zones in the study area. Samples groups taken south of Nogal Canyon have higher average Au values, Au/Ag ratios, and standard deviation of Au/Ag ratios than samples taken in the Pankey Mine area. Wall rocks surrounding the Pankey vein are not as brecciated or altered as rocks sampled in the other mineralized zones. Figure 7 shows the variability of geochemical analyses for gold and silver in the samples. Plotted Au and Ag values from the Pankey Mine area samples show a close correlation so that the Au/Ag ratio plot is flat compared to plotted values from other areas.

Table 2. Mean (average), range (difference between the highest and lowest values), and standard deviation for Au, Ag, and As values (ppm), and Au/Ag ratio from five sample groups taken in mineralized zones in the study area.

(Conversion: 31.103 ppm = 1 troy ounce per ton)

<u>Deposit name</u>		Au	Ag	As	Au/Ag ratio
Pankey Mine area	mean	.18	10.04	5.63	.03
	range	1.31	83.10	15.00	.05
	std. dev.				.03
Taylor shaft area	mean	3.04	22.07	14.96	.35
	range	23.20	172.80	7.81	2.44
	std. dev.				.73
Milliken Park area	mean	1.24	3.20	2.54	.44
	range	14.90	12.24	6.41	1.16
	std. dev.				.47
San Jose Arroyo area	mean	2.54	2.21	3.97	.70
	range	10.60	6.13	5.93	2.14
	std. dev.				1.12
Rhyolite Mine area	mean	.82	5.73	3.63	.25
	range	5.26	21.13	6.00	1.04
	std. dev.				.50

Figure 7. Plotted Au, Ag, and Au/Ag ratio values of samples taken in five mineralized zones in the study area. Samples are listed in order of increasing Au content so that proportional variations are evident.



Analyses of outcrop samples for arsenic, mercury, and antimony indicate anomalies of these elements in zones containing relatively high values of gold and silver, but a clear correlation is not evident. Arsenic ranged from less than 1.0 - 29.0 ppm in twenty-six samples averaging 7.68 ppm As. Of twenty-three samples analysed for mercury, seven were anomalous containing 0.05 - 0.30 ppm Hg. Little variation in antimony was evident in twenty-three outcrop samples which ranged from 0.5 - 7.00 ppm and averaged 1.24 ppm.

Five samples were analysed for gold, silver, platinum, palladium, copper, lead, zinc, molybdenum, arsenic, antimony, and bismuth using a multi-element plasma emission spectrometer. Results from these analyses indicate anomalous concentrations of Pt, As, Cu, Pb, and Zn occur together in mineralized samples. It appears that these metals are concentrated in the fine-grained argillic-ferric fraction of sample separates because their concentrations are significantly reduced in the panned coarse-grained fraction.

Griffitts and others (1971) determined spectrographically detectable concentrations of gold, silver, antimony, beryllium, niobium, lanthanum, molybdenum, zinc, and other elements in magnetically concentrated stream sediment samples in the San Jose Mining District. This sampling was limited to the southern part of the study area. Nonmagnetic concentrates with specific gravities greater than bromoform, obtained from samples collected along faults around Casa

Grande peak, contained more than 500 ppm Au, up to 5000 ppm Ag, up to 150 ppm Be, and between 100 and 150 ppm Sb. More than 500 ppm Nb, and 100 ppm to more than 1000 ppm La were detected in magnetic sediment concentrates sampled outside of altered zones.

DISCUSSION AND CONCLUSIONS

The Nogal Canyon Caldera was proposed by Deal and Rhodes (1976) based on reinterpretation of maps by Furlow (1965) and Farkas (1969), and other reconnaissance mapping in the southern San Mateo Mountains. The proposed caldera boundary, outlined by Chapin (1983), follows a circular trace apparent on satellite imagery. More recent geologic investigation indicate the caldera is broader and more complex than previously suspected. The area contains multiple structural blocks bordered by faults and fracture traces. Late-stage intrusive rocks are exposed along large-scale fracture traces outside the study area interpreted to be caldera ring-fractures (Hermann, unpubl.; Deal and Rhodes, 1976).

The San Jose Mining District is situated in a complexly fractured area along the base of the southeast slope of Vicks Peak. Fracturing in the area include down-to-the-west rotational normal faults that began to form during early eruptive phases of the Nogal Canyon Caldera volcanic sequence. Later volcanotectonic activity and down-to-the-east extensional subsidence east of Vicks Peak produced cross-cutting northwest to east-west trending faults and fracture systems. Areas between Nogal Canyon and the San Jose Arroyo have experienced more subsidence than adjacent blocks.

Fracturing in the study area appear to have been intensified during the emplacement of locally exposed silicic intrusive rocks. Further collapse in areas partially capped by the tuff unit of Milliken Park is attributed to repeated hydrothermal venting in the foot wall of the Rhyolite fault. Similar late-stage volcanotectonic activity is associated with resurgence, subsidence, and epithermal mineralization in the Silverton Caldera of the San Juan volcanic field, Colorado (Steven and Lipman, 1976).

Brittle fracture zones provided structural control for late-stage silicic intrusive rocks and hydrothermal vent systems associated with vein, stockwork, breccia-pipe, and disseminated epithermal deposits in the study area. Widespread argillic-ferric alteration and more localized gold-silver mineralization occur in permeable host rocks below dense flow units of Vicks Peak Tuff, Springtime Canyon Quartz Latite, and the tuff unit of Milliken Park. Mineralized zones at the Pankey and Rhyolite mines are hosted by fractured, moderately welded zones of the upper interval of Vicks Peak Tuff. Light-colored, partially welded zones of the upper interval are mineralized in San Jose Arroyo, Milliken Park, and surrounding the Taylor shaft.

Epithermal Au-Ag deposits associated with low-pH alteration zones, brecciation, and banded quartz veins in similar volcanic settings are attributed to repeated subsurface boiling and hydrothermal eruption initiated by

fracturing and decreased fluid pressure within 1000 feet below the surface (Boyle, 1979; Buchanan, 1981; Robinson and Norman, 1984; Hedenquist and Henley, 1985; Nelson and Giles, 1985). In this process gold, silver, and associated trace elements carried in solution are precipitated as volatile components including CO_2 and H_2S are released from boiling solutions, as the pH, $f(\text{O}_2)$, and K^+/H^+ in remaining fluids increase, and as the temperature decreases.

Acidic hypogene fluids, formed as volatiles liberated during boiling condense in ground water, react with host rocks to produce a distinct assemblage of low-pH alteration products in mineralized zones (Buchanan, 1981). This assemblage includes adularia, illite, and kaolinite which are produced as boiling fluids become increasingly alkaline in active hydrothermal systems studied in New Zealand (Browne, 1978). Advanced argillic alteration and silicification in some permeable zones appear to be produced by supergene acidic fluids. These fluids can be formed by secondary pyrite oxidation and near-surface sulfur-oxidizing bacteria (Crone and others, 1984; Schoen and others, 1973).

Vertical zonation of alteration products detected in brecciated samples from the 90 foot shaft in the Milliken Park area indicates subsurface boiling. The low-permeable zone at the 60 foot level containing relatively high amounts of illite (sericite and hydromica inclusive), smectite, mixed-layer clays, and quartz is similar to alteration

assemblages which form above active boiling zones in New Zealand (Hedenquist and Henley, 1985). This type of self-sealing alteration cap occurs above fossil boiling zones producing precious-metal deposits of the Creede Mining District of Colorado (Robinson and Norman, 1984).

Calcite dissolution, intensified argillic alteration, and silicification in the central part of the Taylor shaft vein are attributed to repeated pulses of hypogene fluids and influx of supergene fluids. X-ray diffraction analyses indicate an inverse relationship between albite and potassic alteration products in mineralized zones. It appears that albite content is comparatively low in the mineralized quartz-rich part of the vein. Alunite and limonite in mineralized zones form as by-products of pyrite oxidation (Boyle, 1979; Blanchard, 1968). Narrow veins of hematite and broad hematitic zones in the study area may have precipitated as chemically distinct shallow oxidized water mixed with hypogene fluids during thermal collapse of hydrothermal systems (Cole and Ravinsky, 1984; Blanchard, 1968). Manganese mineralization appears to have formed late in hypogene and supergene processes.

Widespread, near-surface anomalies of Au, Ag, and associated trace elements have been detected in the San Jose Mining District (Figure 11). Trace amounts of Au, carried in chloride-sulfide complexes can be adsorbed by charged argillic alteration products to produce anomalous haloes

surrounding epithermal gold deposits (Hausen and Kerr, 1968; Boyle, 1979). Boyle (1979) suggests gold transported in solution as Au-As-S and Au-Sb-S complexes can be incorporated into pyrite by replacement.

Analyses of five groups of samples indicate variable proportions of Au and Ag occur in mineralized zones in the study area. Comparatively high Au values and Au/Ag ratios appear to be related to repeated hydrothermal discharge and recharge which resulted in brecciation and alteration. Increased Au/Ag ratios in mineralized zones may have resulted from secondary depletion of silver.

Samples taken in mineralized zones containing high Au and Ag values generally were also anomalous in As, Hg, and Sb. These elements are believed to precipitate together in oxidizing near-surface conditions (Buchanan, 1981). Boyle (1979) has found that there is a marked coherence between Au and As during both hypogene and supergene processes, and As values generally increase approaching enriched gold deposits. Volatile Hg can be separated during boiling and precipitated in the zone of condensation surrounding ore deposits (White and others, 1971).

Preliminary emission spectrometric analyses show interesting anomalous concentrations of platinum and palladium. This data require confirmation by other analytical methods such as neutron activation analyses. Trace amounts of platinum-group metals may be carried by ferromagnesian

minerals destroyed by vapor-phase and hydrothermal processes. Goldschmidt (1954) suggests that platinum group metals can replace Fe in hydrothermal sulfides, arsenides, and oxides.

Practical Features for Exploration

Recent geologic mapping and reconnaissance within the proposed boundaries of the Nogal Canyon Caldera indicate structural blocks in the area have been differentially uplifted and lowered during episodic volcanotectonic activity. Repeated faulting and hydrothermal activity are associated with widespread ferric-argillic alteration and more localized epithermal mineralization. Interpretation of aerial photography and satellite imagery is useful in determining the extent of alteration and delineating major structural features associated with gold-silver deposits in the area.

Zones within the upper interval of Vicks Peak Tuff are the main host rocks for known deposits in the San Jose Mining District. Gold and silver deposits occur within a generally northeast trending fracture zone along the southeast slope of Vicks Peak. Epithermal mineralization is associated with late-phase silicic intrusive rocks which are locally exposed along intersecting faults and fracture systems. Brecciated zones along cross-cutting fracture traces in the area are commonly covered by alluvium, col-

luminium, talus, and hydrothermally altered cap rocks.

Deposits of gold and silver are surrounded by broad alteration haloes containing hydrothermal alteration products associated with boiling. These minerals can be detected in petrographic thin-sections and by X-ray diffraction analyses. Assemblages of low-pH alteration products detected in closely-spaced surface and subsurface samples reflect the extent of hydrothermal activity in mineralized zones.

Relatively high values of Au/Ag are associated with deposits containing comparatively high Au. Similar stockwork and disseminated Au-Ag deposits, associated with anomalous concentrations of As, Hg, and Sb, are thought to form between 100 and 1000 feet below the surface (Buchanan, 1981; Hedenquist and Henley, 1985). Massive sinter deposits which commonly cap similar near-surface epithermal deposits are notably absent in the study area indicating some erosion has occurred since hot springs were active.

Four directional exploration holes, drilled with a reverse circulation rotary drill, were completed during the summer of 1985 in the study area. Unfortunately analyses from bulk samples taken at five foot intervals are not yet available. Further sampling and analyses in altered breccia zones associated with locally exposed intrusive rocks may lead to new drilling targets outside known mineralized zones. Promising areas for continued exploration are shown in Figure 3.

Selected Bibliography

- Atwood, G., 1982, Geology and Geochemistry of the San Juan Peak Area, San Mateo Mountains, Socorro County, New Mexico: with special reference to the geochemistry, mineralogy, and petrogenesis of an occurrence of riebeckite-bearing rhyolite; (MS Thesis) Albuquerque, University of New Mexico, 156 p.
- Blanchard, R., 1968, Interpretation of Leached Outcrops: Nevada Bureau of Mines, Bull. 66, 196 p.
- Bornhorst, T.J., Jones, D.P., Elston, W.E., Damon, P.E., Shafrigullah, M., 1982, New radiometric ages on volcanic rocks from the Mogollon-Datil volcanic field, south western, New Mexico, Isochron/West no. 35, p. 13-15.
- Boyle, R.W., 1979, The geochemistry of gold and its deposits (together with a chapter on geochemical prospecting for the element): Geol. Surv. Canada, Bull. 280, p. 584.
- Brindley, G.W. and Brown, G., 1980, X-ray Diffraction Procedures: Crystal structures of clay minerals and their X-ray identification, published by the Mineralogical Society, London, p. 305-360.
- Browne, P.R.L., 1984, Hydrothermal alteration in active geothermal fields: Ann. Rev. Earth Planet. Sci. v.6, p. 229-250.

- Buchanan, L.J., 1981, Precious Metal deposits associated with Volcanic Environments in the Southwest: Arizona Geological Society Digest, v. XIV, Relations of Tectonics to Ore Deposits, Southern Cordillera, p. 237-262.
- Carrol, D., 1970, Clay Mineralogy: A guide to their X-ray identification: Geologic Society of America, Special Paper, no. 126, vol. vii, 80 p.
- Chapin, C.E., 1983, Selected Tectonic Elements of the Socorro Region: New Mexico Geol. Society Guidebook--34th Field Conference, Socorro Region II, p. 97-98.
- Conrad, W.K., Kay, M.K., Kay, R.W., 1983, Magma Mixing in the Aleutian Arc: Evidence from cognate inclusions and composite xenoliths: Jour. Volcanol. Geotherm. Res., v. 18, p. 279-295.
- Crone, W., Larson, L.T., Carpenter, R.H., Chao, T.T., and Sanzolone, R.F., 1984, A comparison of iron oxide-rich joint coatings and rock chips as geochemical sampling media in exploration for disseminated gold deposits: Journal of Geochemical Exploration, v. 20, p. 161-178.
- D'Andrea-Dinkelman, J.F., Lindley, J.I., Chapin, C.E., and Osburn, G.R., 1983, The Socorro K_2O anomaly: A Fossil geothermal system in the Rio Grande rift: New Mexico Geologic Society Guidebook--34th Field Conference, Socorro Region II, p. 76-77.

- Deal, E.G., 1973, Geology of the Northern Part of the San Mateo Mountains, Socorro County, New Mexico: A study of a rhyolite ash-flow cauldron and role of laminar flow in ash-flow tuffs; (PhD Dissert.) Albuquerque, University of New Mexico, 136 p.
- Deal, E.G. and Rhodes, R.C., 1976, Volcano-Tectonic Structure in the San Mateo Mountains, Socorro County, New Mexico; Cenozoic Volcanism in New Mexico, New Mexico Geological Society Special Publication No. 5, p. 51-56.
- Eggleston, T.L., 1982, Geology of the central Chupadera Mountains, Socorro county, New Mexico: (MS Thesis) Socorro, New Mexico Institute of Mining and Technology, 155 p.
- Elston, W.E., 1978, Mid Tertiary Cauldrons and Their Relationship to Mineral Resources in S.W. New Mexico: Field Guide to Selected Cauldrons and Mining Districts of the Datil-Mogollon Volcanic Field, New Mexico: New Mexico Geologic Society Special Publication No. 7, p.
- Farkas, S.A., 1969, Geology of the Southern San Mateo Mountains, Socorro and Sierra Counties, New Mexico; (PhD Thesis) Albuquerque, University of New Mexico, 137 p.
- Foruria, J., 1984, Geology of part of the southern San Mateo Mountains, Socorro and Sierra Counties, New Mexico; (MS Thesis) Fort Collins, Colorado State University, 140 p.

- Ferguson, C.A., 1985, Geology of the East-central San Mateo Mountains, Socorro County, New Mexico: (MS Thesis) Socorro, New Mexico Institute of Mining and Technology, (in preparation).
- Furlow, J.W., 1965, Geology of the San Mateo Peak area, Socorro County, New Mexico; (MS Thesis) Albuquerque, University of New Mexico, 83 p.
- Goldschmidt, V.M., 1954, Geochemistry: The Platinum Metals; Hydrothermal Deposits: Oxford University Press, London, p. 675-677.
- Griffitts, W.R., Alminas, H.V., and Mosier, E.L., 1971, Analyses and distribution of Pb, Sn, Sr, La, Ag, Be, Zn, Sb, Mo, Nb, and Au within the Vicks Peak, Steel Hill, and Black Hill quadrangles, New Mexico: US Geological Survey Open-File Reports; 71-129 through 71-137.
- Hausen, D.M. and Kerr, P.F., 1968, Fine gold occurrences at Carlin, Nevada; in Ore Deposits of the US: AIME, p. 908-940.
- Hedenquist, J.W. and Henley, R.W., 1985, Hydrothermal eruptions in the Waiotapu Geothermal System, New Zealand: Their Origin, Associated Breccias and Relation to Precious Metal Mineralization: Econ. Geol., v. 80, p. 1640-1668.

- Kedzie, L.L., Sutter, J.F., Chapin, C.E., 1984, High-precision $^{40}\text{Ar}/^{39}\text{Ar}$ age of widespread Oligocene ash-flow tuff sheets near Socorro, New Mexico (abs): Geol. Soc. of America, abstracts with programs.
- Kelley, V.C. and Furlow, J.W., 1965, Lower Paleozoic wedge edges in south-central New Mexico: Geol. Soc. of America, Bull., v.76, p. 689-694.
- Kottlowski, F.E., 1963, Paleozoic and Mesozoic Strata of Southwest and South-Central New Mexico: New Mexico Bureau of Mines and Mineral Resources, Bull. 79, 100 p.
- Lasky, S.G., 1932, The Ore Deposits of Socorro County, New Mexico: New Mexico Bureau of Mines and Mineral Resources Bull. 8, p. 93-118.
- Lipman, P.W., 1984, The Roots of Ash-Flow Calderas: Windows into the tops of Granitic Batholiths: US Geological Survey, (in press).
- Maldonado, F., 1974, Geology of the northern part of the Sierra Cuchillo, Socorro and Sierra Counties, NM: (M.S. Thesis) Albuquerque, University of New Mexico, p. 60.
- Meyer, C. and Hemley, J.J., 1967, Wall Rock Alteration: in Geochemistry of Hydrothermal Ore Deposits; NY, Holt, Rinehart, and Winston, p. 166-235.
- Nelson, C.E. and Giles, D.L., 1985, Hydrothermal Mechanisms and Hot Spring Gold deposits: Econ. Geol., v. 80, p. 1633-1639.

- Neubert, J.T., 1983, Mineral Investigations of the Apache Kid and Withington Wilderness area, US Geological Survey open-file report p. 5-83.
- North, R.M., 1983, History and Geology of the Precious Metal Occurrences in Socorro County New Mexico: New Mexico Geological Society Guidebook--34th Field Conference, Socorro Region II, p. 261-268.
- Osburn, G.R., 1978, Geology of the eastern Magdalena Mountains, Water Canyon to Pound Ranch: (MS Thesis) New Mexico Institute of Mining and Technology, 150 p.
- Osburn, G.R., 1984, Ash-flow tuffs of northeast Mogollon-Datil volcanic field; in New Mexico Geology: New Mexico Bureau of Mining and Mineral Resources, vol. 6, no. 1, p. 10-12.
- Osburn, G.R. and Chapin, C.E., 1983, Nomenclature for Cenozoic Rocks of Northeast Mogollon-Datil volcanic field, New Mexico: Stratigraphic Chart 1, New Mexico Institute of Mining and Technology, Socorro, NM.
- Osburn, G.R. and Chapin, C.E., 1983, Ash-Flow Tuffs and Cauldrons in the Northeast Mogollon-Datil Volcanic Field: A Summary: New Mexico Geological Society Guidebook--34th Field Conference, Socorro Region II, p. 197-204.

- Rendu, J-M, 1984, Geostatistical methods of ore reserve estimation (Review Articles): Mining Geology, Jour. Soc. of Mining Geologists of Japan, v. 37 (3), p. 197-224.
- Robinson, R.W. and Norman, D.I., 1984, Mineralogy and fluid inclusion study of the southern Amethyst vein system, Creede Mining District, Colorado: Econ. Geol., v. 72, p. 439-447.
- Ross, C.T., and Smith R.L., 1961, Ash-flow tuffs--Their origin, geologic relations, and identification: US Geological Survey, Prof. Paper 366, 81 p.
- Rowen, L.C., Wellaufer, P.H., Goetz, A.F.H., Billingsley, F.C., and Stewart, J.H., 1974, Discrimination of rock types and detection of hydrothermally altered areas in south-central Nevada by the use of computer enhanced ERTS images: US Geological Survey Prof. Paper 883, 35 p.
- Schoen, R., White, D.E., and Hemley, J.J., 1973, Argillation by descending acid at Steamboat Springs, Nevada: Clays and Clay Minerals, Pergamon press, vol. 22, p. 1-22.
- Siemers, W.T., 1983, The Pennsylvanian System, New Mexico: Stratigraphy, Petrology, Depositional Environments: New Mexico Geologic Society Guidebook, 34th Field Conference, Socorro Region II, p. 147-155.
- Smith, R.L., 1960, Zones and zonal variations in welded ash-flow tuffs: US Geological Survey, Professional paper 354-F, 15 p.

- Smith, R.L. and Bailey, R.A., 1968, Resurgent Cauldrons: Geological Society of America Memoir 116, p. 613-622.
- Sparks, R.J., Sigurdsson, H., and Wilson, L., 1977, Magma mixing: a mechanism for triggering acid explosive eruptions: *Nature*, v. 267, p. 315-320.
- Steven, T.A. and Lipman, P.W., 1976, Calderas of the San Juan volcanic field, southwestern Colorado: US Geological Survey Prof. Paper 958, 35 p.
- Travis, R.B., 1955, Classification of Rocks: Colorado School of Mines Quart., Vol. 50, no. 1, 98 p.
- United States Bureau of Mines Mineral Yearbooks, 1933-1941, Gold, silver, copper, lead, and zinc in New Mexico; Appendices and reviews by Henderson, C.W., and Martin, A.J.
- Vincent, R.K., and Rouse, G., 1977, Landsat detection of hydrothermal alteration in the Nogal Canyon Cauldon, New Mexico: Internat. symposium remote sensing environment, 11th Ann Arbor, April 25-29, p. 579-590.
- Walker, C.W., Renault, J.R., 1972, Determinative Tables of $2\theta_{Cu}$ and $2\theta_{Fe}$ for Minerals of Southwestern US: Circular 127, NM State Bureau of Mines and Mineral Resources.
- White, D.E., Muffler, J.P., and Truesdell, A.H., 1971, Vapor-Dominated Hydrothermal Systems compared with Hot-Water Systems: *Econ. Geol.*, v. 66, p. 75-97.

Appendix I: Sample preparation and procedures for semi-quantitative X-ray analyses (Caroll, 1970; Brindley and Brown, 1980). Reproduced X-ray diffraction traces also included.

Three groups of samples weighing 400 to 600 grams were collected in the field and crushed into fragments less than 0.5 inches in diameter with a jaw crusher. A portion of the crushed samples composed of fine- to coarse-grained aggregates was stirred and agitated in beakers containing distilled water. The water suspensions were then left to stand for 10 minutes. Small portions were then drawn off the top with an eye dropper, dripped on to a glass slide, and left to evaporate at room temperature. This procedure produces sample slides surfaced by phyllosilicate minerals less than 2 microns in diameter with C axes oriented perpendicular to the slide.

Untreated sample slides were first run from 40 to 2 degrees 2θ in the XRD, then placed in a container of vaporous ethylene glycol for 12 hours and re-run from 13 to 2 degrees 2θ . Some of these samples were successfully heated to more than 350 degrees centigrade for 30 minutes and re-run from 10 to 8 degrees 2θ while still hot. X-ray diffraction reflection traces from each run were used to estimate comparative amounts of major clay groups and other detected minerals.

Kaolinite group minerals in sample slides produced commonly sharp, relatively intense K_1 (001) basal reflections centering near 12.4 degrees 2θ , and K_2 (002) reflections at 24.9 degrees 2θ . Some samples showed comparatively broad, weak K_1 and K_2 peaks indicating a lower degree of crystallization. Illite was recognized by commonly diffuse I_1 (001) and I_2 (002) basal reflections centering near 8.8 and 17.7 degrees 2θ . Smectite produced commonly diffuse S_1 (001) basal reflections between 5.2 and 7.1 degrees 2θ which shifted position in glycolated, and heated samples (Walker and Renault, 1972). Randomly-stratified mixed-layer clays produced irregular basal reflections which shifted positions in glycolated and heated samples indicating disordered structures composed of interlayered illite and smectite (Brindley and Brown, 1980). Representative intensities of peaks for quartz (26.6 degrees 2θ), orthoclase (adularia inclusive) (27.5 degrees 2θ), albite (27.9 degrees 2θ), and alunite (29.8 and 30.9 degrees 2θ) are also shown (Walker and Renault, 1972).

Diffraction traces were produced using nickel-filtered, copper K α radiation on a Rigaku Geirgerflex DMAX X-ray diffractometer. The heights of reflection peaks of clays were measured from diffraction traces and standardized so that comparative unitless values could be calculated. X-ray reflection traces of untreated, glycolated, and heated sample slides were used to estimate comparative proportional semiquantitative values (parts in 10) for major clay groups. The following formulas were used to obtain comparative semiquantitative numeric values for kaolinite, illite (sericite and hydromica inclusive), smectite, and mixed-layer clays (T = constant, g = peak from glycolated run, h = peak from heated run):

$$T = I_{lh} + K_1$$

$$\text{Illite} = \frac{I_{lg}}{T} \times 10$$

$$\text{Kaolinite} = \frac{K_1}{T} \times 10$$

$$\text{Smectite} = \frac{.25S_1 I_{lg}}{T} \times 10$$

$$\text{Mixed-layer Illite-Smectite} = \frac{I_{lh} - (.25 S_1 + I_{lg})}{T} \times 10$$

	S ₁	I ₁	M-L	K ₁	I ₂	K ₂	Qtz	Orth	Alb	Alun	
Angle 2θ	5.2-7.1	8.8	10.5-11.5	12.4	17.7	24.9	26.6	27.5	27.9	29.8	

40 w.											
u	-	.3	.45	1.4	.5	.95	2.35	1.45	1.0	.45	
g		.25	.35	1.25							
h		-									
20 w.											
u	-	.2	.3	.5	-	-	2.95	1.8	1.2	.5	
g		.25	.5	.6							
h											
15 w.											
u	-	.32	.43	.9	.58	.7	2.85	2.55	.8	.45	
g		.3	.4	.95							
h		-									
10 w.											
u	-	.3	.3	.82	.4	.7	2.0	1.7	1.3	.6	
g		.4	.4	.8							
h		-									
A.											
u	.3	2.1	5.4	.6	26.6	2.7	19.5	7.8	.2	.5	.6
g		9.7	5.4	.6	22.3						
h			7.8								
B.											
u		4.5	.6	.5	6.3	.2	3.6	3.1	.75	-	.35
g		.5	.5	.55	5.9						
h			.8								
C.											
u	2.6	3.1	3.9	-	45.5	.78	25.0	2.6	.8	-	.5
g		.7	2.6	-	43.7						
h			5.2								
D.											
u	-	1.0	.45	4.15	.2	2.4	2.75	1.6	.3	.6	
g			.7	4.5							
h			1.0								
2 east											
u		.75	.7	.5	5.2	.1	3.25	2.3	1.1	-	-
g		1.4	.65	.7	5.2						
h			.3								
5 e.											
u	-	.4	.5	.6		.5	3.15	1.5	.9	-	
g			.4	.5	.8						
h			.45								

Appendix III: Rhyolite Mine sample map (Neubert, 1983);

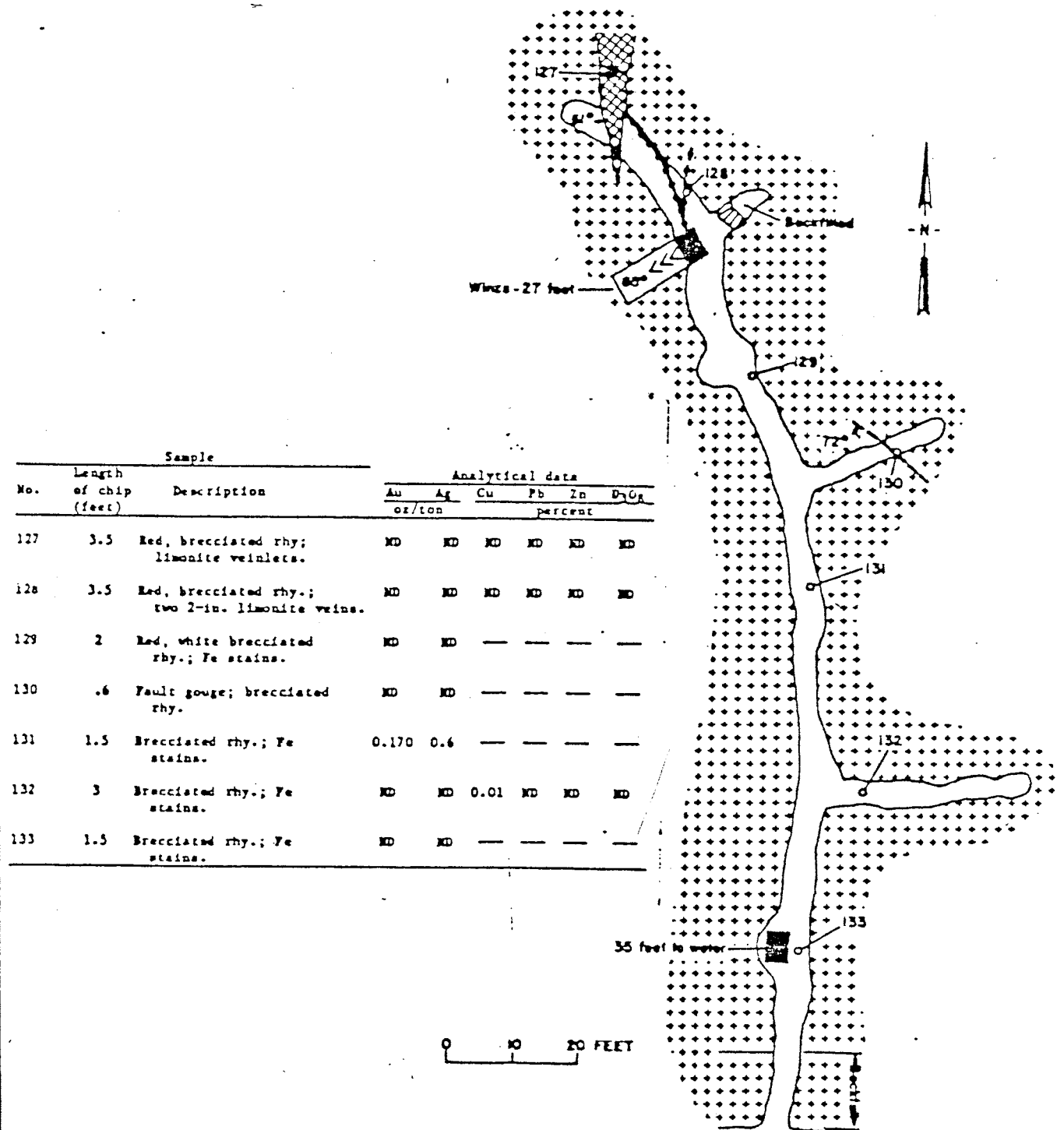


Figure 8.—Map showing the Rhyolite Mine and sample localities 127-133. Table shows sample data; symbols are: rhy., rhyolite; ND, not detected; —, not analyzed.

Appendix IV: Geochemical analyses data:

The following list includes analyses of samples provided by the current owners of the Apache Group lode mining claims, various mining companies, and selected geochemical data from open-file reports by the USGS and the US Bureau of Mines, and Foruria (1984). Sampling by: A, B, and L (Apache Claims owners), C (Calahan Mining Co.), F (Foruria, 1984), N (Newmont Exploration Ltd.), P (Pioneer Nuclear, Inc.), and X (USGS)(locations shown in Figure 11). The list below contains analyses from samples taken in five mineralized zones used to determine ranges, means, and standard deviations shown in Table 2. Samples given in parts per million (ppm).

Pankey Mine area:

sample no.	Au	Ag	As	Hg	Sb	Au/Ag
1 F1824	.07	4.30	3.0		tr.	.02
2 F1825	1.33	84.20	2.0		1.0	.02
3 F1826	.05	1.50	1.0		tr.	.03
4 F1829	.02	8.60	4.0		tr.	.002
5 F1832	.06	1.10	4.0		tr.	.05
6 F1842	.38	7.90	12.0		1.0	.05
7 F1851	.06	1.30	3.0		2.0	.05
8 F1861	.03	1.90	16.0		1.0	.02
9 X90	.05	3.10				.02
10 X91	.15	6.00				.03

11	X94	.03	2.50			.01
12	X96	.06	1.60			.04
13	X99	.11	4.70			.02

Taylor shaft area:

sample no.	Au	Ag	As	Hg	Sb	Au/Ag	
14	Al01a	.12	1.56			.08	
15	Al01b	.62	18.04			.03	
16	Al01c	1.62	12.75			.13	
17	Al01d	3.42	7.78			.44	
18	Al03	2.34	9.11	12.81		.26	
18c	Al03*	3.42	6.02		1.35	.56	
	(coarse fraction, not averaged)						
19	Al19	tr.	.31				
20	F1886	.87	15.5			.06	
21	F1887	23.20	173.00			.14	
22	P10	.99	20.20	5.0	.05	2.0	.05
23	P11	1.16	7.70	10.0	.03	2.0	.15
24	P12	1.32	16.90	18.0	.30	1.0	.08
25	P13	.27	3.90	29.0	.05	2.0	.07
26	N900	.49	.20				2.49

Milliken Park:

sample no.	Au	Ag	As	Hg	Sb	Au/Ag
27 A112a	.62	1.87				.33
28 A112b	.62	0				
29 A112c	.62	9.95				.06
30 A112d	.62	0				
31 A112d*	1.00	.70				
32 A113	14.93	12.44	6.51		.88	1.20
33 A114*	.22	0	.10			
34 C401	.03					
35 C402	.12					
36 C403	.65					
37 C404	.81					
38 C405	.16					
39 N894	.13	.80				.16
40 N895	.38	.80				.48
41 N896	.03	.20				.15
42 F1908	.03	.30				.10
43 F1909	.07	1.90	1.0		1.0	.04

Mineralized zone along the San Jose Arroyo:

sample no.	Au	Ag	As	Hg	Sb	Au/Ag
44 A109	9.33	6.22				1.50
45 A110	tr.	.09				
46 A115*	10.64	4.75	6.93		.83	2.24
47 C417	.06					

48	C418	1.03				
49	C419	1.49				
50	N879	.06	.60			.10
51	N883	.11	1.20			.09
52	N885	.04	.20			.20
53	F1914	.14	2.40	1.0	1.0	.06

Rhyolite Mine area:

sample no.	Au	Ag	As	Hg	Sb	Au/Ag	
54	A106	0	21.15				
55	P03	0	.02	7.0	tr.	1.0	
56	P10	.99	20.20	5.0	.05	2.0	.05
57	P19	.03	.24	5.0			.12
58	F1916	.05	.90	1.0		1.0	.06
59	F1917	.04	1.40	1.0		1.0	.03
60	F1920	.04	.20	1.0		1.0	.20
61	F1921	.08	1.90	3.0		7.0	.04
62	F1925	.17	2.40	6.0		1.0	.41
63	N886	0	.20				
64	N892	0	6.60				
65	N893	.65	.60				1.08
66	X131	5.29	18.67				.28

Other analyses of samples taken in the study area:

sample no.		Au	Ag	As	Hg	Sb	Au/Ag
67	A102	tr.	.31				
68	A104	0	6.84				
69	A105	tr.	2.52				
70	A108	.03	.16				.20
71	B1	0	.49				
72	B2	0	.40				
73	B3	0	.19				
74	B4	0	.09				
75	B5	0	.19				
76	B6	0	.19				
77	B7	0	.28				
78	B8	0	.09				
79	B9	0	.09				
80	B10	0	.28				
81	C417	0	.05				
82	C418	0	1.05				
83	C419	0	1.50				
84	C420	0	39.50				
85	F1038	0	.20				
86	F1863	0	1.30				
87	F1893	0	.30				
88	F1896	0	.20				
89	F1904	0	.20				

sample no.	Au	Ag	As	Hg	Sb	Au/Ag
90 F1905	0	.30				
91 F1907	0	.80				
92 F1919	0	.90				
93 F1924	0	.50				
94 G77	0	.62				
95 G78	tr.	34.21				
96 L20	tr.	2.49				
97 L29	0	.25				
98 L30	0	.28				
99 L31	0	.40				
100 L32	0	.19				
101 L33	0	.16				
102 L34	0	.34				
103 L35	0	.12				
104 L36	.03	.34				.09
105 N878	0	.40				
106 N887	0	.20				
107 N891	0	.20				
108 N900	.49	.20				2.49
109 P01	0	.20	3.0	.01	1	
110 P02	0	.30	6.0	.01	2	
111 P05	1.67	10.70	10.0	.09		.16
112 P06	.08	.60	24.0	.01	1	.13
113 P08	0	.02	3.0	.01	1	

The following analyses of selected samples (indicated above by *) were reanalysed using a Jarrel-Ash multi-element plasma emission spectrometer.

sample no.		Au	Ag	Pt	Pd	Cu	Pb	Zn	Mo	As	Sb	Bi
18	Al03*	2.34	9.11	3.02	-	76.96	91.92	73.79	6.00	12.81	1.35	-
18c	Al03* (panned coarse fraction)	3.42	6.02	-	-	27.70	33.73	54.67	13.47	8.25	1.12	.06
31	Al12d*	1.00	.70	.03	.07	41.75	18.95	10.93	9.78	6.51	.88	.44
33	Al14*	.22	-	.08	-	15.83	-	30.31	3.58	.10	-	.13
46	Al15*	10.64	4.75	-	-	42.75	60.64	8.82	8.32	6.93	.83	.43
114	Al16	.75	4.42	.04	-	61.99	-	-	13.78	31.41	-	.31

ACKNOWLEDGEMENTS

The following people made significant contributions to the formulation and completion of this work. These individuals include professors, staff, and students at New Mexico Institute of Mining and Technology, University of New Mexico, and employees of the US Bureau of Land Management, Pioneer Nuclear, Inc., Exxon Minerals Company, Chem-gold, Inc., Socorro Engineering, and Academy Corp.

Clay Smith (Director of Alumni Relations, Professor of geology, NMIMT)

George Austin (Deputy Director of NM Bureau of Mining and Mineral Resources, Professor of geology, NMIMT)

Glenn Osburn (Geologist, Instructor of geology, NMIMT)

Lynn Branvold (Senior Chemist, Professor of geochemistry, NMIMT)

Raul Compose-Marquetti (Geologist, Technology Application Center, UNM)

Darrel Dean (Geologist, Exxon Minerals Company)

Paul Eimon (Geologist, Pioneer Nuclear, Inc.)

Rick Robinson (Geologist, Pioneer Nuclear, Inc.)

Terry Brown (Geologist, Chem-gold, Inc.)

Mike Hermann (M.S. in geology candidate, NMIMT)

Cortney Hesse (M.S. in geology candidate, NMIMT)

Jim Dodson (M.S. in geology candidate, NMIMT)

Curt Verploegh (Chief Metalurgist, Academy Corp.)

Charles Ferguson (Geology graduate, M.S., NMIMT)

Bertrand Gramont (M.S. in geology candidate, NMIMT)

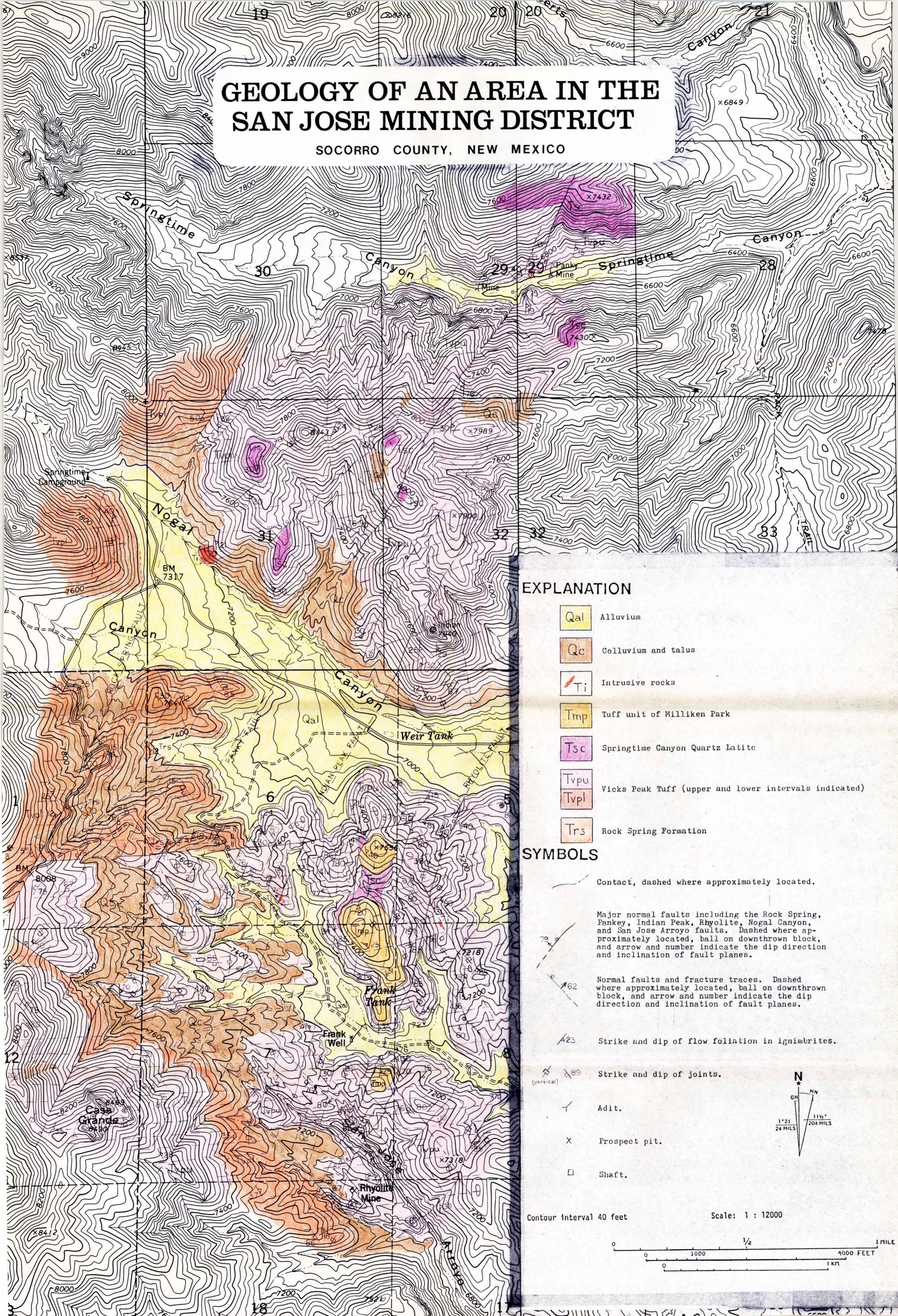
Ted Jochems (M.S. in geology candidate, NMIMT)

Robert Bewley (Geographer, BLM)

Jon Mortensen (P.E., Socorro Engineering)

GEOLOGY OF AN AREA IN THE SAN JOSE MINING DISTRICT

SOCORRO COUNTY, NEW MEXICO

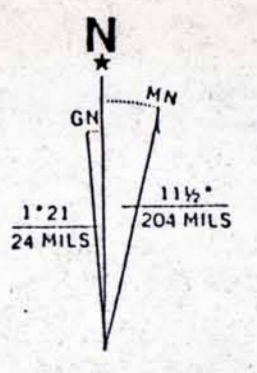


EXPLANATION

- Qal Alluvium
- Qc Colluvium and talus
- Ti Intrusive rocks
- Tmp Tuff unit of Milliken Park
- Tsc Springtime Canyon Quartz Latite
- Tvp Vicks Peak Tuff (upper and lower intervals indicated)
- Trs Rock Spring Formation

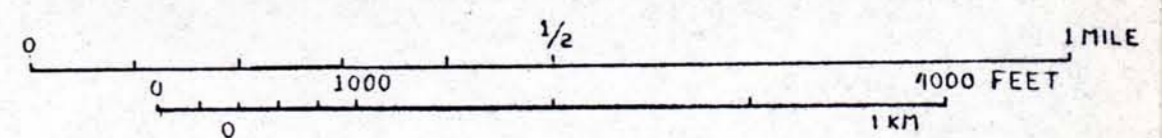
SYMBOLS

- Contact, dashed where approximately located.
- Major normal faults including the Rock Spring, Pankey, Indian Peak, Rhyolite, Nogal Canyon, and San Jose Arroyo faults. Dashed where approximately located, ball on downthrown block, and arrow and number indicate the dip direction and inclination of fault planes.
- Normal faults and fracture traces. Dashed where approximately located, ball on downthrown block, and arrow and number indicate the dip direction and inclination of fault planes.
- Strike and dip of flow foliation in ignimbrites.
- Strike and dip of joints.
- Adit.
- Prospect pit.
- Shaft.



Contour Interval 40 feet

Scale: 1 : 12000



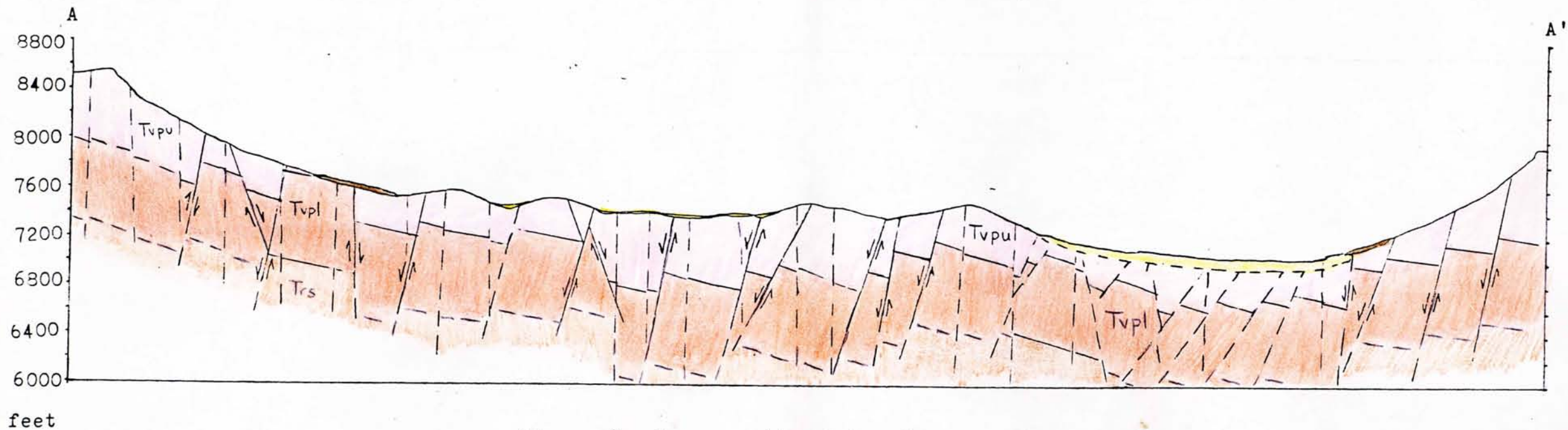
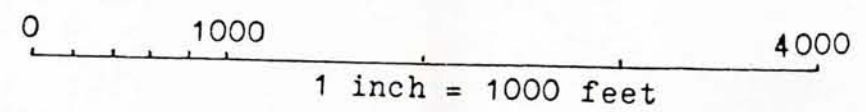


Figure 9. Cross-section A to A' across the central part of the study area from Casa Grande northeast to Indian Peak.



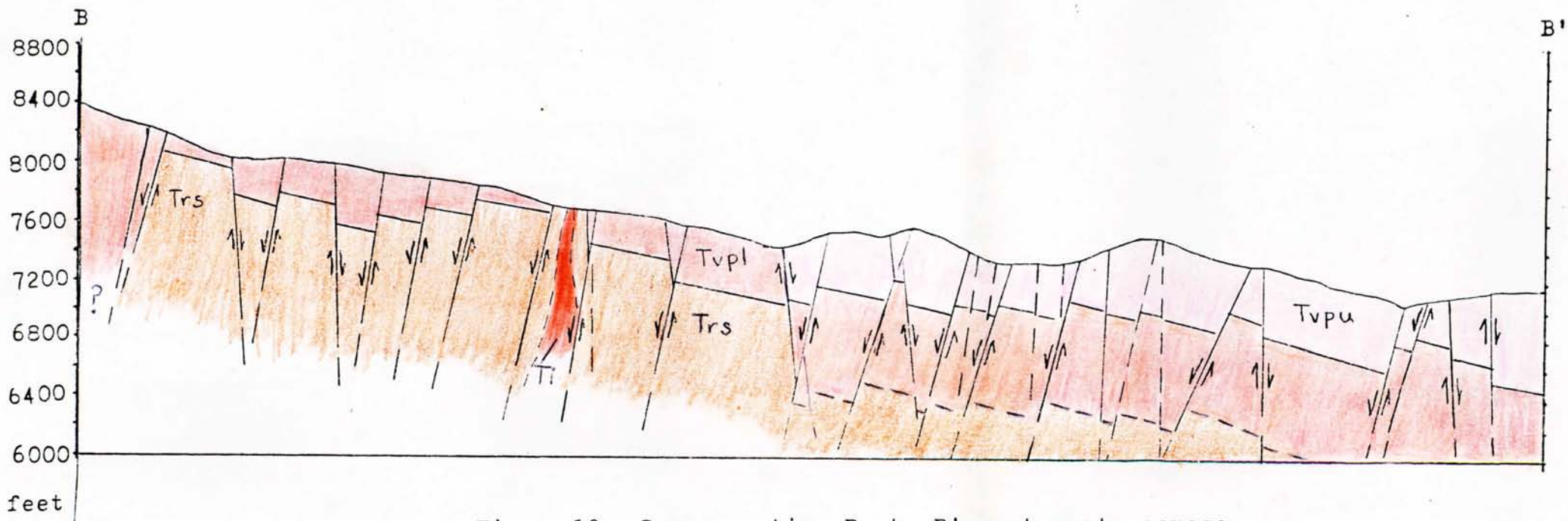
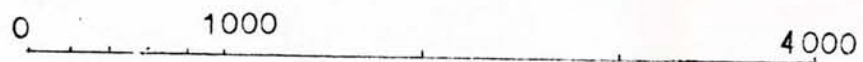


Figure 10. Cross-section B to B' east-west across the central part of the study area.



1 inch = 1000 feet

30

F1851 • F1861
 F1832 • F1842
 F1826 • F1829
 F1824 • F1825
 F1824
 A90,91,94,96,99

Pankey Mine area
 Mean Au: .18 ppm
 Mean Au/Ag: .03


• F1038

31

32

Figure 11: Map showing locations of samples listed in Appendix IV. Mean Au (ppm) and Au/Ag indicated in separate mineralized zones. Apache load mining claim block outlined.

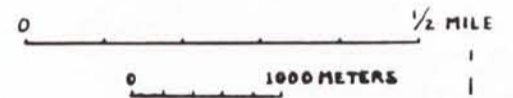
T.8 S.
 T.9 S.

Drill holes showing direction, horizontal projection, and inclination angle (45 degrees): 

Taylor shaft area
 Mean Au: 3.04 ppm
 Mean Au/Ag: .35

5

Approximate scale:



• L32
 • L31
 • L30
 • G78
 • L35
 • L36
 • L33
 • L34
 • B1
 • B2
 • B3
 • B4
 • B5
 • B6
 • B7
 • B8
 • B9
 • B10
 • B11
 • B12
 • B13
 • B14
 • B15
 • B16
 • B17
 • B18
 • B19
 • B20
 • B21
 • B22
 • B23
 • B24
 • B25
 • B26
 • B27
 • B28
 • B29
 • B30
 • B31
 • B32
 • B33
 • B34
 • B35
 • B36
 • B37
 • B38
 • B39
 • B40
 • B41
 • B42
 • B43
 • B44
 • B45
 • B46
 • B47
 • B48
 • B49
 • B50
 • B51
 • B52
 • B53
 • B54
 • B55
 • B56
 • B57
 • B58
 • B59
 • B60
 • B61
 • B62
 • B63
 • B64
 • B65
 • B66
 • B67
 • B68
 • B69
 • B70
 • B71
 • B72
 • B73
 • B74
 • B75
 • B76
 • B77
 • B78
 • B79
 • B80
 • B81
 • B82
 • B83
 • B84
 • B85
 • B86
 • B87
 • B88
 • B89
 • B90
 • B91
 • B92
 • B93
 • B94
 • B95
 • B96
 • B97
 • B98
 • B99
 • B100

Milliken Park area
 Mean Au: 1.24 ppm
 Mean Au/Ag: .44

8

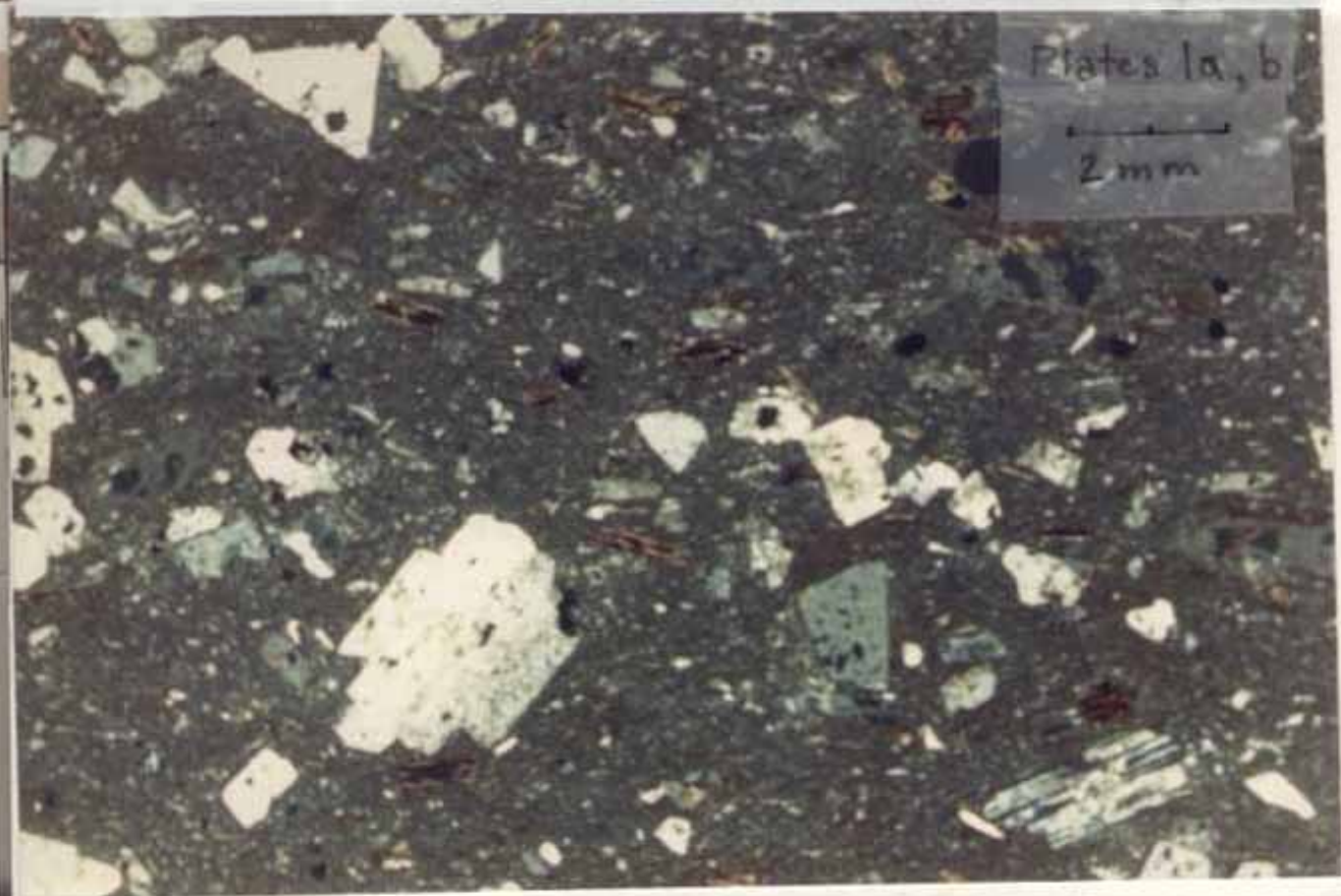
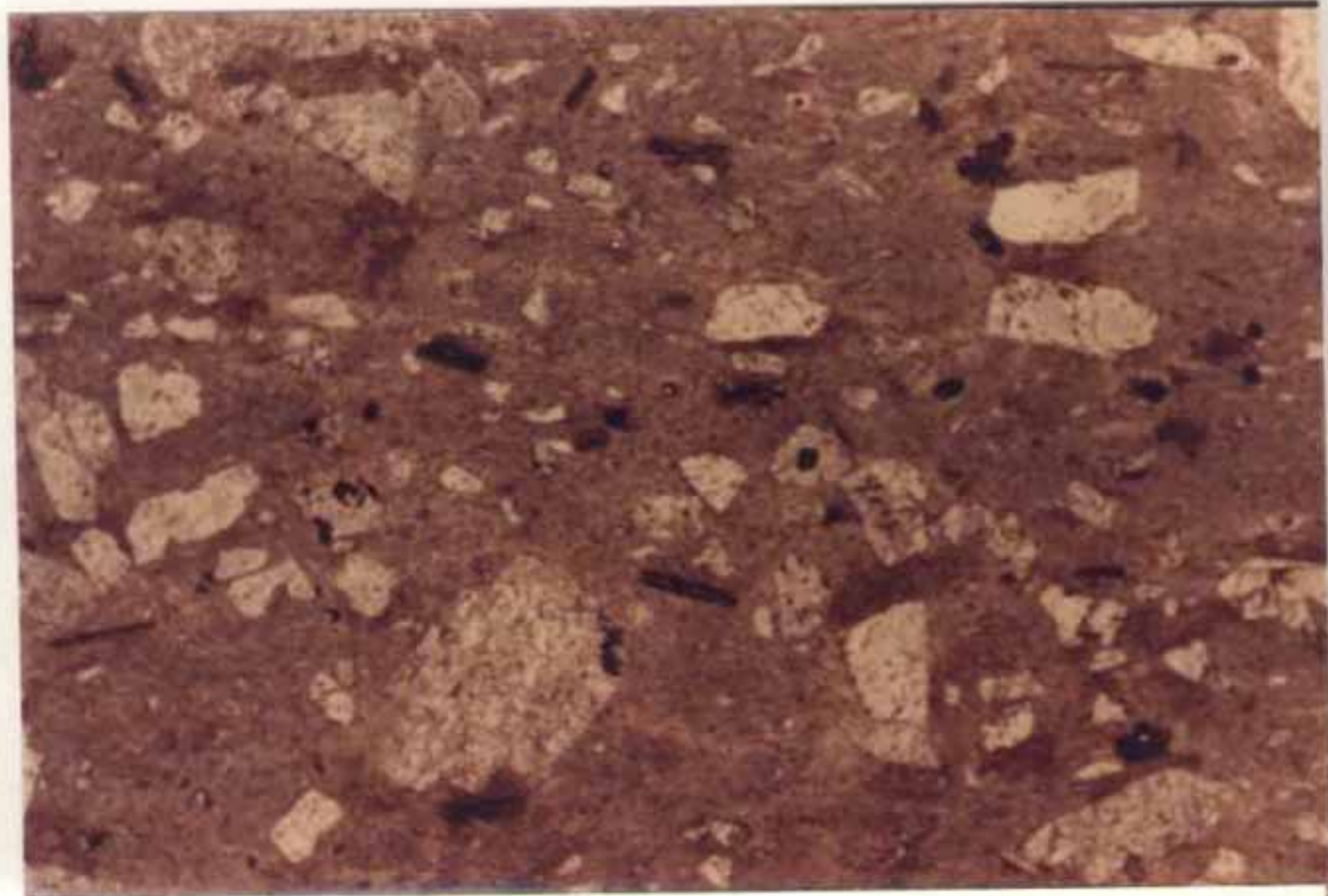


San Jose Arroyo area
 Mean Au: 2.54 ppm
 Mean Au/Ag: .70

Rhyolite Mine area
 Mean Au: .82 ppm
 Mean Au/Ag: .25

R.6W. | R.5W.

F1920
 F1921
 X131
 A105
 P03
 NB92
 NB93
 P01
 B10
 F1917
 F1919
 F1924
 • N887
 • P02



Plates 1a, b

2 mm

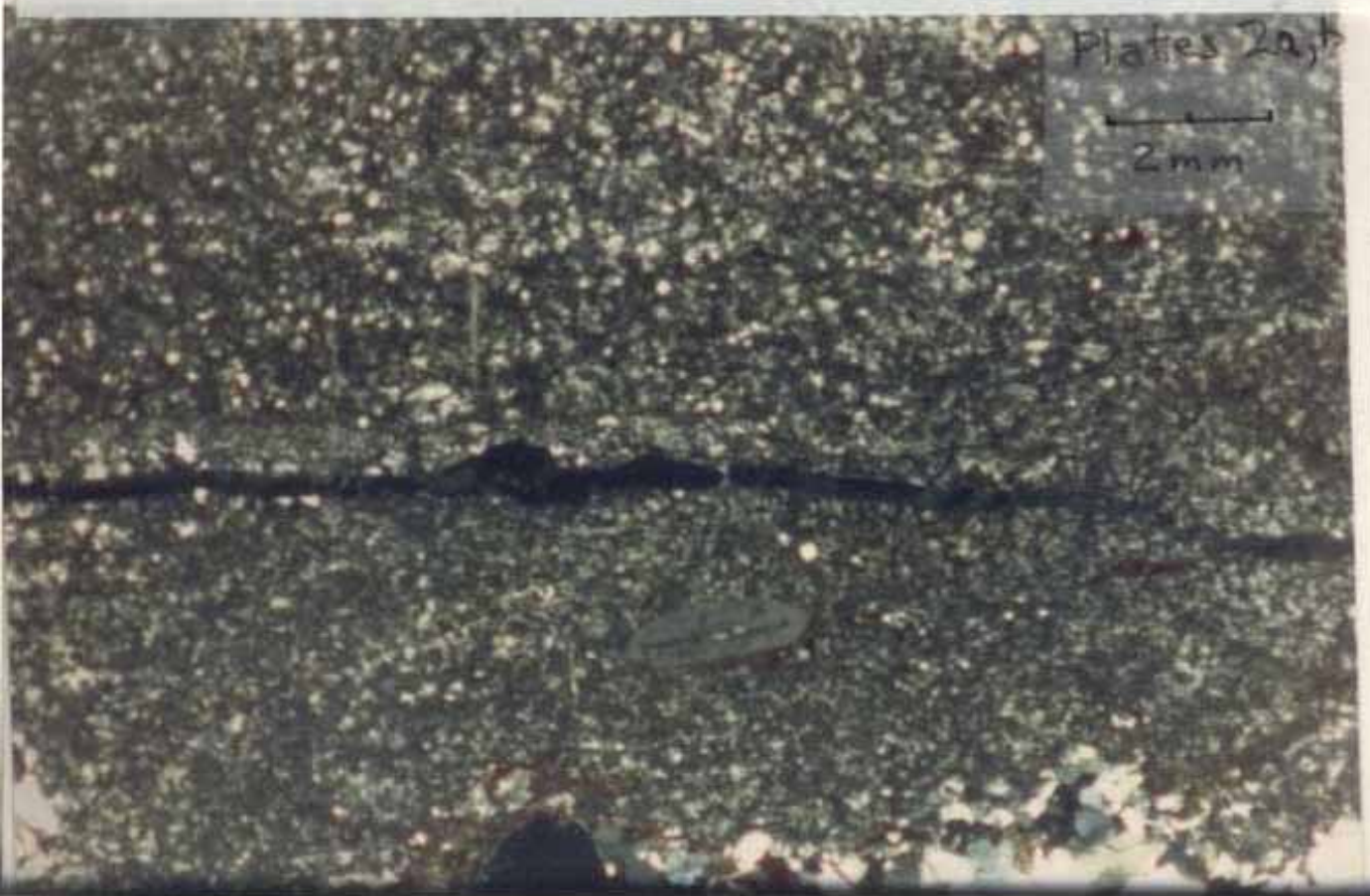
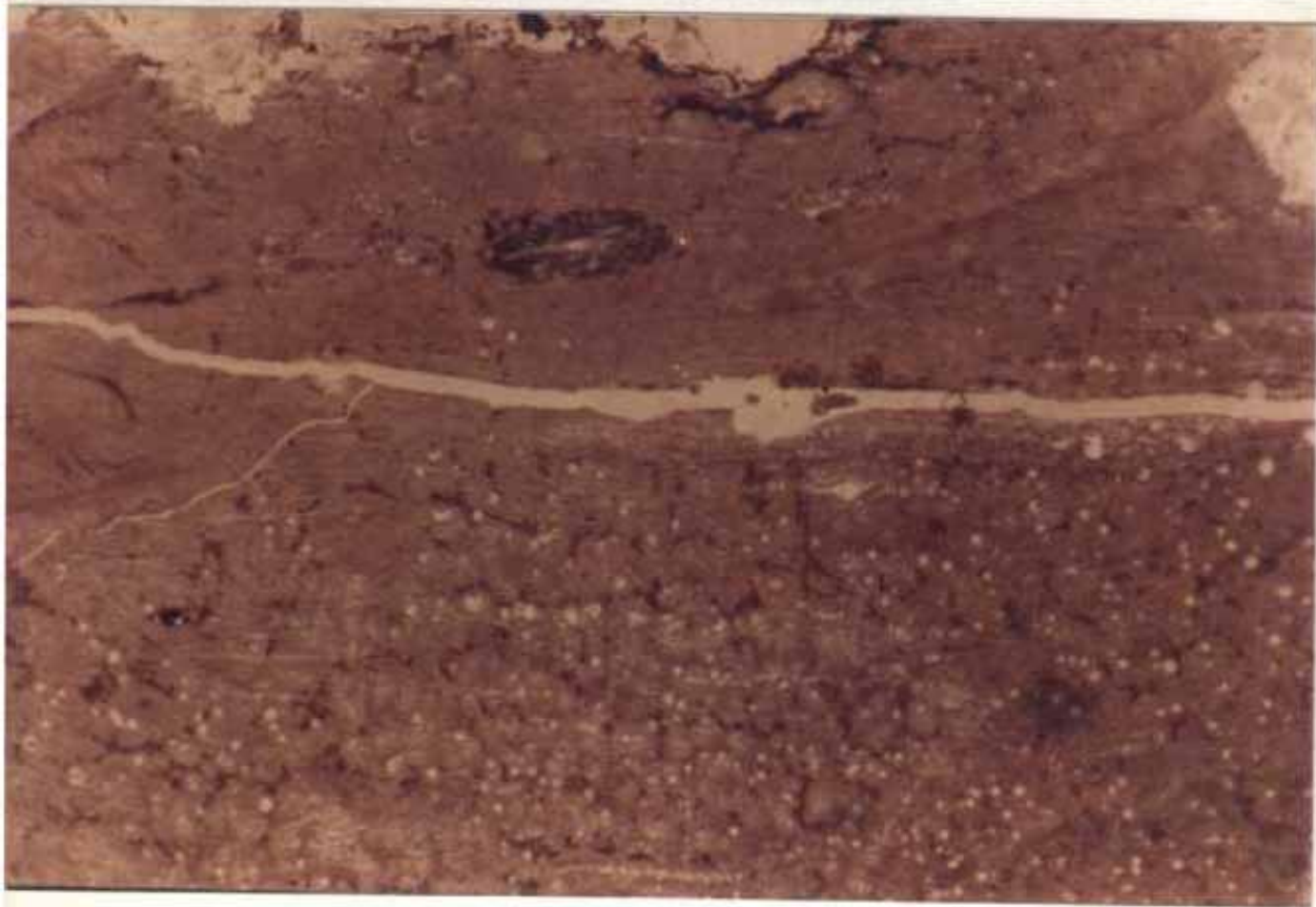
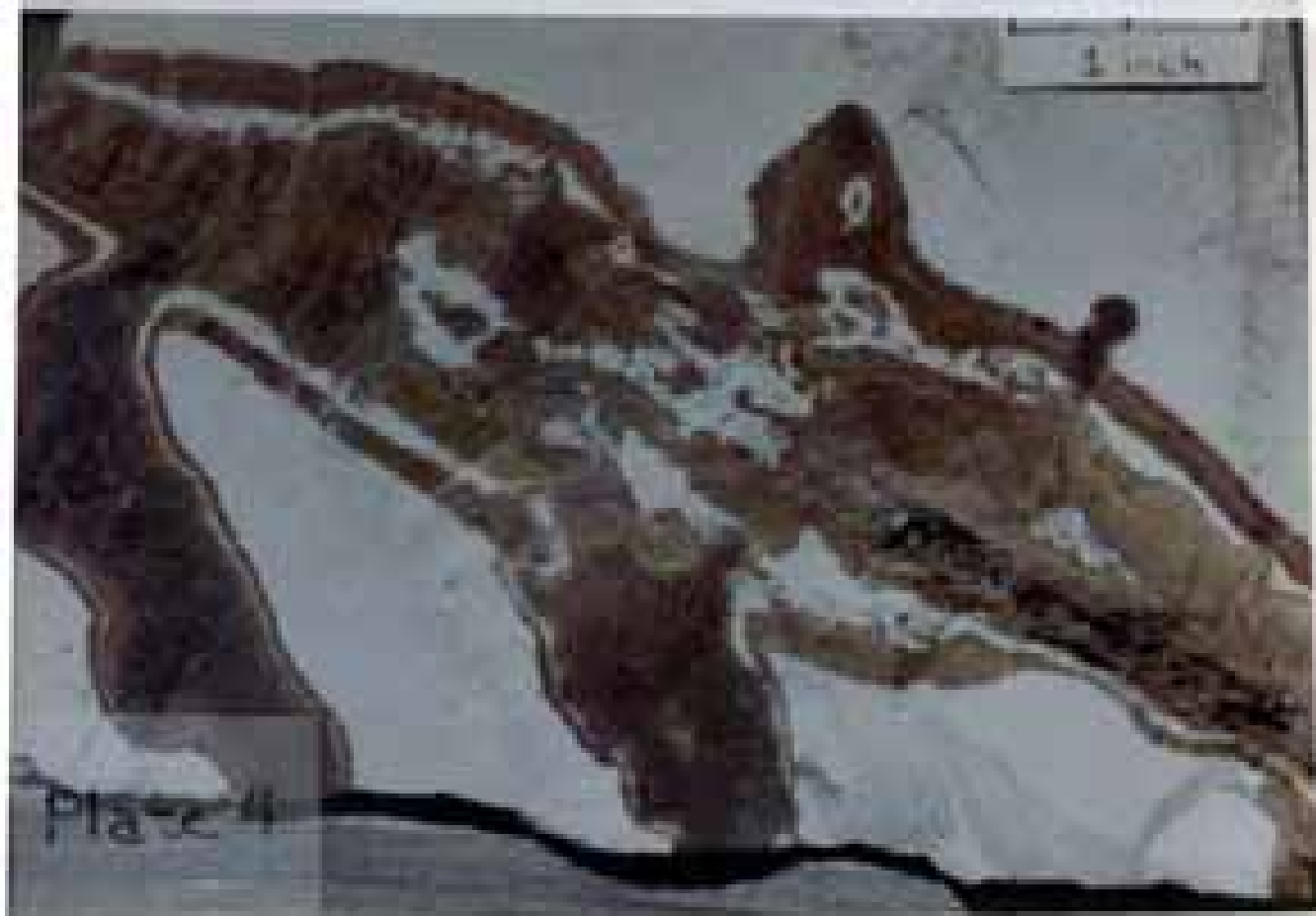


Plate 3

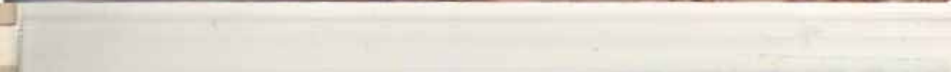


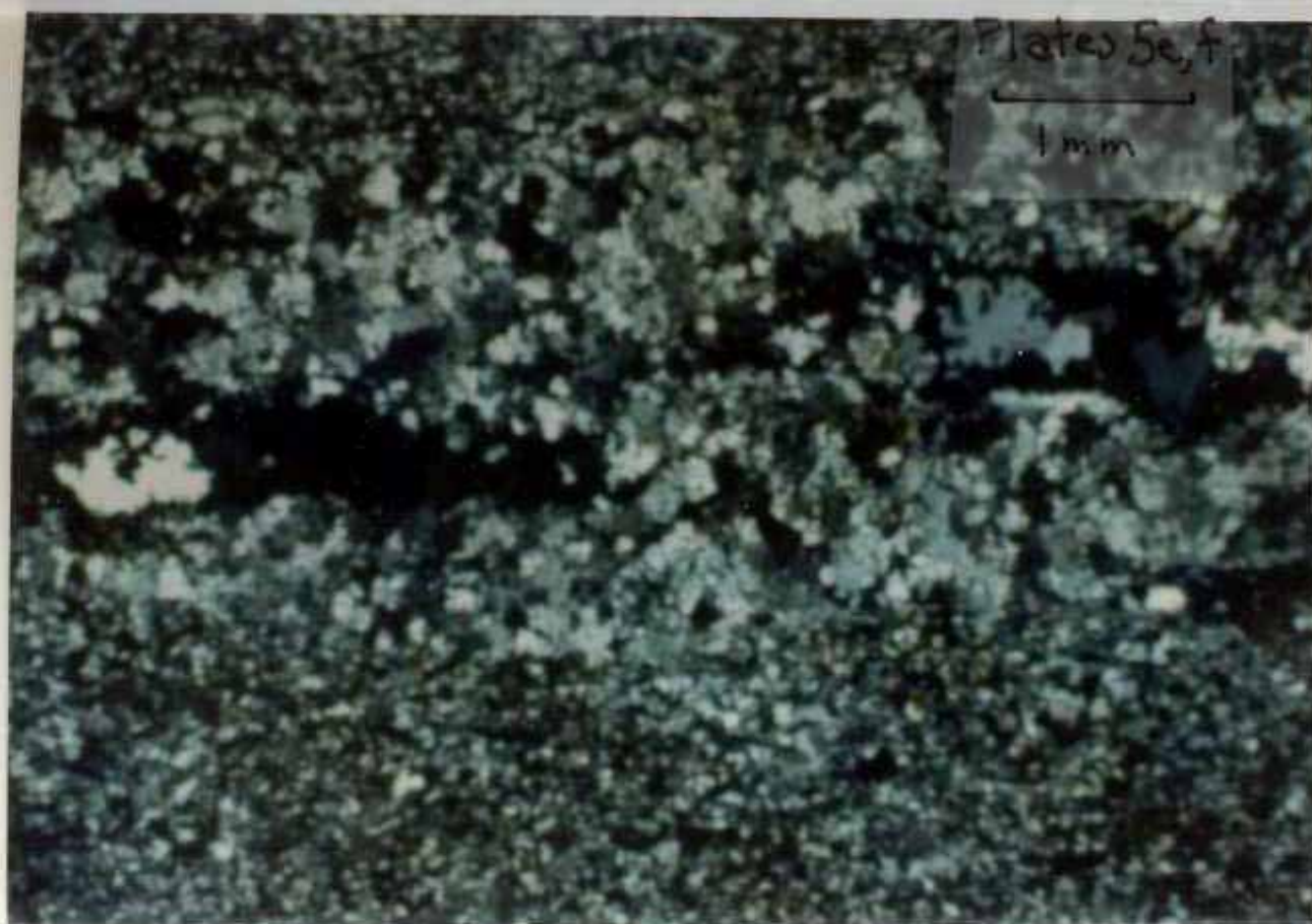
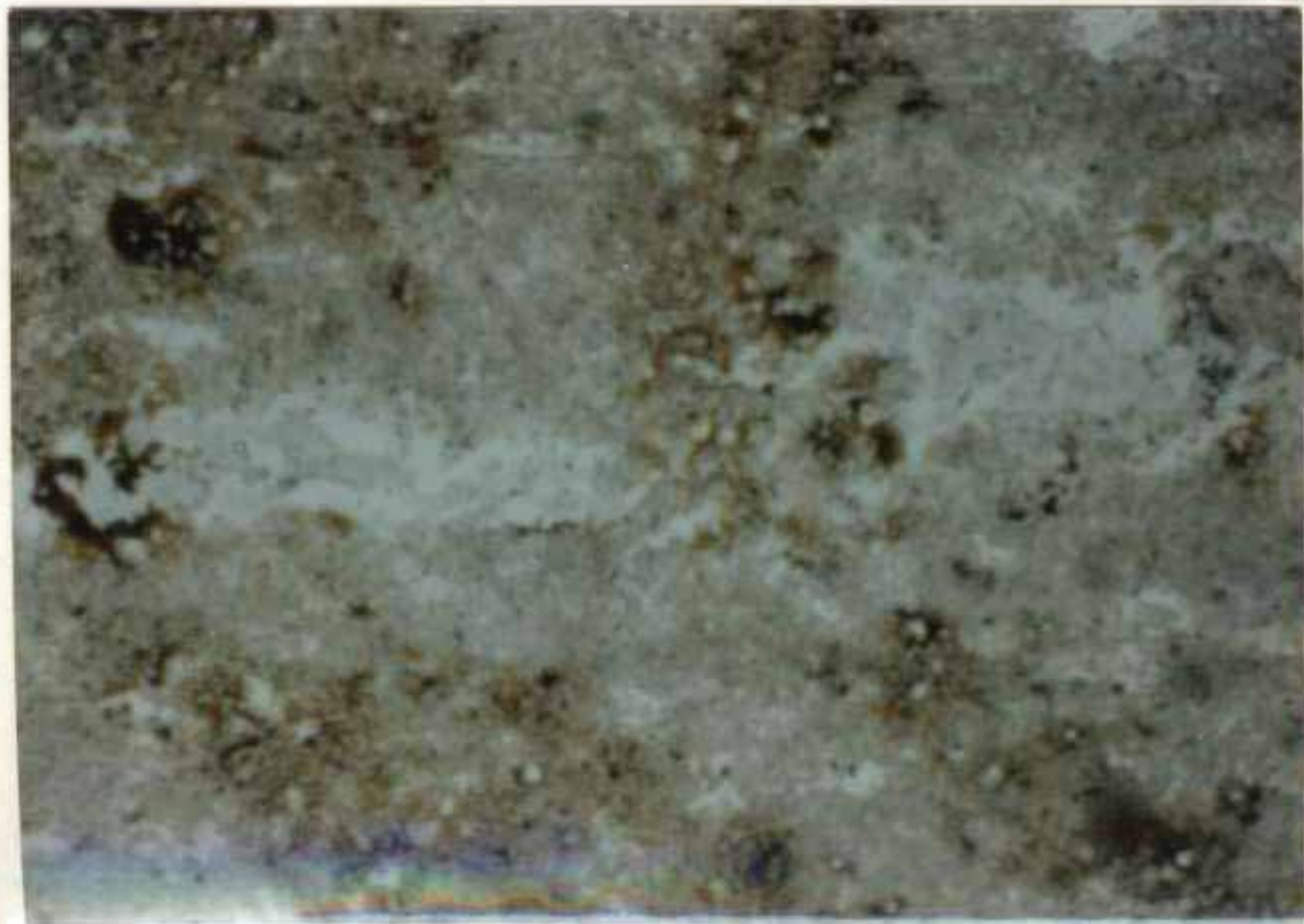
1 inch

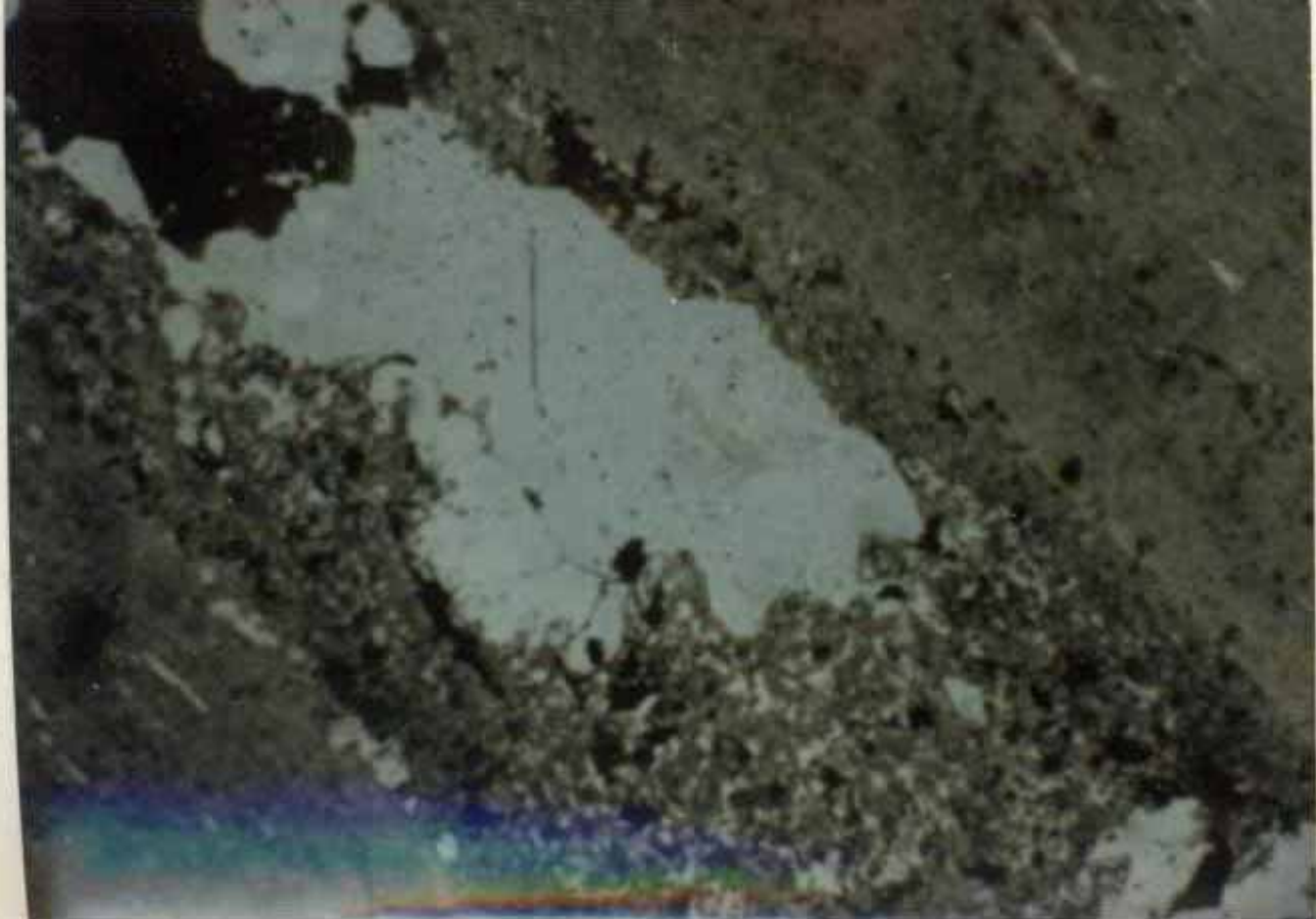
Plate 4

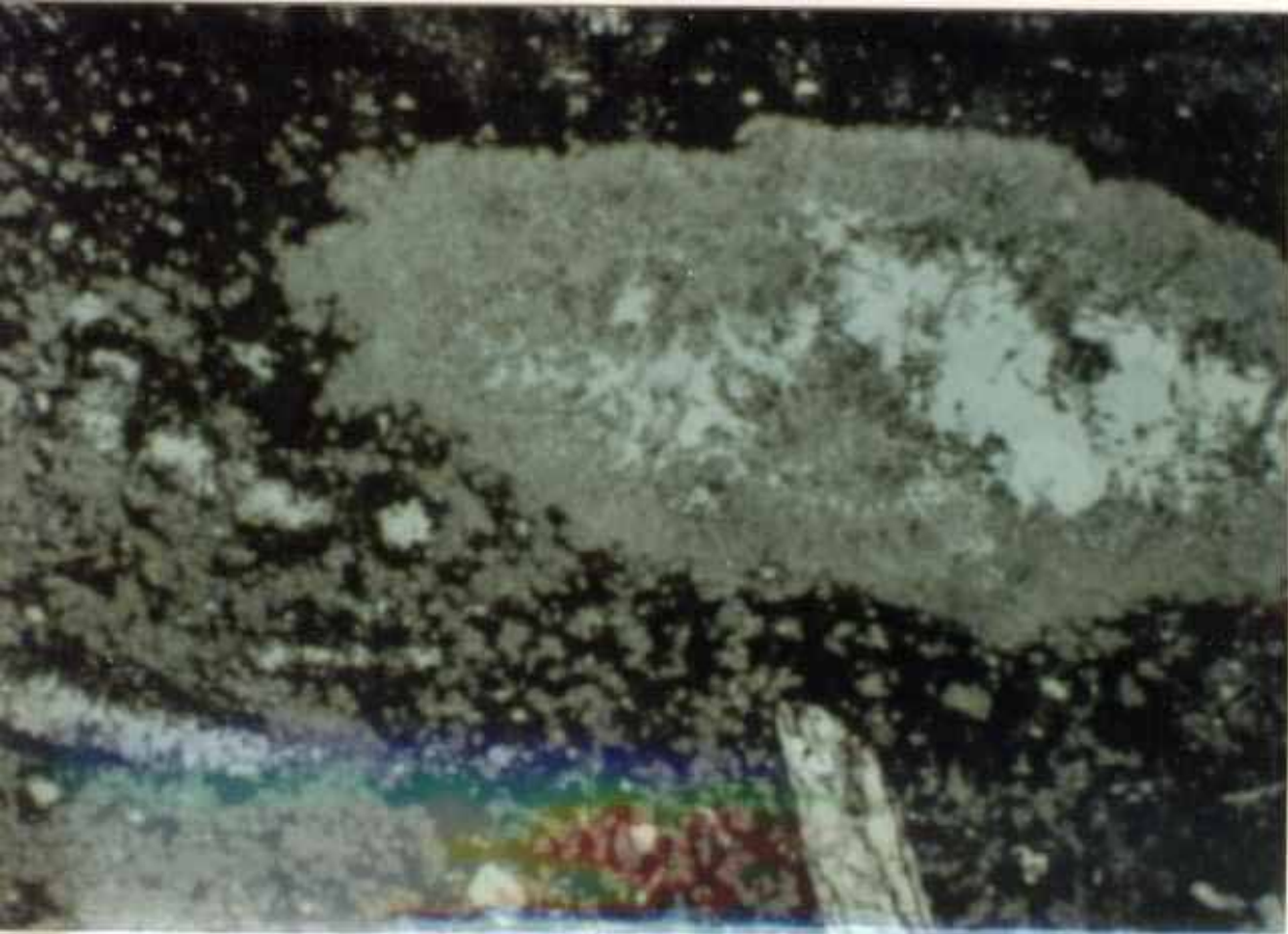




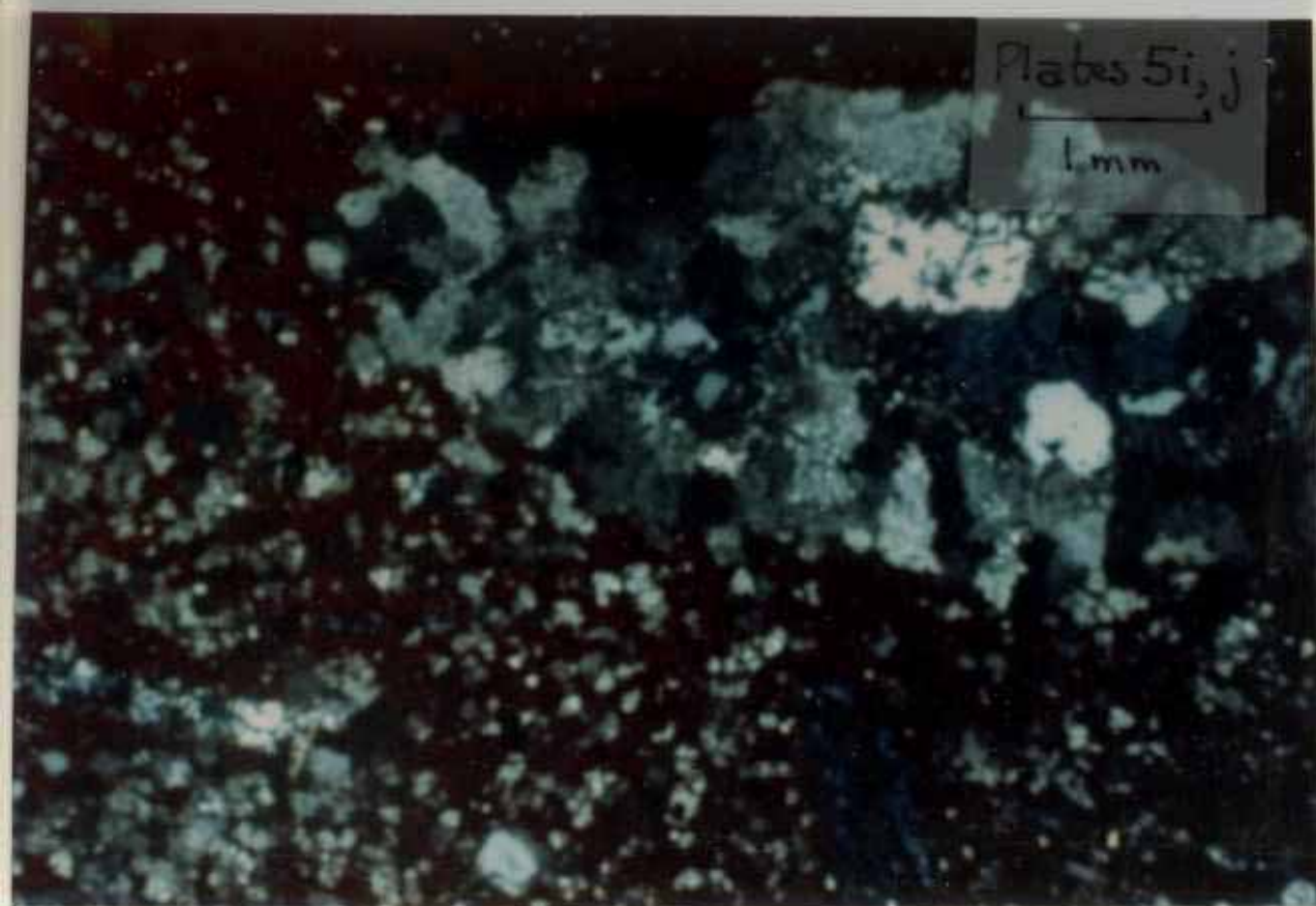




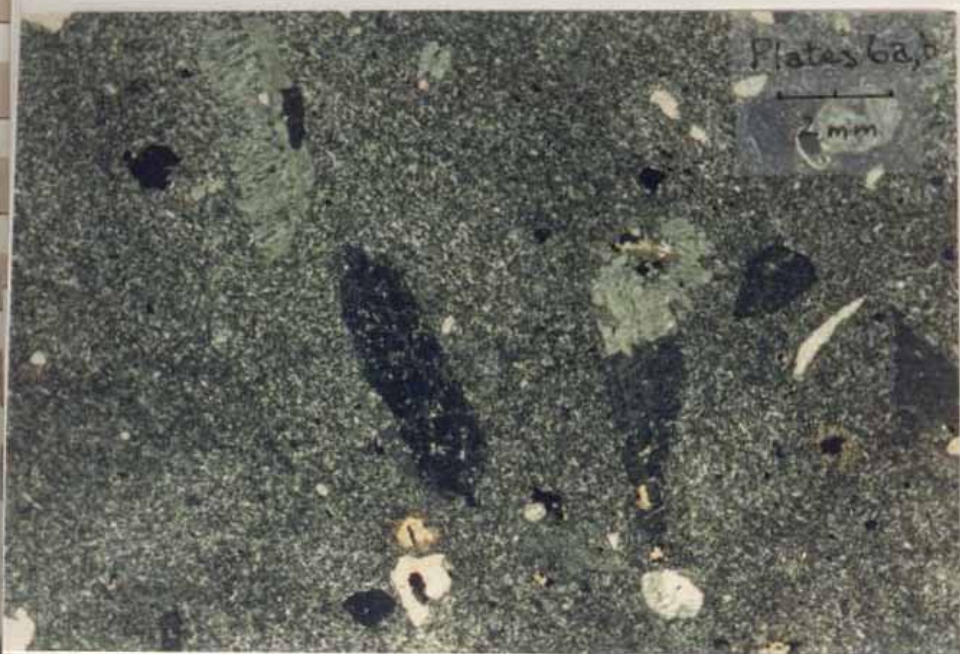
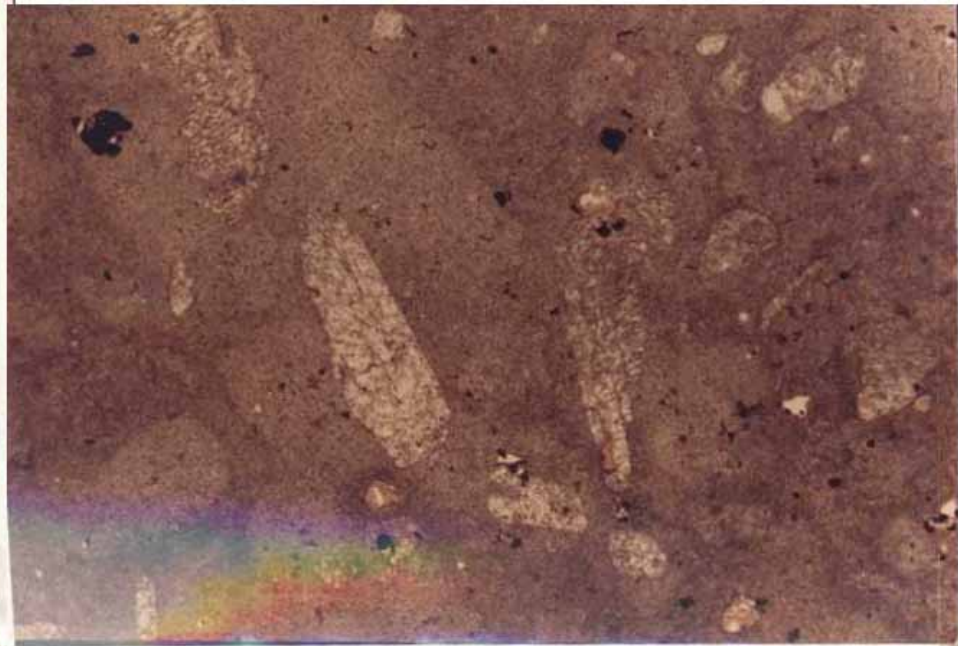




Photomicrograph of a mineral specimen showing a large, light-colored, irregularly shaped inclusion within a darker matrix. The inclusion has a granular texture. Below the inclusion, there is a thin, horizontal layer of material with a distinct color gradient from blue to red. A small, light-colored, elongated object is visible in the lower right quadrant.



Plates 5i, j
1mm



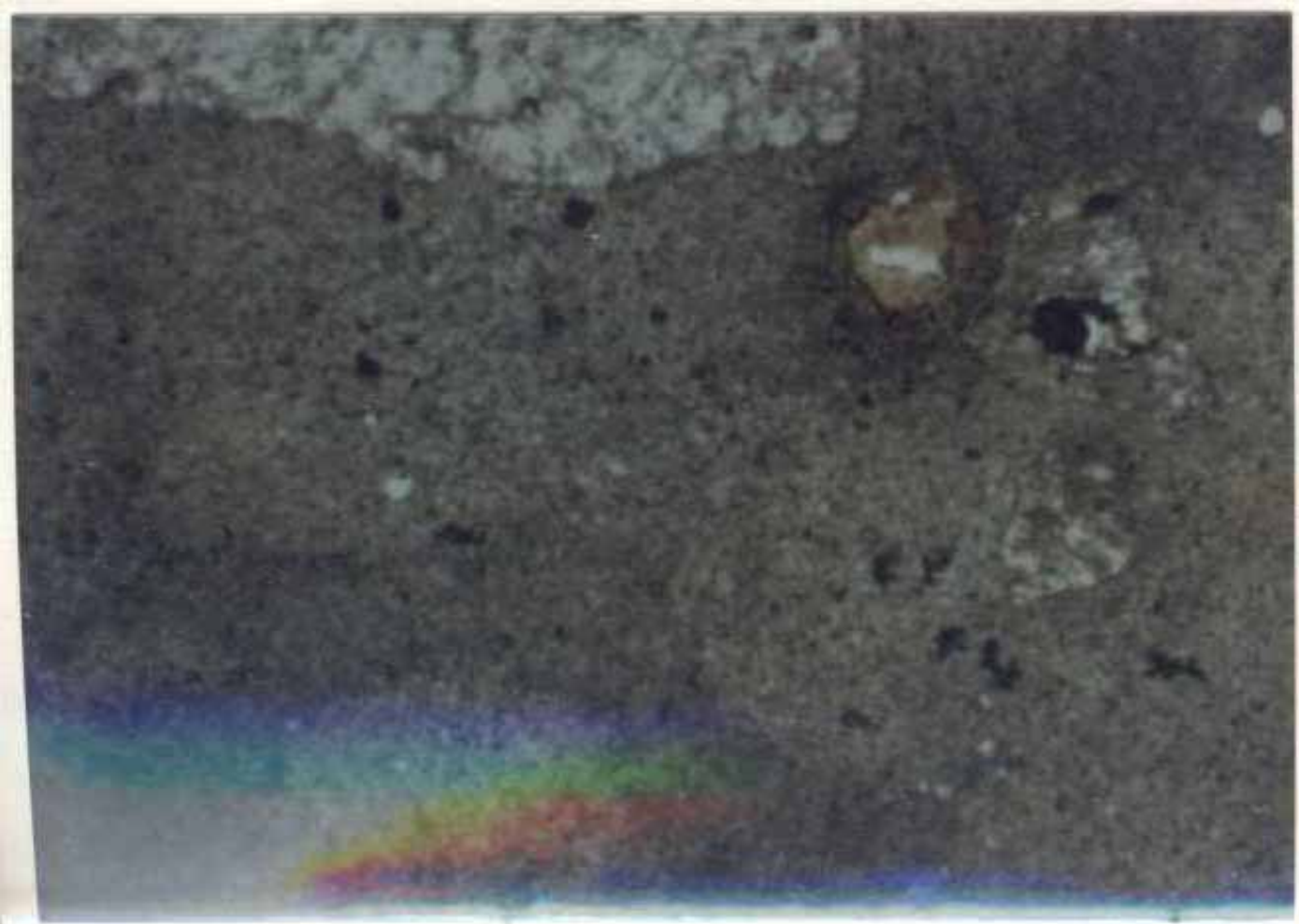
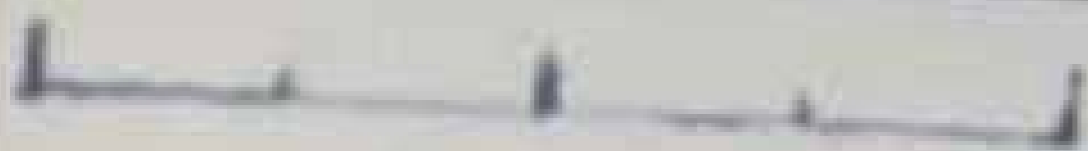
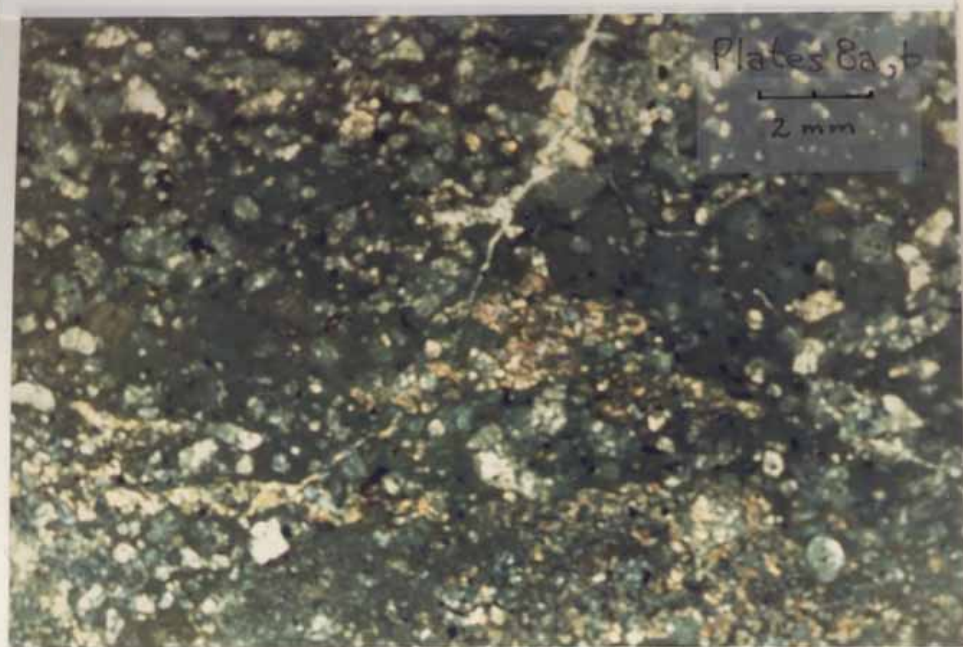
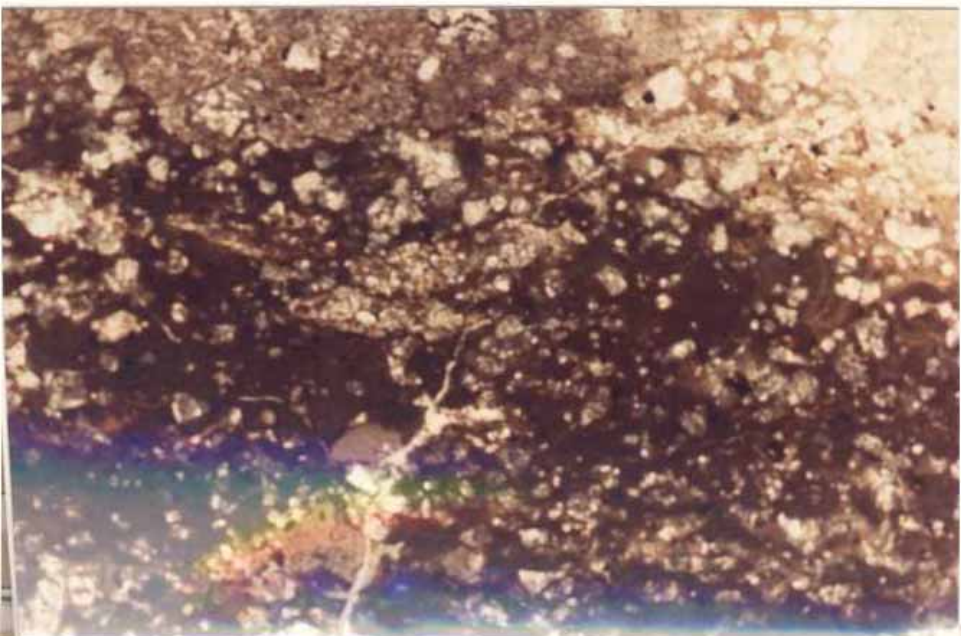
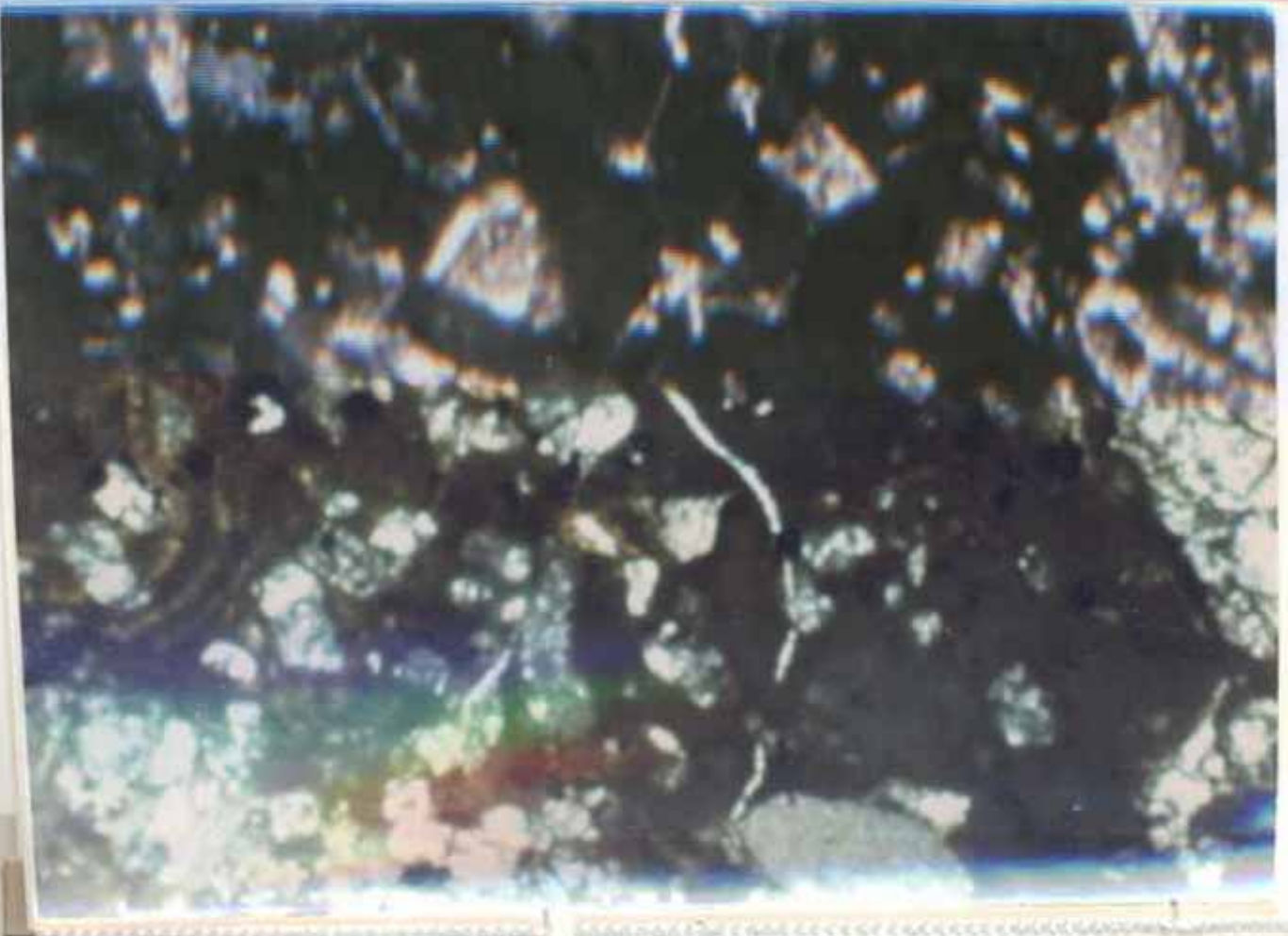


Plate 7



1 inch





Plates 8c, 9
| mm

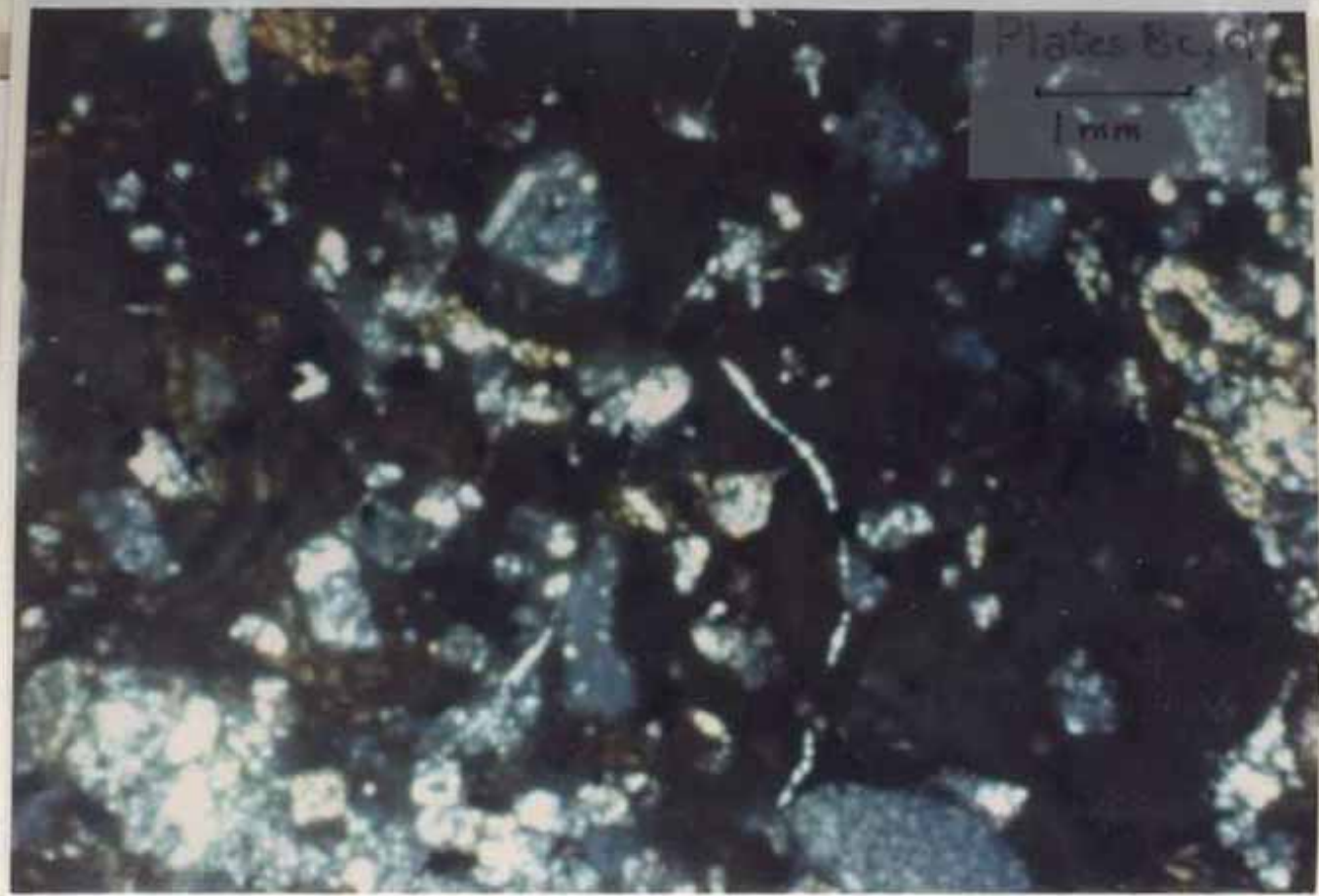


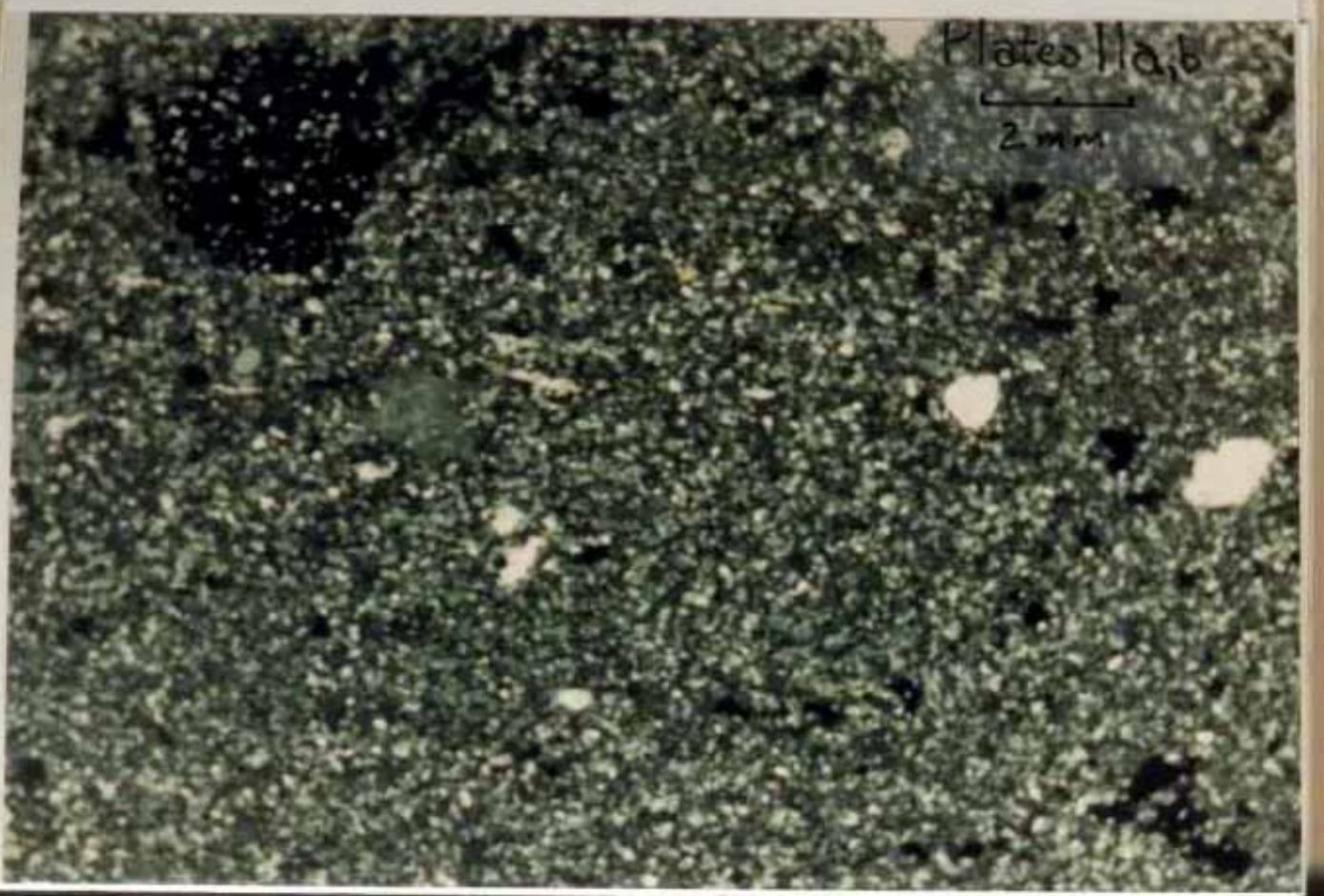
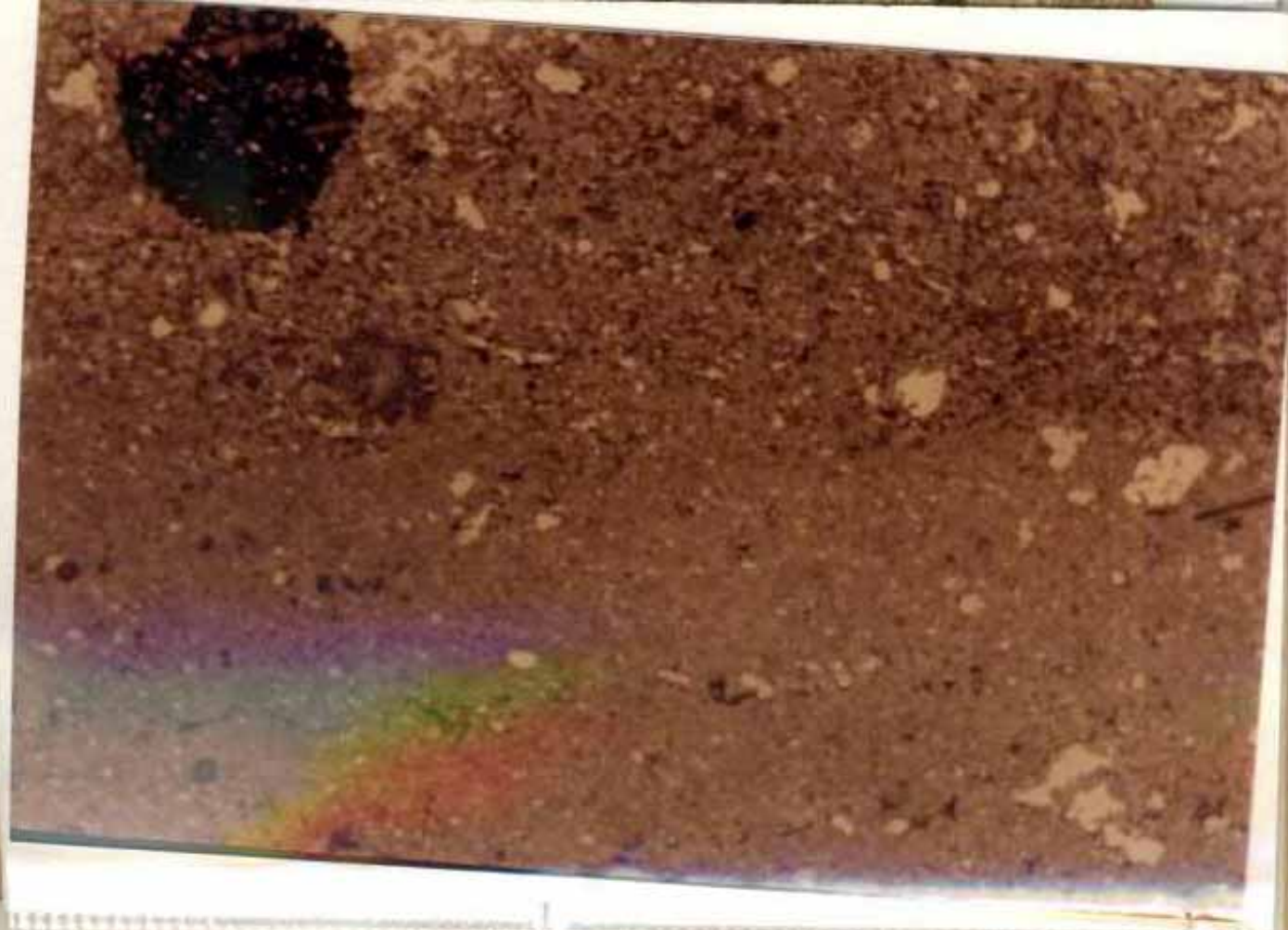
Photo 9

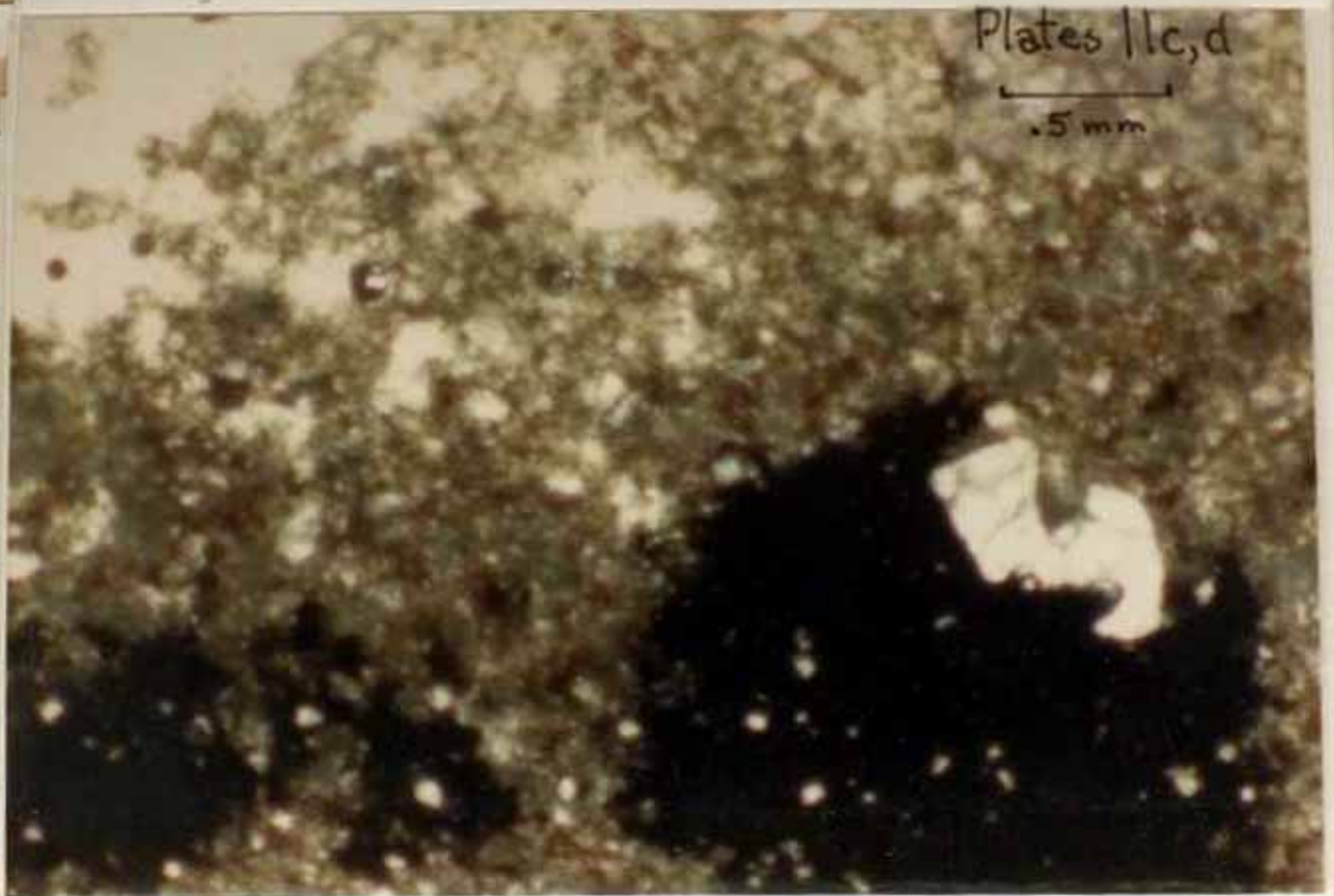


Plate 10

1 cm







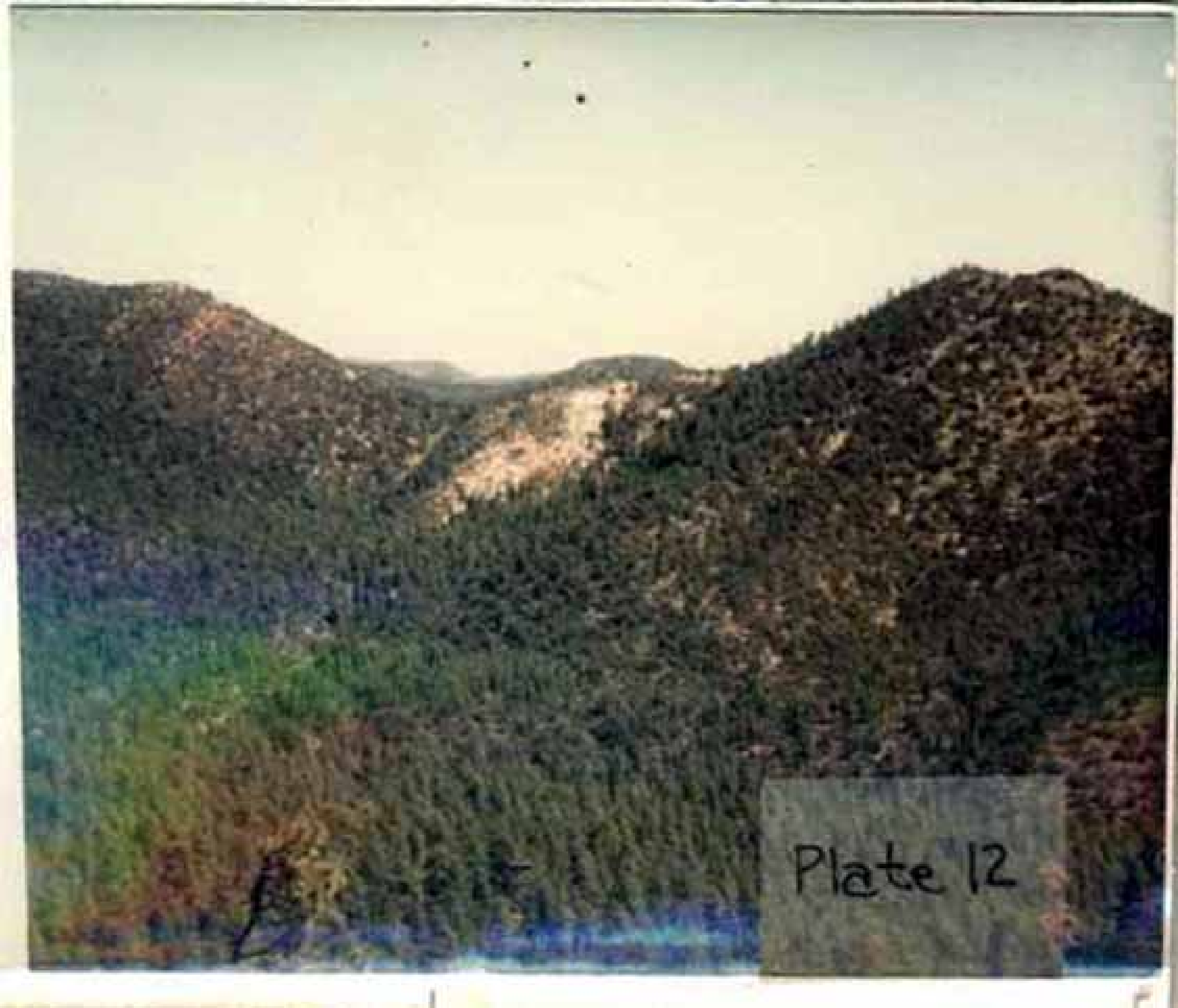


Plate 12

Plate 13: North slope of Springtime Canyon
the Pankey fault and vein outcrop with adit.

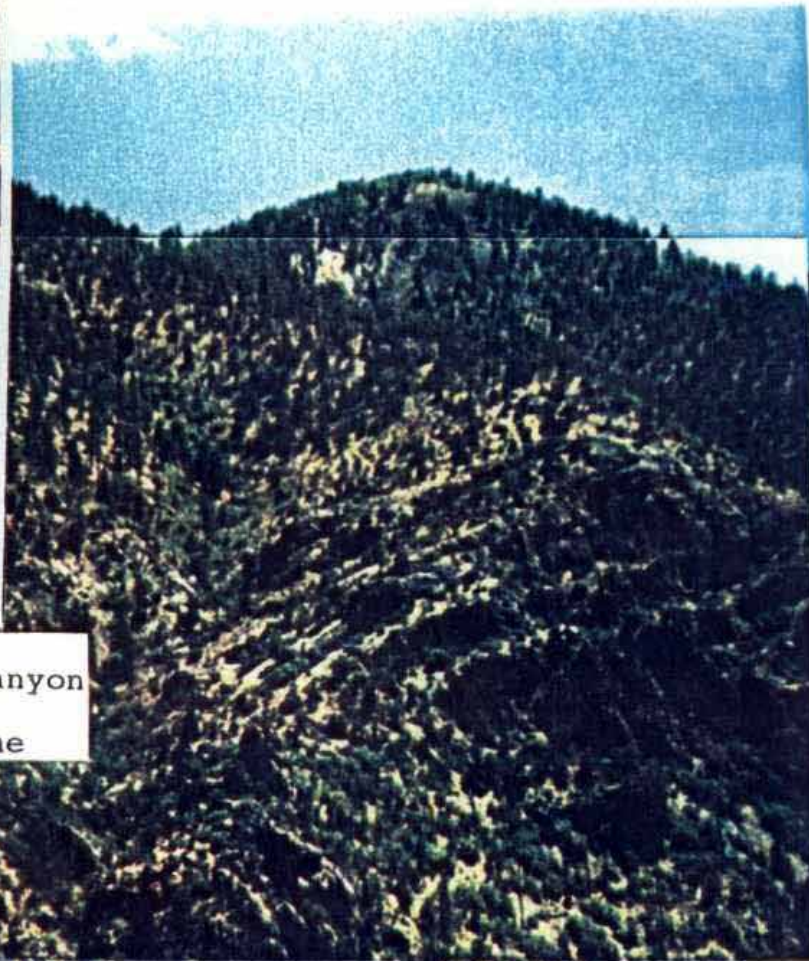
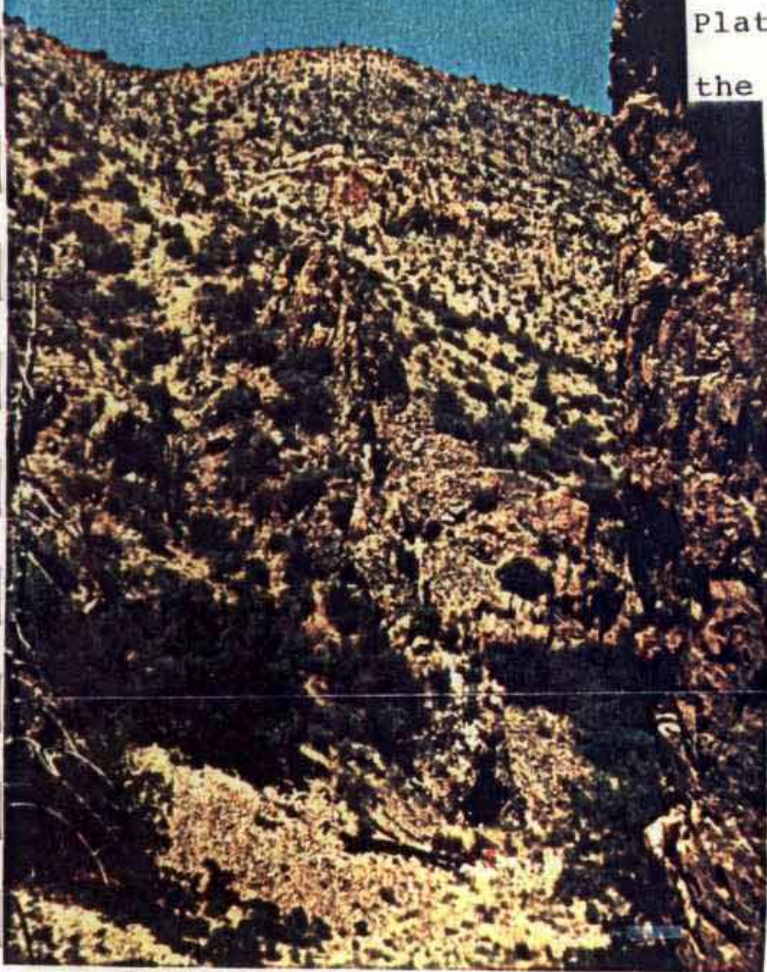


Plate 14: South slope of Springtime Canyon
showing the south-trending trace of the
Pankey fault.



Plate 15: Caved workings in the south-facing slope of the San Jose Arroyo.

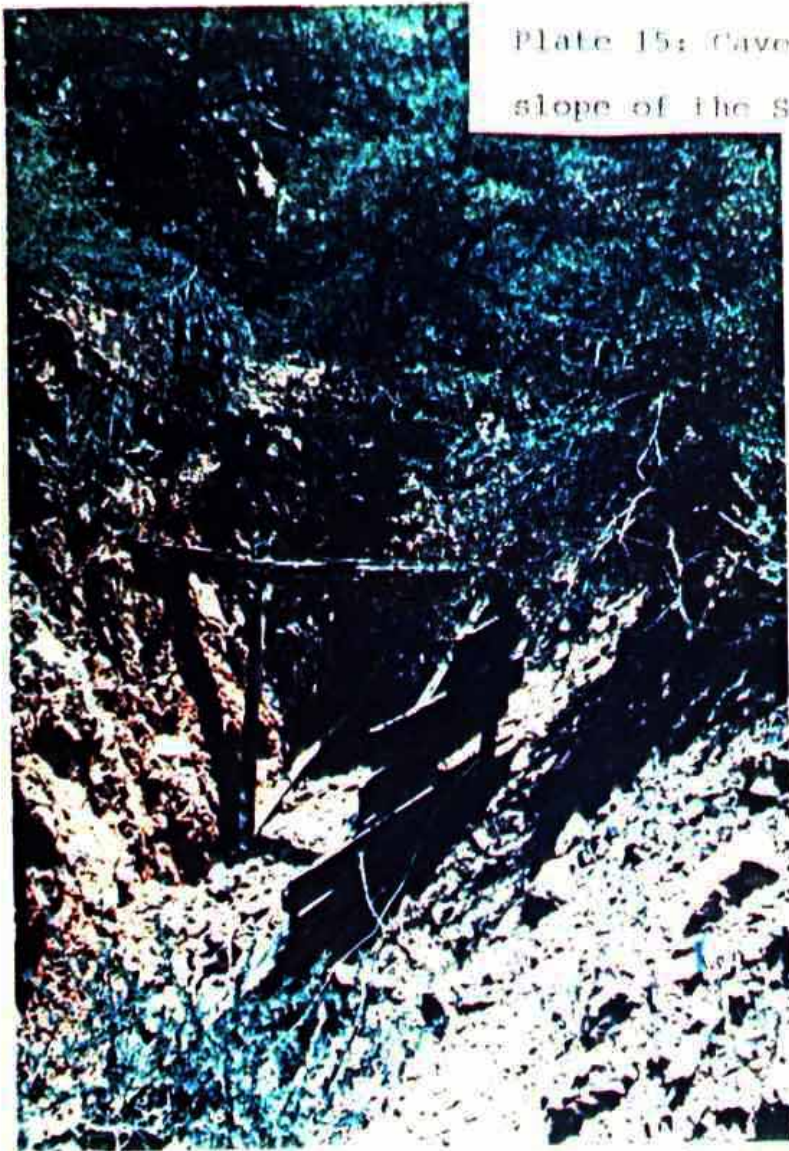
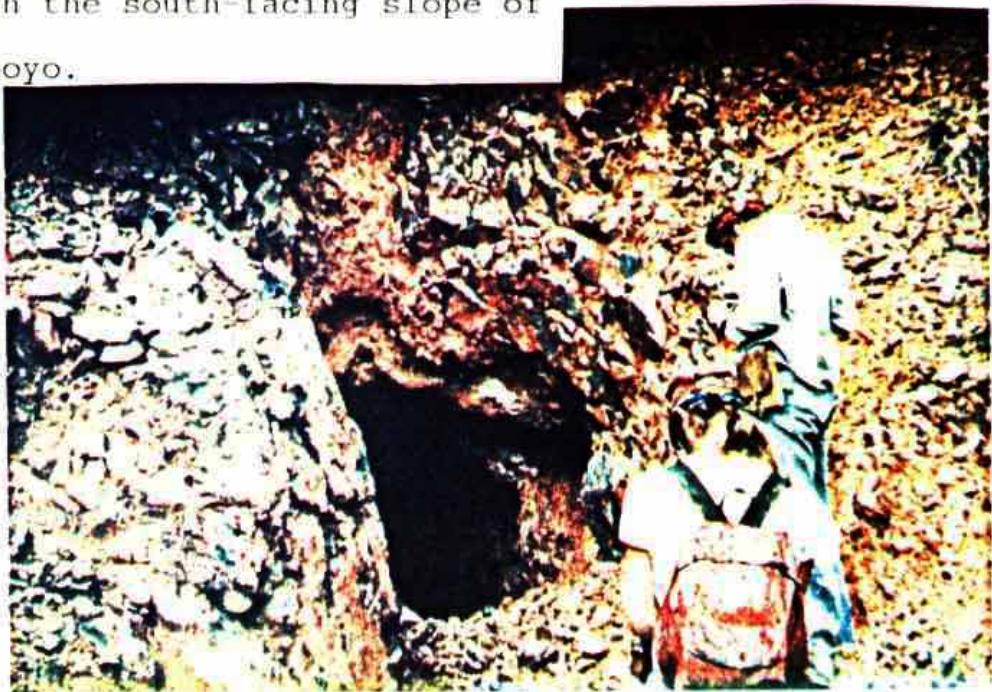
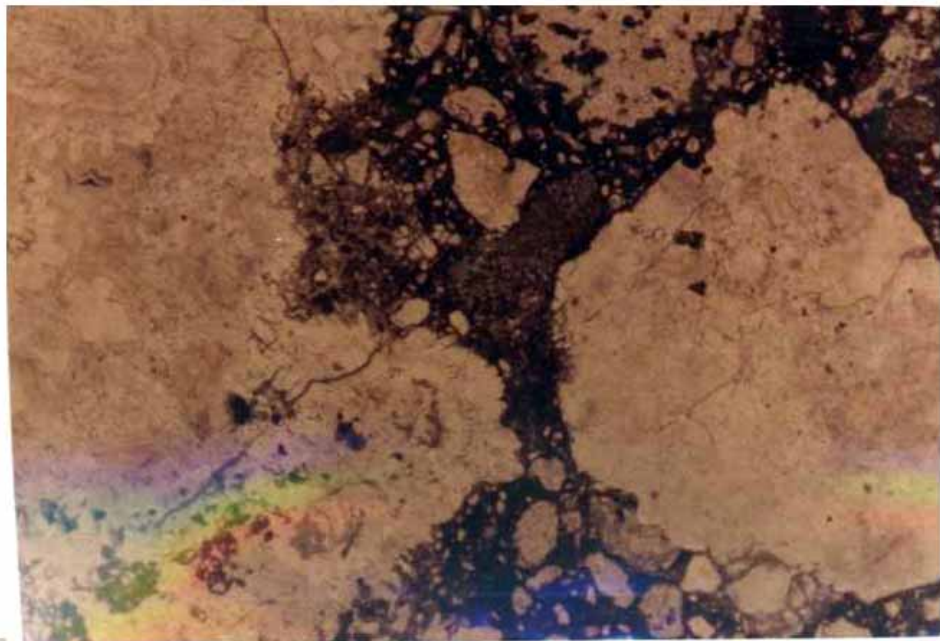


Plate 16: Adit in the south-facing slope of the San Jose Arroyo.





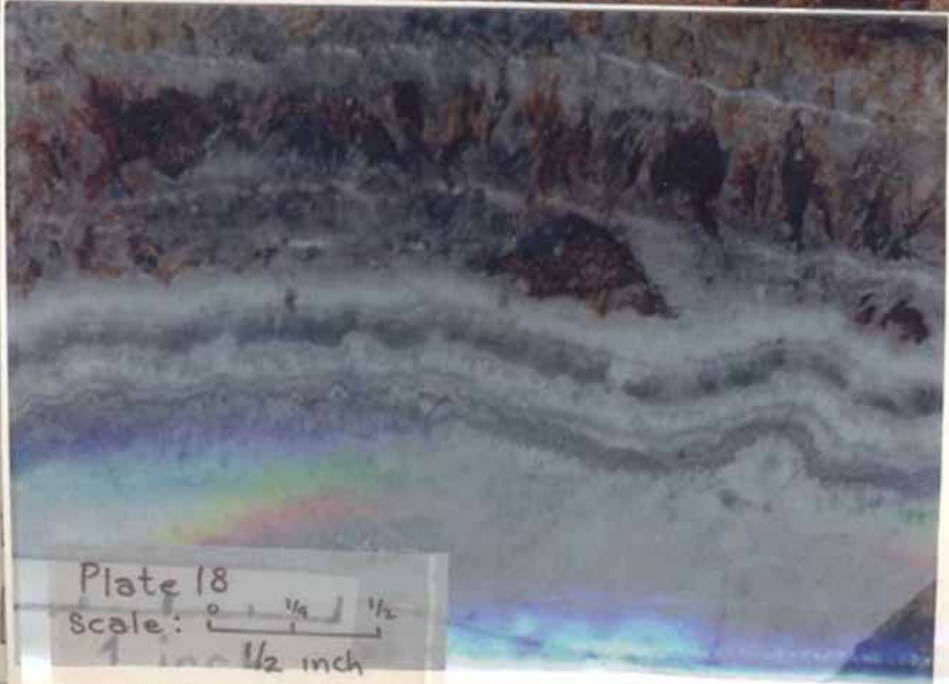


Plate 18

scale: 0 $\frac{1}{4}$ $\frac{1}{2}$
1 $\frac{1}{2}$ inch